

Environmental Risk Assessment of Mechanically Strengthened
Cellulose-Based Electrospun Nanocomposite Fibrous
Membranes

by

Nasrin Attari

THESIS PRESENTED TO ÉCOLE DE TECHNOLOGIE SUPÉRIEURE
IN PARTIAL FULFILLMENT FOR THE DEGREE OF
DOCTOR OF PHILOSOPHY
Ph.D.

MONTREAL, "9 MAY, 2024"

ÉCOLE DE TECHNOLOGIE SUPÉRIEURE
UNIVERSITÉ DU QUÉBEC



Nasrin Attari, 2024



This Creative Commons license allows readers to download this work and share it with others as long as the author is credited. The content of this work cannot be modified in any way or used commercially.

BOARD OF EXAMINERS

THIS THESIS HAS BEEN EVALUATED

BY THE FOLLOWING BOARD OF EXAMINERS

M. Robert Hausler, Thesis supervisor
Department of Construction Engineering, École de technologie supérieure

Mrs. Nicole Demarquette, Chair, Board of Examiners
Department of Mechanical Engineering, École de technologie supérieure

M. Mathias Glaus, Member of the Jury
Department of Construction Engineering, École de technologie supérieure

M. Patrick Drogui, External Independent Examiner
Institut National de la Recherche Scientifique

THIS THESIS WAS PRESENTED AND DEFENDED

IN THE PRESENCE OF A BOARD OF EXAMINERS AND THE PUBLIC

ON "19 MARCH, 2024"

AT ÉCOLE DE TECHNOLOGIE SUPÉRIEURE

Dedication

*This dissertation is dedicated to my husband **Vahid**, my sister **Mina**, my brothers **Peiman**, and **Atta**, my **Mom** for the tremendous love, and support at all times,*

and

*to the loving memories of my dear **dad**, whose unwavering belief in my potential guided me through every stage of this academic endeavor. Your spirit lives on in the pages of this thesis.*

FOREWORD

It is with great pleasure that I present this foreword for my Ph.D. thesis on the sustainable development of mechanically strengthened cellulose-based electrospun nanocomposite fibrous membranes. This research represents a significant contribution to the field of materials science, specifically in the area of advanced membrane technology. Sustainable development has become a pressing issue in today's world, as we strive to find innovative solutions that meet our societal needs while minimizing our impact on the environment. The development of cellulose-based electrospun nanocomposite fibrous membranes aligns perfectly with this goal, as it offers a sustainable alternative to traditional materials and methods. The objective of this research is to explore the fabrication techniques, material properties, and structural characteristics of these membranes, with a particular focus on enhancing their mechanical strength. By incorporating various nanocomposite fillers, such as nanocrystals and nanofibers, into the cellulose matrix, we aim to overcome the inherent limitations of cellulose-based materials and create membranes that are not only sustainable but also mechanically robust. Throughout this thesis, we delve into the fundamental principles of electrospinning, nanocomposite synthesis, and mechanical testing methodologies. We investigate the influence of different processing parameters, such as electrospinning parameters, filler concentration, and heat post-treatment, on the final properties of the membranes. Additionally, we evaluate the environmental impacts of the electrospinning method and compare it to the conventional wet spinning (NIPS) method emphasizing their potential to contribute to sustainable development. The significance of this research lies in its contributions to the field of sustainable materials and the advancement of nanocomposite fibrous membranes. By understanding the underlying mechanisms and optimizing the fabrication processes, we can unlock the full potential of these membranes and pave the way for their widespread adoption in various industries.

I would like to express my sincere gratitude to my supervisor and mentors for their guidance and support throughout this research journey. Their expertise and encouragement have been invaluable in shaping the outcome of this thesis. I also extend my appreciation to the Arbour and

VIII

Molson Foundations, ETS University, and the Biointerface research center at McGill University for providing the necessary resources and infrastructure for this research.

ACKNOWLEDGEMENTS

Completing this PhD thesis has been an extraordinary journey, and I am deeply grateful to all those who have supported and contributed to its realization. I am deeply thankful to my husband, Dr. Vahid Attari, for his boundless love, support, understanding, and encouragement. My Family's belief in my dreams and their unwavering support have been the driving force behind my accomplishments. I would like to express my heartfelt gratitude to my supervisor, Dr. Robert Hausler. His guidance, expertise, and unwavering support have been invaluable throughout this entire process. His belief in my abilities and his encouragement have been a constant source of motivation. I extend my sincere appreciation to the members of my thesis committee, Dr. Mathias Glaus, Dr. , and Dr. Nicole Demarquette, for their insightful feedback, constructive criticism, and valuable suggestions that have significantly improved the quality of this work. I am truly grateful to Dr. Martha Cerruti for her generosity and support throughout my research project. The access to Bio-Interface Laboratory at McGill University and lab equipment has been invaluable in helping me conduct my experiments and gather essential data for my study. I am indebted to my colleagues and friends at STEPPE-ETS for their camaraderie, stimulating discussions, and unwavering encouragement during the highs and lows of this journey. Your support has made this challenging endeavor more enjoyable and rewarding. My gratitude also extends to the faculty and staff of ETS University, whose dedication to academic excellence has provided a nurturing environment for research and learning. Last but not least, I acknowledge the financial support provided by Arbour Foundation, Molson Foundation, and ETS University which made this research possible. To everyone who has played a part in shaping this thesis and my academic pursuits, I offer my sincerest thanks. Your contributions, big and small, have left an indelible mark on this work. With humility and a sense of fulfillment, I dedicate this thesis to all those who believe in the power of knowledge and the pursuit of truth.

Développement durable de membranes fibreuses nanocomposites électrofilées à base de cellulose renforcées mécaniquement

Nasrin Attari

RÉSUMÉ

La technologie à membrane a été utilisée pour la purification de l'eau, le traitement des eaux usées et le retraitement des eaux polluées ces dernières années. Les technologies de filtration à base de membranes peuvent être utilisées dans la purification de l'eau dans la métallurgie primaire, la transformation des métaux, les secteurs pétroliers, etc. Une méthode innovante et durable pour séparer sélectivement les molécules et les ions a été développée à l'aide de membranes nanocomposites polymères constituées d'une phase polymère continue et d'une phase de nanofiller. Cette technologie a été reconnue pour son potentiel à contribuer à la fois à la durabilité et à l'efficacité des applications de filtration. L'équilibre entre durabilité et efficacité est de la plus haute importance dans les technologies membranaires pour assurer des performances optimales tout en minimisant l'impact environnemental. Pour relever les défis associés à la technologie des membranes, nous avons tout d'abord optimisé les paramètres du matériau, c'est-à-dire la concentration d'acétate de cellulose (CA) et la composition du solvant du mélange N, N-diméthylformamide (DMF)/acétone et les paramètres du processus de fabrication de la membrane par électrofilage, c'est-à-dire le débit de la solution, la tension, la distance entre la distance entre spinneret et le collecteur et le temps de traitement. Deuxièmement, nous avons développé et comparé des membranes nanofibreuses en acétate de cellulose (CA) renforcées de nanofibrilles de cellulose (CNF) et de nanocristaux de cellulose (CNC). Plusieurs propriétés dont les morphologies, les interactions chimiques et la résistance mécanique des membranes, ont été étudiées après leur synthèse à l'aide de la technique d'électrofilage et après leur traitement thermique. Les solutions de polymères étaient composées de divers pourcentages massique de CNC, de CNF oxydés par le 2,2,6,6-tétraméthyl-1-pipéridinyloxy (TEMPO) (c'est-à-dire de 0% à 1 %) et de 15% massique de CA résolu dans une fraction volumique égale (1/1) de solvant de mélange DMF/acétone. D'après notre étude, les propriétés de renforcement des nanofiller TOCNF étaient supérieures à celles des nanofiller CNC. La membrane nanofibreuse composite 0.25TOCNF/CA traitée thermiquement a atteint une résistance à la traction et un allongement maximaux au point de rupture de 33.31 MPa et 1.8%, respectivement. Les relations processus-structure-propriété décrites dans cette étude peuvent faciliter la fabrication et améliorer l'efficacité de l'application de membranes nanocomposites électrofilées pour la purification de l'eau. D'autre part, la durabilité est une considération fondamentale lors du développement et de la mise en œuvre des technologies membranaires. Ces technologies offrent plusieurs avantages qui contribuent à une approche plus durable. Cette étude évalue l'impact environnemental de la méthode conventionnelle de filage humide (NIPS) et de la technique innovante de filage à sec (électrofilage) pour les membranes nanofibreuses électrofilées nanocomposites à base de cellulose. L'analyse du cycle de vie (ACV) de la membrane nanocomposite 0.25TOCNF/CA a été réalisée afin de comprendre les impacts environnementaux du processus de fabrication et d'évaluer le potentiel d'utilisation dans des applications industrielles et autres nécessitant une évaluation de l'empreinte environnementale. Les résultats seront précieux pour les chercheurs,

les ingénieurs et les décideurs travaillant dans le domaine du traitement de l'eau et de la technologie membranaire. Plusieurs méthodes d'évaluation d'impact ont été utilisées dans cette analyse, y compris les méthodes de demande énergétique cumulée (CED) et IMPACT2002+. Afin de prendre en compte les variations dans les résultats et de faire face aux incertitudes associées, nous avons utilisé la simulation de Monte-Carlo et effectué une analyse de sensibilité. Nous avons également examiné les incertitudes liées à la méthode d'Évaluation des Impacts du Cycle de Vie (EICV), ainsi qu'aux paramètres et sources de données. Les résultats suggèrent que l'utilisation de la technique d'électrofilage pour la fabrication de membranes est un choix plus durable sur le plan environnemental par rapport à la méthode NIPS, notamment en ce qui concerne les catégories d'impact du changement climatique et de l'épuisement des ressources fossiles. Cependant, l'analyse des incertitudes a révélé que des conclusions définitives ne pouvaient pas être tirées concernant les catégories d'impact de l'eutrophisation et de la toxicité. L'énergie totale utilisée par la méthode NIPS pour un filage par lots de 50g de solution polymère à 0.25TOCNF/CA était de 1030MJ, tandis que pour le processus d'électrofilage, elle était de 768MJ. La consommation d'énergie fossile non renouvelable par la méthode NIPS est supérieure à celle de la méthode d'électrofilage. Ainsi, la méthode d'électrofilage est plus efficace que la méthode NIPS en termes de consommation d'énergie. La méthode NIPS a un impact plus important sur l'environnement en raison de sa consommation d'eau plus élevée et du rejet d'eaux usées contaminées par des solvants, et d'une contribution plus élevée à la toxicité cancérigène pour l'homme, non cancérigène, principalement en raison d'une plus grande demande d'électricité.

Mots-clés: Electrofilage, Nanocelluloses, Acétate de Cellulose, Nanofibres Composites Électrofilées, Propriétés Mécaniques, Analyse du Cycle de Vie, Impacts Environnementaux, OpenLCA

Environmental Risk Assessment of Mechanically Strengthened Cellulose-Based Electrospun Nanocomposite Fibrous Membranes

Nasrin Attari

ABSTRACT

Membrane technology has been employed for water purification, wastewater treatment, and reprocessing of polluted water in recent years. Membrane-based filtration technologies can be used in water purification in primary metallurgy, metal processing, petroleum sectors, etc. An innovative sustainable method to selectively separate molecules and ions has been developed using polymer nanocomposite membranes that consist of a continuous polymer bulk phase and a nanofiller phase. This technology has been recognized for its potential to contribute to both sustainability and efficiency in filtration applications. The balance between sustainability and efficiency is of utmost importance in membrane technologies to ensure optimal performance while minimizing environmental impact. To address the challenges associated with the membrane technology, firstly, we have optimized the material parameters, i.e., cellulose acetate (CA) concentration and N, N-dimethylformamide (DMF)/ acetone mixture solvent composition and electrospinning membrane fabrication process parameters, i.e., feed flow rate, voltage, tip-to-collector distance, and processing time. Secondly, we developed, and compared the nanofibrous cellulose acetate (CA)-based membranes reinforced with cellulose nanofibrils (CNFs) and cellulose nanocrystals (CNCs). Several properties including the morphologies, chemical interactions, and mechanical strength of the membranes were investigated after they were synthesized using the electrospinning technique and after they were heat treated. The polymer solutions were composed of various weight percentages of CNCs, 2,2,6,6-tetramethyl-1-piperidinyloxy (TEMPO)-mediated oxidized CNFs (i.e., 0 wt% to 1 wt%), and 15 wt% of CA solved in an equal (1/1) volume fraction of DMF/ acetone mixture solvent. Based on our study, the reinforcing properties of TOCNF nanofillers were superior to CNC nanofillers. Heat-treated 0.25TOCNF/CA composite nanofibrous membrane achieved maximum ultimate tensile strength and elongation at the break-point of 33.31 MPa and 1.8%, respectively. The process-structure-property relationships outlined in this study can facilitate the fabrication and improve the efficiency of the application of electrospun nanocomposite membranes for the purification of water. On the other hand, sustainability is a fundamental consideration when developing and implementing membrane technologies. These technologies offer several advantages that contribute to a more sustainable approach. This study evaluates the environmental impact of the conventional wet spinning method (NIPS) and the innovative dry spinning technique (electrospinning) for cellulose-based nanocomposite electrospun nanofibrous membranes. Life cycle assessment (LCA) of the 0.25TOCNF/CA nanocomposite membrane was conducted to understand the environmental impacts of the fabrication process and to evaluate the potential for use in industrial and other applications that require an assessment of the environmental footprint. The findings will be valuable for researchers, engineers, and policymakers working in the field of water treatment and membrane technology. Several impact assessment methods were used in this analysis, including the Cumulative Energy Demand (CED) and IMPACT2002+ methods. In order to consider the variations in results and tackle the associated uncertainties, we employed

Monte Carlo simulation and conducted sensitivity analysis. We also delved into uncertainties linked to the Life Cycle Impact Assessment (LCIA) method and the parameters and data sources. The results suggest that employing the electrospinning technique for membrane fabrication is a more environmentally sustainable choice compared to the NIPS method, particularly concerning climate change and fossil depletion impact categories. However, the uncertainty analysis revealed that definitive conclusions couldn't be reached regarding the impact categories of eutrophication and toxicity. The total energy that the NIPS method uses for one batch spinning of 50 gr of 0.25TOCNF/CA polymeric solution was 1030 MJ while for the electrospinning process was 768 MJ. The nonrenewable fossil fuel energy consumption by the NIPS method is more than the electrospinning method. So, the electrospinning method is more efficient than the NIPS method in terms of energy consumption. The NIPS method has a greater impact on the environment due to its higher water consumption and solvent-contaminated wastewater release, and a higher contribution to human carcinogenic, non-carcinogenic toxicity, mainly due to more electricity demand.

Keywords: Electrospinning, Nanocelluloses, Cellulose Acetate, Composite Electrospun Nanofibers, Mechanical Properties, Life Cycle Assessment, Environmental Impacts, OpenLCA

TABLE OF CONTENTS

	Page
INTRODUCTION	1
CHAPTER 1 PROBLEM STATEMENT, RESEARCH OBJECTIVES, AND ORIGINAL CONTRIBUTIONS	3
1.1 Problem statement and research objectives	3
1.2 Original contributions of the study	4
CHAPTER 2 BACKGROUND AND LITERATURE REVIEW	7
2.1 The enhancement of mechanical properties of the membranes	7
2.2 Life cycle assessment of nanocomposite fibrous membrane production processes	12
CHAPTER 3 METHODOLOGY	17
3.1 Materials	17
3.2 Membrane production and characterization methodology	18
3.2.1 Preparation of spinning polymer solutions	18
3.2.2 Membrane synthesis by electrospinning process	20
3.2.3 Hollow-fiber and flat-sheet membrane preparation by NIPS method	22
3.2.4 Exploring Material and Operating Parameters in Electrospinning	22
3.2.5 Heat post-treatment of CNC/CA, TOCNF/CA composite nanofibers	23
3.2.6 Solution characterization	23
3.2.7 Membrane characterization	23
3.3 Life Cycle Assessment methodology	25
3.3.1 Goal and scope definition	25
3.3.2 System boundary	26
3.3.3 Life Cycle Inventory	27
3.3.4 Life Cycle Impact Assessment	31
3.3.5 Life Cycle Interpretation	32
CHAPTER 4 RESULTS	35
4.1 Optimization of the Electrospinning Process	35
4.1.1 Material and electrospinning process parameters	36
4.1.2 Structural effects of material parameters	37
4.1.3 Structural effects of electrospinning parameters	38
4.1.4 The effects of material and electrospinning parameters on the porosity of ENM samples	39
4.1.5 Conclusion	41
4.2 Mechanical reinforcement of cellulose acetate nanofibrous membranes	43
4.2.1 Nanocomposite spinning solution characterization	43
4.2.2 Structural effects: HPT process	44

4.2.3	Structural effects: nanofiller loading	46
4.2.4	FTIR spectroscopy	47
4.2.5	Mechanical properties	50
4.2.6	Conclusion	55
4.3	Life Cycle Assessment: environmental impacts of cellulose-based nanocomposite membrane fabrication process	56
4.3.1	Life Cycle Impact Assessment (CED and IMPACT2002+ methods)	56
4.3.2	Environmental impacts of synthesis process of 0.25TOCNF/CA nanofibrous membrane by electrospinning technique	58
4.3.3	Environmental impacts of synthesis process of 0.25CNF/CA hollow-fiber membrane via NIPS method	61
4.3.4	Comparative analyses of 0.25TOCNF/CA membrane production by electrospinning and wet spinning methods	66
4.3.5	Interpretation of environmental impacts of synthesizing 0.25TOCNF/CA ENM and HFM samples	73
CHAPTER 5	DISCUSSION	77
CONCLUSION	81
RECOMMENDATIONS	85
BIBLIOGRAPHY	87

LIST OF TABLES

		Page
Table 2.1	Recent experimental studies on the mechanical properties and the microstructure of polymeric nanocomposite membranes	11
Table 2.2	Recent LCA studies on the manufacturing process of polymeric membranes	15
Table 3.1	Caption for LOF	18
Table 3.2	The properties and the characterization of spinning solutions	19
Table 3.3	The composition and formulation of synthesized nanocomposite ENMs	20
Table 3.4	Per FU based material requirements and energy consumption for 0.25TOCNF/CA electrospun membrane fabrication by Electrospinning method	26
Table 3.5	Per FU based material requirements and energy consumption for 0.25TOCNF/CA hollow-fiber membrane fabrication by NIPS method	26
Table 3.6	Per FU based life cycle inventory for the production of 0.25TOCNF/CA nanocomposite membrane by electrospinning and wet spinning methods	29
Table 3.7	Synthesis data inventory for the production of 1.14 gr CA and 10 gr TEMPO-CNF	30
Table 4.1	The mechanical properties of CNC/CA nanocomposite ENMs	54
Table 4.2	The mechanical properties of TOCNF/CA composite ENMs	54
Table 4.3	Per FU Based CED and IMPACT2002+ results for the production of 0.25TOCNF/CA nanocomposite membrane by Electrospinning and NIPS methods	57
Table 4.4	Caption for LOF	71
Table 4.5	Uncertainty results for life cycle impact assessment of 0.25TOCNF/CA ENM and HFM	74

LIST OF FIGURES

		Page
Figure 3.1	Caption for LOF	18
Figure 3.2	Various conventional and innovative methods for membrane fabrication in a glance: (A) Electrospinning process along with heat treatment, (B) Hollow-fiber fabrication by Non-solvent Induced Phase Separation (NIPS), (C) Flat sheet membrane fabrication by NIPS method	21
Figure 3.3	System boundary of electrospun nanocomposite membrane fabrication process	27
Figure 3.4	Overall scheme of a)IMPACT2002+ and b)CED impact assessment methods, an interconnection between LCI results and damage categories based on midpoint and energy categories	32
Figure 4.1	The morphological characterization of synthesized nanofibrous ENM samples to investigate the structural effects of material parameters	37
Figure 4.2	The morphological characterization of synthesized nanofibrous ENM samples to investigate the structural effects of electrospinning process parameters	40
Figure 4.3	The effect of different compositions of DMF/acetone solvent mixtures on porosity(ϵ) of the synthesized ENM samples with the same CA concentration of 10 wt.% at constant electrospinning conditions	41
Figure 4.4	The effect of CA concentration on porosity ϵ of the synthesized ENM samples with the same solvent composition of (1:1) at constant electrospinning conditions	42
Figure 4.5	The effect of various electrospinning parameters on porosity(ϵ) of the synthesized ENM samples at constant CA concentration and solvent mixture composition	42
Figure 4.6	The impact of CNC/TOCNF loading on a) conductivity and b) viscosity of the spinning solutions	44
Figure 4.7	SEM images, fiber diameter distribution and range for pristine CA nanofibers and CNC/CA and TOCNF/CA ENMs as-spun and after HPT process (a)Pristine CA nanofibers as-synthesized (b)Pristine	

	CA nanofibers after HPT (c) to (r) CNC/CA and TOCNF/CA composite nanofibers as-spun and after HPT process (s) Mean fiber diameter vs. nanofiller loading (t)Fiber diameter range vs. nanofiller loading	45
Figure 4.8	FTIR spectra of ENMs (a) CNC/CA composite ENMs (b) TOCNF/CA composite ENMs as-spun	48
Figure 4.9	FTIR spectra of 0.5CNC/CA electrospun nanofibrous membrane samples as-spun and after HPT process	49
Figure 4.10	The effect of (a) CNC and (b) TOCNF nanofillers on mechanical properties of CA ENMs as-spun and after HPT process	51
Figure 4.11	Variations of tensile strength of CNC/CA and TOCNF/CA ENMs as a function of nanofiller loading and heat treatment process	53
Figure 4.12	CED for material and energy requirement processes of electrospinning 50gr 0.25TOCNF/CA	58
Figure 4.13	IMPACT2002+ results (a) contribution to impact category (b) relative Impact, for the environmental impacts of producing 0.25CNF/CA electrospun nanofibrous membrane	59
Figure 4.14	CED results for the environmental impacts of producing 0.25CNF/CA hollow-fiber membrane via NIPS method	62
Figure 4.15	IMPACT2002+ results (a) Contribution to impact category (b) Relative Impact, for the environmental impacts of producing 0.25CNF/CA hollow-fiber membrane via NIPS method	63
Figure 4.16	Comparative CED results for the energy consumption for the production of 0.25CNF/CA ENM and HFM via Electrospinning and NIPS methods	66
Figure 4.17	Comparing IMPACT2002+ results for the environmental impacts of producing 0.25CNF/CA ENM and HFM via Electrospinning and NIPS methods	68
Figure 4.18	Relative endpoint damages of producing one functional unit of the final product by NIPS and electrospinning processes	71
Figure 4.19	Contribution to endpoint damages of producing one functional unit of the final product by NIPS and electrospinning processes	72

Figure 4.20 Comparative uncertainty boxplots for ENM and HFM samples
manufacturing processes by electrospinning and NIPS methods 73

LIST OF ABBREVIATIONS

ETS	École de technologie supérieure
e.g.	Exempli gratia. (For example)
i.e.	Id est, (That is)
et. al.	Et Alia, (And others)
ENM	Electrospun Nano-fibrous Membrane
HFM	Hollow-fiber Membrane
NIPS	Nonsolvent Induced Phase Separation
TIPS	Thermal Induced Phase Separation
HPT	Heat Post Treatment
SEM	Scanning Electron Microscope
TEM	Transmission Electron Microscope
FTIR	Fourier Transform Infrared Spectroscopy
ATR	Attenuated Total Reflection
DMF	N-diMethylformamide
CA	cellulose acetate
NCs	nano-celluloses
CNC	cellulose nano-crystal
CMC	cellulose micro-crystal
TOCNF	TEMPO-oxidized cellulose nano-fibril

XXIV

TEMPO	2,2,6,6-tetramethyl-1-piperidinyloxy
PVDF	Poly(vinylidene fluoride)
CH	chitosan
PEO	poly(ethylene oxide)
PLA	poly(lactic acid)
NaCl	sodium chloride
NaBr	sodium bromide
UTS	Ultimate Tensile Strength
UF	Ultra Filtration
DS	Degree of Substitution
TCD	Tip to Collector Distance
DI	De-Ionized
FU	Functional Unit
LCA	Life Cycle Assessment
ACV	Analyse du Cycle de Vie
LCIA	Life Cycle Impact Assessment
LCI	Life Cycle Inventory
CED	Cumulative Energy Demand
ROW	Rest of World
GLO	Global

AAP	Aquatic Acidification Potential
AEP	Aquatic Ecotoxicity Potential
AEUP	Aquatic Eutrophication Potential
GWP	Global Warming Potential
IRP	Ionizing Radiation Potential
MEP	Mineral Extraction Potential
HCTP	Human Carcinogenic Toxicity Potential
HNCTP	Human Non-Carcinogenic Toxicity Potential
LUP	Land Use Potential
NREP	Non-Renewable Energy Potential
OLDP	Ozone Layer Depletion Potential
RIP	Respiratory Inorganics Potential
ROP	Respiratory Organics Potential
TANP	Terrestrial Acid/Nutri Potential
TEP	Terrestrial Ecotoxicity Potential
HH	Human Health
EQ	Ecosystem Quality
CC	Climate Change
RD	Resource Depletion
CF	Characterization Factor
CV	Coefficient Variation

LIST OF SYMBOLS AND UNITS OF MEASUREMENTS

ρ	Density
ϵ	Porosity
μ	Viscosity
Mn	Molecular Weight
g	Gram
kg	Kilogram
h	Hour
nm	Nanometer
μm	Micrometer
cm	Centimeter
km	Kilometer
wt %	Weight Percent
vol%	Volume Percent
MPa	Megapascal
GPa	Gigapascal
ppm	Part per million
g/ml	Gram per millilitre
mmol/g	Milimole per gram
$\mu\text{ s}$	Microsecond

XXVIII

cp	Centipoise
ml/min	Mililitre per minute
°C	Degree Centigrade
rpm	Round per minute
W_w	Wet sample weight
W_d	Dry sample weight
ρ_w	Density of the water
ρ_p	Density of the polymer
N	Newton
kg SO_2 eq.	Kilograms of sulfur dioxide-equivalents
kg TEG water	Kilograms of triethylene glycol to water
kg PO_4 P-lim	Kilograms of phosphate ion equivalents into a P-limited water
kg CO_2 eq.	Kilograms of carbon dioxide-equivalents
kBq C-14 eq.	Kilobecquerel of Carbon-14-equivalents
MJ surplus	Additional energy needed for future use of substitutes, inferior quality, sources of material or energy supply in megajoules
kg C_2H_3Cl eq	Kilograms of Vinyl chloride-equivalents
m_2 org.arable	Square meter of organic arable land
MJ primary	Energy intensity level of primary energy in megajoules
kg CFC-11 eq.	Kilograms of Trichlorofluoromethane-equivalents
kg $PM_{2.5}$ eq.	Kilograms of particulate matter-equivalents

kg C_2H_4 eq.	Kilograms of Ethylene-equivalents
kg TEG soil	Kilograms of triethylene glycol to soil
DALY	Disability-adjusted life years

INTRODUCTION

Cellulose-based nanocomposite membranes have emerged as a prominent area of research and innovation in the field of membrane technology Pinnau & Freeman (2000). Leveraging cellulose, one of the most abundant and sustainable natural polymers, these membranes hold great promise for various applications, especially in filtration processes Battirola, Andrade, Marson, Hubinger & do Carmo Gonçalves (2017). One of the key fabrication methods for these membranes is electrospinning, an innovative and versatile technique that enables the production of nanofiber assemblies with high porosity, controllable thickness, and a high surface-to-volume ratio Zhou, Lin & Wu (2016). The mechanical properties of membranes play a pivotal role in their performance in pressure-driven filtration processes, influencing factors such as filtrate flux and selectivity Jonoobi, Harun, Mathew & Oksman (2010); Voisin, Bergström, Liu & Mathew (2017). To enhance the mechanical strength of cellulose-based membranes, nanofillers like cellulose nanocrystals (CNCs) and cellulose nanofibrils (CNFs) are introduced into the polymer matrix. Furthermore, heat post-treatment (HPT) is employed as a technique to reinforce the membrane structure.

As the membrane industry expands, considerations of sustainability and environmental impact have gained prominence Prézéus, Tiruta-Barna, Guigui & Remigy (2021); Kim (2020). This project explores the environmental aspects of cellulose-based nanocomposite membrane manufacturing, introducing the concept of Life Cycle Assessment (LCA) as a crucial methodology for evaluating the overall environmental footprint. In addition, a comparative analysis is undertaken between the electrospinning and wet spinning methods for membrane fabrication, examining their respective life cycle assessments. This project aims to provide insights into the broader environmental implications of cellulose-based nanocomposite membrane production and guide informed decisions toward more sustainable membrane manufacturing processes.

This PhD thesis is organized in four chapters, which are briefly described here. The thesis's research objectives along with its scope are described in chapter 1. The chapter 2 provides a background and an overview of recent researches on the mechanical reinforcement of membranes and life cycle assessment of membrane manufacturing processes.

The chapter 3 discusses the methodology of membrane synthesis and characterization, experimental measurements, and more specific information regarding the life cycle assessment methodology.

Chapter 4 including three sections discusses the findings of this research. The section 4.1 focuses on the optimization of the electrospinning process to obtain an ultimate optimum electrospun cellulose acetate membrane. In Section 4.2, the mechanical reinforcement of electrospun cellulose acetate nanocomposite fibrous membranes, and the structural impacts of thermal treatment and nanofiller loading are discussed. The research's third phase, outlined in section 4.3, focuses on evaluating the environmental repercussions of the electrospun membrane manufacturing process and making a comparative analysis between the electrospinning technique and the traditional wet spinning method.

The conclusions from the present research work are addressed at the end of this Ph.D. thesis, along with some recommendations for more future research in this area.

CHAPTER 1

PROBLEM STATEMENT, RESEARCH OBJECTIVES, AND ORIGINAL CONTRIBUTIONS

1.1 Problem statement and research objectives

Water purification process plays a crucial role in addressing global water scarcity and ensuring access to safe drinking water. However, conventional water purification methods are often associated with limitations such as high energy consumption, chemical usage, and inefficient removal of contaminants. To improve the performance of water treatment processes, there is an urgent need to develop sustainable and efficient water purification technologies, and nanotechnology offers a promising solution. Cellulose-based nanocomposite electrospun nanofibrous membranes have gained significant attention due to their unique properties, such as high surface area, mechanical strength, and excellent chemical stability. These membranes have the potential to revolutionize water purification applications by effectively removing contaminants and pollutants from water sources. However, there are still several challenges that need to be addressed in the development of these membranes. One of the main challenges is achieving optimal mechanical properties while maintaining the desired filtration efficiency. Traditional cellulose-based membranes often lack the necessary mechanical strength, leading to reduced lifespan and compromised performance. Their mechanical limitations, particularly in terms of strength and durability, impede their widespread implementation.

Furthermore, with the growing concern for environmental damages, and also increasing demand for sustainable and environmentally friendly solutions in various industries, the pursuit of eco-friendly and resource-efficient technologies has become imperative. As the demand for membranes continues to grow across various industries, understanding the environmental implications of their production becomes paramount. The current state of knowledge in LCA often focuses on the operational phase of processes, neglecting the environmental footprint of membrane fabrication and potential end-of-life disposal solutions. Additionally, while some studies exist on the subject, there is a lack of comprehensive evaluations that encompass various

impacts such as global warming, human carcinogenic toxicity, human non-carcinogenic toxicity, fossil resource scarcity, and marine eco-toxicity. The problem statement revolves around the need for a holistic and detailed assessment of the environmental performance of membrane manufacturing processes, providing valuable insights for sustainable decision-making and contributing to the ongoing discourse on eco-friendly technologies.

The overall objective of this study is to develop a sustainable mechanically strengthened cellulose-based electrospun nanocomposite fibrous membrane.

The specific objectives of the present research are:

- Optimizing the material parameters, i.e., CA concentration, solvent mixture composition, and the electrospinning parameters, i.e., feed flow rate, tip to collector distance (TCD), voltage, and process time.
- Investigating the impacts of material and electrospinning parameters on morphological and structural properties of CA electrospun membranes.
- Exploring the effects of thermal treatment and nanofiller loading on the mechanical properties of the nanocomposite fibrous membranes.
- Evaluation of the environmental impacts of membrane manufacturing process by electrospinning via life cycle assessment.
- Comparative life cycle assessment of cellulose acetate membrane fabrication processes by the conventional wet spinning method (NIPS) and the innovative dry spinning technique (electrospinning).

1.2 Original contributions of the study

By addressing the challenges associated with the mechanical development of cellulose-based nanocomposite electrospun nanofibrous membranes and assessing the environmental performance of different membrane fabrication methods, this research endeavors to contribute to the development of efficient and sustainable solutions for clean water production. The findings of this research will be valuable for researchers, engineers, and policymakers working in the field

of water treatment and membrane technology. Moreover, by employing LCA methodology, the research aims to systematically assess and quantify the environmental burdens associated with each stage of the manufacturing process. The anticipated contributions include the identification of hotspots and environmentally sensitive stages in the life cycle, allowing for targeted improvements and the development of more sustainable practices. The study seeks to establish a framework for the eco-design of cellulose-based membranes, fostering advancements in sustainable membrane technology.

The successful development of such membranes would have significant implications in the field of water purification. It would contribute to the advancement of sustainable and cost-effective water treatment technologies, making clean drinking water more accessible to communities facing water scarcity. The outcomes of this research are anticipated to have direct applications in water purification technologies. The development of mechanically reinforced cellulose-based membranes is expected to extend their operational lifespan, and improve overall efficiency in removing contaminants from water sources. The practical implications include the potential deployment of these membranes in water treatment plants, decentralized purification systems, and point-of-use devices, contributing to sustainable and reliable access to clean water.

This work maps the process-structure-property hierarchy of CA-based nanofibrous composite membranes. At the most general level, we consider the main polymer material, nanofillers, and the solvent. As the process level, we dissolved the polymer solution using the ultrasonication technique until the nanofillers were well dispersed and well distributed in the spinning solution. The membrane samples were then synthesized by electrospinning and their structure was investigated using a Scanning Electron Microscope (SEM). Two nanofibrous and bead-formed microstructures are shown as possible example structures. As the property level, the synthesized sample was further characterized to determine the chemical properties, and mechanical properties using Fourier transform infrared spectroscopy (FTIR), and universal tensile testing, respectively. Following the fabrication and mechanical characterization phases of the research, the comparative environmental impacts assessment of the cellulose-based nanocomposite fibrous membrane samples fabricated by the NIPS method and the electrospinning technique were conducted. A

specific focus of this study was to explore if the electrospinning technique provides intrinsic benefits over the established phase inversion method when environmental impacts are considered.

CHAPTER 2

BACKGROUND AND LITERATURE REVIEW

This chapter serves as the foundation for contextualizing and delving into the research topic within the existing body of knowledge. This chapter critically examines relevant scholarly literature, theories, and empirical studies to identify gaps, establish the rationale for the research, and articulate the significance of the chosen area of investigation. Section 2.1 summarizes the most recent work in the field of mechanical enhancement of nanocomposite membranes. The predominant focus in the current state of membrane technology in LCA is on the operational phase of processes, neglecting the environmental impact related to membrane fabrication and potential end-of-life disposal solutions. Consequently, there is limited research in this field, and section 2.2 provides an overview of the related LCA works.

2.1 The enhancement of mechanical properties of the membranes

Membranes serve as semi-permeable barriers regulating the exchange of substances between two adjoining phases, and they play pivotal roles in advanced separation technologies. The transformative era of membrane technology began with the invention of reverse osmosis by Reid and Breton in 1959 Reid & Breton (1959), along with the development of the asymmetric cellulose acetate (CA) membrane by Loeb and Sourirajan in 1962 Sidney & Srinivasa (1964). This breakthrough led to numerous applications, including molecular separation methods, i.e., reverse osmosis, nanofiltration, ultrafiltration, and microfiltration Glater (1998); Matsuura (2020), supporting chemical transformations in catalytic membranes, membrane reactors Marcano & Tsotsis (2002), and bioreactors Judd (2008), as well as applications in energy storage Kausar (2017) and sustainable energy production Goodenough (2014). Membranes also hold significance in diverse medical and biological fields, including dialysis, drug release, and cell culture Adiga, Jin, Curtiss, Monteiro-Riviere & Narayan (2009). Over the past few years, membrane technology has found extensive use in the purification of water, treatment of wastewater, and the reclamation of contaminated water sources Kugarajah *et al.* (2021). The swift

progress in membrane science and technology can be credited to the straightforwardness, minimal energy usage, ease of management and expansion, adaptability, and environmentally conscious nature inherent in numerous membrane-based technologies. Also, using high-performance materials, membrane technologies have found a broad range of applications in industry and human life Fane, Wang & Jia (2011). As the most prevalent membrane material, polymers are mainly used in the membrane industry because they are comparatively inexpensive, environmentally friendly, and easy to process. Other performance requirements must be considered, including selective permeation, mechanical strength, thermal properties, and physiochemical stability, before practical application of a membrane material Pinnau & Freeman (2000); Yadav *et al.* (2021); Park, Hoek & Tarabara (2013). Additionally, polymer-based nanocomposites, which comprise a polymer bulk phase (i.e., continuous phase) and a nanofiller phase (i.e., dispersed phase) provide a promising solution to take advantage of synergistic interactions between the polymer bulk and the nanofiller Bay, Zarybnicka, Jancar & Crosby (2020); Wen, Yuan, Ma, Wang & Liu (2019); Divya & Oh (2022).

Cellulose Acetate (CA) is one of the most abundant polymer resources, an ester derivative of cellulose, an essential ingredient of green plant cell walls, and also one of the most favorable biodegradable polymers for the preparation of polymeric membranes. The most common type of CA has an acetate group on two of its three hydroxyls Babaei-Ghazvini & Acharya (2022); Fischer *et al.* (2008); Salama, Mohamed, Aboamera, Osman & Khattab (2018); Jiang *et al.* (2020); Lee, Nishino, Sohn, Lee & Kim (2018). CA-based membranes are widely used in filtration-based processes in particular water purification Voisin *et al.* (2017); Goetz, Naseri, Nair, Karim & Mathew (2018), wastewater treatment Del Río De Vicente (2021); Abdullah, Yusof, Lau, Jaafar & Ismail (2019), biosensors Vaidya & Wilkins (1994), blood purification Janeca, Rodrigues, Gonçalves & Faria (2021), and tissue engineering Stamatialis *et al.* (2008). This popularity originates from extensive bio-compatibility, biodegradability Wsoo, Shahir, Mohd Bohari, Nayan & Razak (2020), nontoxic nature, good chemical, thermal Etemadi, Yegani & Babaeipour (2016), and mechanical properties and relatively low cost Aboamera, Mohamed, Salama, Osman & Khattab (2019). Of the conventional methods for polymeric

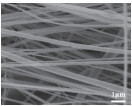
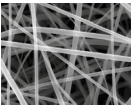
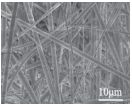
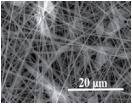
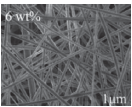
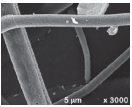
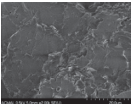
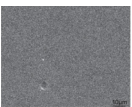
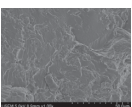
membrane fabrication (i.e., sintering, track-etching, stretching, and phase inversion), phase inversion is the most widely used in both industry and academia Ismail *et al.* (2020). The non-solvent induced phase separation (NIPS) process is predominantly used on an industrial scale to fabricate porous asymmetric flat sheets and hollow-fiber membranes (HFMs) due to the relative simplicity of its set-up Battirola *et al.* (2017). In comparison, electrospinning is an innovative, simple, and useful technique for producing various fiber assemblies by properly controlling the polymer solution and electrospinning parameters. In general, the electrospun fiber diameters can range from 50 nm to 10 μ m in thickness Doshi & Reneker (1995). The fibers can be spun into non-woven structures having high porosity, high surface-to-volume ratio, controllable thickness, and high alignment of nanofibers, which are desirable in water and wastewater treatment applications Zhou *et al.* (2016); Aruchamy, Mahto & Nataraj (2018); Burger, Hsiao & Chu (2006). CA as a hydrophilic polymer and an excellent electrical conductor is ideal for wet spinning and electrospinning methods, respectively Wsoo *et al.* (2020); Jung *et al.* (2016); Vatanpour *et al.* (2022). CA electrospun nanofibrous membranes (ENMs) have a high specific surface area, uniform morphology, high interconnected porosity resulting in high permeability flux Zhou *et al.* (2016), controllable thickness, high alignment of nanofibers Aruchamy *et al.* (2018), and good mechanical strength Suja, Reshmi, Sagitha & Sujith (2017); Lee *et al.* (2018) in comparison to the membranes fabricated by other techniques (e.g., phase inversion method). On the other hand, the conventional non-solvent induced phase separation (NIPS) process is predominantly used on an industrial scale to fabricate porous asymmetric flat sheets and hollow-fiber membranes (HFMs) due to the relative simplicity of its set-up Battirola *et al.* (2017).

Mechanical characteristics of membranes play a significant role in the performance of pressure-driven water purification processes in terms of water flux and selectivity. A method for strengthening polymer membranes is to introduce nanofillers to the polymer matrix and then heat post-treated afterwards. When nanofillers like cellulose nanocrystals (CNCs) and cellulose nanofibrils (CNFs) are introduced to a CA polymer solution and heat post-treatment (HPT) is performed, the fiber linkages and mechanical properties can be improved Wsoo *et al.* (2020); Jiang *et al.* (2020); Jonoobi *et al.* (2010); Voisin *et al.* (2017). CNCs and CNFs are renewable

nanoparticles originating from cellulose and depending on the source and preparation process, their lengths may vary between 100 and 2000 nm, and diameters range between 2 and 20 nm. Chemical or enzymatic pre-treatments can be used for their preparation to greatly influence their characteristics Mokhena, Jacobs & Luyt (2018); Goetz *et al.* (2018); Ma, Burger, Hsiao & Chu (2014). The most important pre-treatments are TEMPO-mediated oxidation, mechanical refining, hydrolyzation, and carboxymethylation. The key point in 2,2,6,6-tetramethyl-1-piperidinyloxy (TEMPO)-mediated oxidation is the negatively charged surface of the crystals and the fibrils. The individual fiber and crystal due to electrostatic repulsion forces can stay free and result in an improved dispersion Patiño-Masó *et al.* (2019); Levanic *et al.* (2020). Furthermore, in order to cross-link the CNCs and TEMPO-oxidized cellulose nanofibrils (TOCNFs) and improve the fibrous linkages, the HPT process is recommended. The number of fiber cross-links per fiber length is the prominent factor that highly affects the tensile strength and Young's modulus of CA nanocomposite ENMs Liu & Tang (2007). The mechanical properties of polymeric membranes can significantly impact their performance and longevity. Membranes with poor mechanical properties are prone to fouling, degradation, and damage, leading to decreased efficiency and increased operational costs. Polymer nanocomposites have superior mechanical and physical properties over host polymers, due to the good affinity between the polymer and nanofiller and the high rigidity and high aspect ratio of nanofillers.

The microstructure, materials, mechanical properties, and nanofiller loading of cellulose-based nanocomposite membranes fabricated by different techniques are summarized in Table 2.1. These nanocomposite polymers exhibit enhanced mechanical properties (e.g., ultimate tensile strength, elongation at break, and Young's modulus) due to the reinforcing effects of CNC and CNF nanofillers. The CNC as a filler has been used for reinforcing CA Jiang *et al.* (2020); Sun *et al.* (2015), Poly(vinylidene fluoride) (PVDF) Wang *et al.* (2019b); Lalia *et al.* (2014), poly(lactic acid) (PLA) Gaitán & Gacitúa (2018), chitosan-poly(ethylene oxide) (CH-PEO) Wang *et al.* (2019a). CNC-reinforced CA nanocomposite ENMs in the loading range of 0 to 1 wt% showed the optimal UTS of 5.72 MPa and 16.7 MPa for 0.105 wt% CNC/CA ENM Jiang *et al.* (2020) and 0.5 wt% CNC/CA ENM Sun *et al.* (2015), respectively. CNF filler has been successfully used to

Table 2.1 Recent experimental studies on the mechanical properties and the microstructure of polymeric nanocomposite membranes

Material	Fabrication method	Cellulose function	Mechanical properties				Microstructure	Ref.
			NCs ¹ Conc. (wt%)	UTS (MPa)	Strain at break(%)	Modulus (GPa)		
CNC/CA	Electrospinning	filler/matrix	0.105	5.72	2.47	–		Jiang <i>et al.</i> (2020)
CNC/CA			0.5	16.7	1.24	1.68		Sun, Boluk & Ayranci (2015)
CNC/PVDF ²		filler	4	3.3	88.1	3e-3		Wang, Cheng, Wang, Ni & Han (2019b)
CNC/PVDF			2	17.2	–	0.105		Lalia, Guillen, Arafat & Hashaikeh (2014)
CNC/CH ³ -PEO ⁴			6	5.76	8	2.45		Wang <i>et al.</i> (2019a)
CMC ⁵ /PLA ⁶			1	3.75	20	–		Gaitán & Gacitúa (2018)
CNF/PLA	Extrusion		5	34.8	3	1.27		Ghasemi, Behrooz, Ghasemi, Yassar & Long (2018)
CNF/CA	TIPS	filler/matrix	5	65	–	2.5		Sharma, Mandal & Goswami (2021)
CNF/CA	NIPS		5	47.6	2.5	2.7		Cindradewi <i>et al.</i> (2021)

1 Nanocelluloses

2 Poly(vinylidene fluoride)

3 Chitosan

4 Poly (ethylene oxide)

5 Cellulosemicrocrystal

6 Poly(lactic acid)

reinforce PLA Ghasemi *et al.* (2018) and CA Sharma *et al.* (2021); Cindradewi *et al.* (2021). TIPS and NIPS techniques were used to synthesize CNF-reinforced CA nanocomposite flat sheet membranes. Among the samples shown in Table 2.1, the optimal mechanical properties were achieved for films with a CNF/CA concentration of 5 wt %. The SEM micrograph of this sample, however, indicates a dense bulk structure making them incomparable to fibrous ENMs. In spite of the higher tensile strength of membrane mats fabricated by phase inversion, fibrous-structured electrospun membranes are more advantageous in separation processes because of their higher specific surface area and superior selective permeation.

2.2 Life cycle assessment of nanocomposite fibrous membrane production processes

Although research on understanding the mechanism of membrane fabrication dates back to the 19th century Loeb & Sourirajan (1962); Strathmann, Kock, Amar & Baker (1975); Tucker, Stanger, Staiger, Razzaq & Hofman (2012), environmental concerns related to membrane fabrication have gained prominence in recent years, with research efforts primarily focused on discovering and substituting novel and environmentally friendly synthesis techniques Prézélus *et al.* (2021); Kim (2020). Numerous life cycle assessment (LCA) investigations have been conducted regarding different separation processes. The predominant focus in most of these studies revolves around the operational phase of the process, emphasizing chemical and energy demands, identified as the primary contributors to environmental impact. Nevertheless, these inquiries have often fallen short in adequately evaluating the environmental effects of membrane manufacturing and examining potential end-of-life disposal solutions for used membranes Coutinho de Paula & Amaral (2017); Banerjee (2023).

In recent years, the membrane community has gained a profound understanding of the principles and mechanisms underlying fabrication methods. With membrane technology expanding into diverse markets, researchers have shifted their focus to evaluating its growing environmental impact and overall sustainability, as highlighted in prior works Szekely, Jimenez-Solomon, Marchetti, Kim & Livingston (2014); Li, McGinnis, Wong & Renneckar (2013b). Sustaining the growth of the membrane industry requires a nuanced understanding of the environmental

footprint of each fabrication method, prompting informed choices favoring more sustainable and environmentally friendly membrane manufacturing processes. The concept of "sustainability" spans a broad and at times elusive spectrum, urging researchers to explore all conceivable avenues for enhancing the sustainability and eco-friendliness of membrane technology Cseri, Razali, Pogany & Szekely (2018). In this context, a fundamental question arises: "How can we precisely quantify the sustainability improvements in production processes?" The answer lies in Environmental Life Cycle Assessment (LCA), a methodology designed to comprehensively address this query. For a more robust evaluation of sustainability in membrane production, it becomes pivotal to quantitatively assess the impact of the entire process from multiple perspectives, including global warming, human carcinogenic toxicity, human non-carcinogenic toxicity, fossil resource scarcity, and marine ecotoxicity, utilizing the LCA approach.

LCA stands as a well-established environmental assessment tool, providing analytical insights into the cumulative environmental impacts associated with a product, process, or human activity across its entire life cycle. This life cycle spans from raw material extraction (cradle) through production, use, and eventual end-of-life disposal (grave) Curran (2013); Malara *et al.* (2021). A holistic LCA methodology proves beneficial across diverse domains, offering insights not only for methodological comparisons but also for formulating enhancement strategies, advancing product and process development, and assisting decision-makers in making well-informed choices Gu, Reiner, Bergman & Rudie (2015); Malara *et al.* (2021); Gallo Stampino *et al.* (2021). LCA facilitates the selection of the most environmentally friendly fabrication method through quantified indices (LCA scores) related to environmental impact. The LCA process encompasses four interrelated phases: (1) goal and scope definition to establish objectives and the functional unit, (2) system boundary delineation involving the quantification of material and energy flows in a life cycle inventory (LCI), (3) transformation of inventory data into comparable potential environmental impacts via life cycle impact assessment (LCIA) methodologies (e.g., ReCiPe endpoint, IPCC GWP100a), and (4) data analysis, review, the generation of meaningful insights, decision-making, recommendations, and the formulation of improvement strategies

aimed at minimizing the environmental footprint of products and processes Turk *et al.* (2020); Li, Hashaikeh & Arafat (2013a); Prézélus *et al.* (2021).

Although the membrane process is recognized as a developed environmentally friendly technology and is considered a key player in various industries, it is not widely known that the fabrication of the membrane itself generates a significant amount of waste. LCA of the production process of nanocomposite polymer membranes still represents a challenge and to the best of the authors' knowledge, few life cycle assessment studies have addressed the environmental aspects of the membrane fabrication process (summarized in table 2.2), and it is likely due to its complexity involving many different chemicals and polymers. Several LCA studies on polymer membranes are available in the literature, with many of them focused on membrane processes (i.e., filtration, desalination, water and wastewater treatment technologies) Hancock, Black & Cath (2012); Razali *et al.* (2015); Abdelrazeq, Khraisheh, Ashraf, Ebrahimi & Kunju (2021); Nakhate, Moradiya, Patil, Marathe & Yadav (2020); Coday, Miller-Robbie, Beaudry, Munakata-Marr & Cath (2015). Each study developed a life cycle inventory (LCI) to account for various reference flows such as construction materials, chemicals required for operation (primarily anti-scaling and disinfection chemicals), and materials used for membrane fabrication. A primary conclusion from these studies is that energy consumption during the operation phase of the plants is the single greatest contributor to its negative environmental impacts, accounting for greater than 85% of the environmental impacts.

A recent review study by Kim *et al.* in 2020 focused on the sustainability of membrane fabrication by immersion precipitation method. Based on the review paper, mass intensity (total mass of materials used to produce a specified mass of product) and huge amounts of solvent-contaminated wastewater are the main contributors to the negative environmental impact of the NIPS method Kim (2020). Prézélus *et al.* (2021) implemented a generic LCA approach to list material and energy flows as a function of operating conditions for UF HFMs prepared by the NIPS method. They assessed the contribution of material and energy to the environmental impacts of HFM fabrication. The results show that water consumption is the most important contributor to the negative environmental impacts of membrane fabrication via

Table 2.2 Recent LCA studies on the manufacturing process of polymeric membranes

Year	Membrane Type	Membrane Fabrication Method	FU ¹	LCA approach	LCIA methodology	Observations	Ref.
2021	Polymer	NIPS ²	1000 m ² of the HFM ³	Cradle-to-Gate	ReCipe-16(World-H)	The choice of solvent and polymer and the source of electricity were identified as the major determinants of environmental impact and cost.	Yadav <i>et al.</i> (2021)
2021	Polymer	NIPS	1 m ² of filtration surface of HFM	Cradle-to-Gate	ReCipe-16(Midpoints)	Solvent has been identified as major contributors to environmental impacts.	Prézélus <i>et al.</i> (2021)
2021	Polymer	Electrospinning	The storage capacity delivered by the fiber-based SIB anodes	Cradle-to-Gate	Eco-Indicator 99	Thermal treatment process contributes more to the environmental impact in the production phase.	Malara <i>et al.</i> (2021)
2018	Polymer	NIPS	1 kg of spun yarn	Cradle-to-Gate	ReCiPe endpoint	Reducing of the impact caused by the wet spinning process improved the production process.	Piccinno, Hirschier, Seeger & Som (2018)
2014	Polymer	NIPS	The supply of one cubic meter of drinking water	Cradle-to-Grave	CED-ReCipe	Electricity consumption contributes most significantly.	Manda, Worrell & Patel (2014)
2015	Polymer	Electrospinning	Production of 1 g spun yarn	Cradle-to-Gate	CED-ReCipe	Electricity consumption contributes most significantly.	Piccinno, Hirschier, Seeger & Som (2015)

1 Functional Unit

2 Nonsolvent Induced Phase Separation

3 Hollow-Fiber Membrane

the NIPS method. Based on the study of Manda *et al.* Manda *et al.* (2014), the use of electricity, CA production, and the use of the solvent NMP contribute significantly to most impact categories in CA membrane production by the NIPS method. From an environmental point of view, the more important and strict disadvantage of the NIPS method as a conventional method which is on the watch list of researchers and environmental agencies is the huge amount of solvent-contaminated wastewater. It has been estimated that more than 50 billion liters of wastewater are discharged from the membrane manufacturing industry every year Razali *et al.* (2015). According to a survey carried out by Razalie *et al.* in 2015 Razali *et al.* (2015), sadly, approximately 70 percent of membrane fabrication industries flushed contaminated wastewater down the sink. 31% of the companies directly drain down the sink without any treatment and 38% of them dilute

the contaminated wastewater with excess water to lower the solvent concentration below the threshold level (100 ppm) and then drain down the sink Mehrabani, Vatanpour & Koyuncu (2022). It is worth noting that the solvent concentration in membrane wastewater is relatively low and mild, and can easily be treated with an appropriate solution. Malara et al. Malara *et al.* (2021) provided an LCA of electrospun Fe_2O_3 -based fibers (composed of polyacrylonitrile (PAN), N,N-dimethylformamide (DMF) and iron(II) acetate ($FeAc_2$)) for battery applications. They demonstrated that heat treatment process shows the greater environmental impact in the production phase. Abbasi et al. Abbasi (2014) characterized the environmental impact of the electrospinning process to produce polymeric fibers at a larger scale. It has been shown that when this technique is used at the industrial scale, the consumption of electrical energy could possibly cause the largest environmental impact. Another study by Piccinno et al. Piccinno *et al.* (2015); Foroughi, Rezvani Ghomi, Morshedi Dehaghi, Borayek & Ramakrishna (2021) showed that mainly energy consumption of the electrospinning technique has a high impact on the environment.

The main objective of this study was to investigate the comparative environmental impacts of an established method and a novel technique for the synthesis of nanocomposite polymer membranes. A specific focus of this study was to explore if the electrospinning technique provides intrinsic benefits over the established phase inversion method when environmental impacts are considered. The scope of the study focused primarily on the optimized enhancement of mechanical properties of the cellulose acetate nanocomposite membrane and secondary on the evaluation of the environmental impacts of two scenarios of synthesized reinforced nanocomposite membrane samples by electrospinning and non-solvent induced phase separation methods. A key step to determining the most sustainable membrane production process and the environmental impact of the different approaches consists of their detailed Life Cycle Assessment (LCA), not only to compare the different methodologies but, also, to drive improvement actions Gallo Stampino *et al.* (2021).

CHAPTER 3

METHODOLOGY

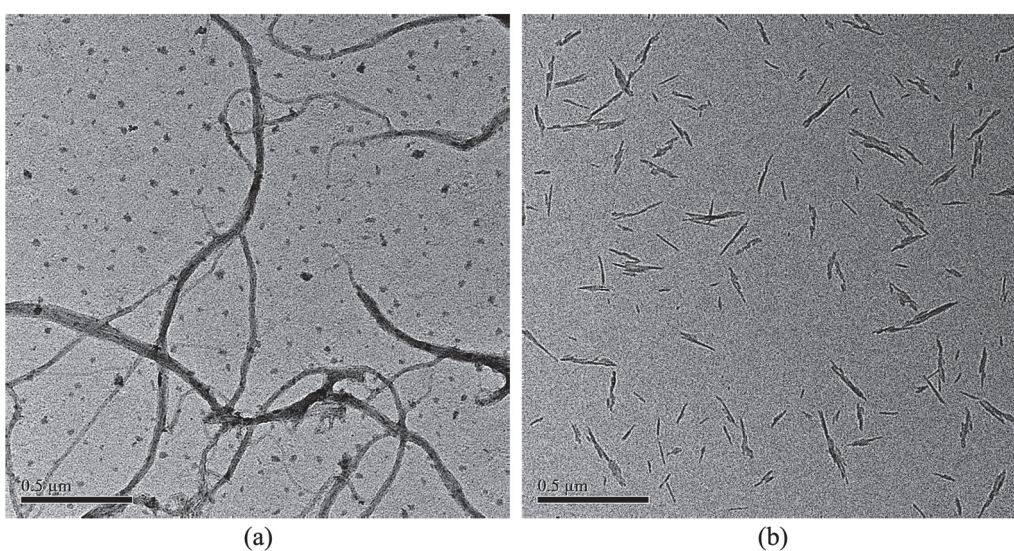
3.1 Materials

Cellulose Acetate (CA, $M_n=50000$, $\rho=1.3 \text{ g/mL}$, and average degree of substitution, $DS \approx 1.2$), received from Sigma-Aldrich Chemistry, was used as the matrix polymer. Freeze-dried powder 2,2,6,6-tetramethyl-1-piperidinyloxy (TEMPO)-oxidized cellulose nanofibrils (TOCNFs, 98 wt% dry powder) and freeze-dried powder cellulose nanocrystals (CNCs, 98 wt% dry powder), purchased from Cellulose LAB, Canada were used as nanofillers in the preparation of ENMs. Different volume ratios of N-dimethylformamide, DMF, and acetone, purchased from Fisher Chemical Co., were used as the solvent without further purification.

The characteristic properties of CNC and TOCNF and TEM images of these nanofillers provided by Cellulose LAB are presented in Table 3.1 and Figure 3.1, respectively. The degree of substitution (DS) which refers to the average amount of hydroxyl groups in repeating units that were substituted with carboxyl groups is determined by the ability to chemically modify the repeating unit and is given in the table. The amount of carboxyl groups is determined by conductimetric titration of CNF after TEMPO-mediated oxidation using the curve of conductivity versus amount (mL) of added sodium hydroxide Habibi, Chanzy & Vignon (2006). The content of sulfate groups, after hydrolysis, is determined by potentiometric titration. TEM images of TOCNF show a high degree of fibrillation, with diameters and lengths of a few micrometers. The TOCNF bundles form an entangled network. CNCs, on the other hand, have a cylindrical shape and are narrower (5-20 nm) and shorter (100-250 nm) because acid treatment dissolves the amorphous regions of the cellulose fibers, exposing the crystallites. Therefore, CNC has a lower aspect ratio than CNF.

Table 3.1 Properties of CNC and TOCNF nanofillers¹

CNC properties	Units	Value
Degree of Substitution	%	5
Degree of Surface Substitution	%	>15
Content of Sulfate groups	g/100g CNC	0.8
Fiber Dimensions		width 5-20 nm, length 100-250 nm
TOCNF properties	Units	Value
Content of Carboxyl groups	mmol/g	1-1.2
Fiber Dimensions		width 50 nm, length 0.5 – 80 μm

Figure 3.1 TEM images of a) TOCNF and b) CNC²

3.2 Membrane production and characterization methodology

3.2.1 Preparation of spinning polymer solutions

The polymer solutions for the optimization phase of research were prepared by dissolving a determined concentration of CA polymer (10, 15, and 20 wt%) in DMF:acetone mixture solvent (volume ratios of 1:0, 1:1, and 2:8) using a magnetic stirrer for 24 hours until a homogeneous solution obtained. The solution codes and their characterization are listed in table 3.2. The

¹ Source of the data: Cellulose LAB Company

² Source of the TEM images: Cellulose LAB Company

solutions were named xCAy/z where x, y, and z represented the amount of CA, and the volume fractions of DMF and acetone, respectively.

Table 3.2 The properties and the characterization of spinning solutions

Sample code	Solution Code	CA Conc. (wt%)	Solvent Comp. (v/v%)	Solution Characterization		Electrospinning Parameters			
				Viscosity (cp)	Conductivity (μS)	Voltage (v)	Flow Rate (ml/min)	TCD (mm)	Process Time(h)
ENM1	10CA1/0	10	1/0	1812	7.7	35	5	150	1
ENM2	10CA1/0								2
ENM3	10CA1/1		1/1	827.8	6.38				
ENM4	10CA1/1						2		
ENM5	10CA2/8		2/8	664	6.08		5		
ENM6	10CA2/8							100	
ENM7	15CA1/1	15	1/1	1370	6.72		2	150	
ENM8	15CA1/1					25		100	1
ENM9	15CA1/1					35			
Failed	15CA1/0		1/0	2025	8.1	NA	NA	NA	NA
Failed	15CA2/8		2/8	983	6.28				
Failed	20CA0/1	20	1/0	2761	8.5				
Failed	20CA1/1		1/1	1752	7.81				
Failed	20CA2/8		2/8	1017	6.84				

For the second phase of the project, nanocomposite NCs/CA spinning solutions were prepared as follows. The calculated amount of CA (optimized 15 wt%), 7.5 gr, was stirred in half the volume of solvent (optimized (1:1) volume ratio) for 24 h using a magnetic stirrer at 300 rpm at ambient temperature until the polymer was homogeneously dissolved. The different loadings of CNCs or TOCNFs, i.e., 0, 0.25, 0.5, 0.75, and 1 wt% were first homogeneously dispersed in the calculated volume of acetone by magnetic stirrer for 24 hours, followed by ultrasonication for 3 minutes. Then, a determined volume of DMF solvent was poured into NCs/acetone suspension and mixed for another 24 hours. NCs/acetone-DMF suspension was then added to CA/solvent and stirred at 60°C for an additional 12 hr followed by ultrasonication for 3 minutes until homogeneous dispersion of nanofiller was achieved. As outlined by Cindradewi et al. Cindradewi *et al.* (2021) and Cai et al. Cai, Li, Liu & Mai (2019), NCs in the loading range of 0 wt% to 1 wt% can be well-dispersed in the spinning solutions, especially at the lower loadings in accordance with the above-described methodology. Table 3.3 summarizes the detailed sample codes, the values of

CA concentration, Solvent composition, and nanofiller loading, and the implementation of the HPT process in the synthesis process. The samples were named xCNC/CA where x represented the amount of CNC or TOCNF in the nanocomposite ENMs.

Table 3.3 The composition and formulation of synthesized nanocomposite ENMs

Sample code	CA concentration (wt%)	Concentration	Solvent Comp. (DMF:acetone)	CNC Load-ing (wt%)	TOCNF Load-ing (wt%)	HPT Process
CA	15		(1:1)	0		×
CA-HPT				0		✓
0.25CNC/CA				0.25		×
0.25CNC/CA-HPT				0.25		✓
0.5CNC/CA				0.5		×
0.5CNC/CA-HPT				0.5		✓
0.75CNC/CA				0.75		×
0.75CNC/CA-HPT				0.75		✓
1CNC/CA				1		×
1CNC/CA-HPT				1		✓
0.25CNF/CA					0.25	×
0.25CNF/CA-HPT					0.25	✓
0.5CNF/CA					0.5	×
0.5CNF/CA-HPT					0.5	✓
0.75CNF/CA					0.75	×
0.75CNF/CA-HPT					0.75	✓
1CNF/CA					1	×
1CNF/CA-HPT					1	✓

3.2.2 Membrane synthesis by electrospinning process

Electrospinning (See Figure 3.2(a)) is a simple and adjustable method of producing various fiber assemblies by properly controlling polymer solution and electrospinning parameters. In this method, polymer solution is stretched using electrostatic forces to fabricate electrospun nanofibrous membranes (ENMs) by overcoming surface tension. In this technique, which is based on the electric field between polymer solution droplets in the needle existence and the collector, the conical-shaped droplets are stretched out and form nanofibers collecting on the collector Attari & Hausler (2020); Aruchamy *et al.* (2018); Pan *et al.* (2019). Its set-up consists of a 20 mL BD plastic syringe as the solution container which is connected to a nozzle with an inner diameter of 0.8 mm to form the fibers.

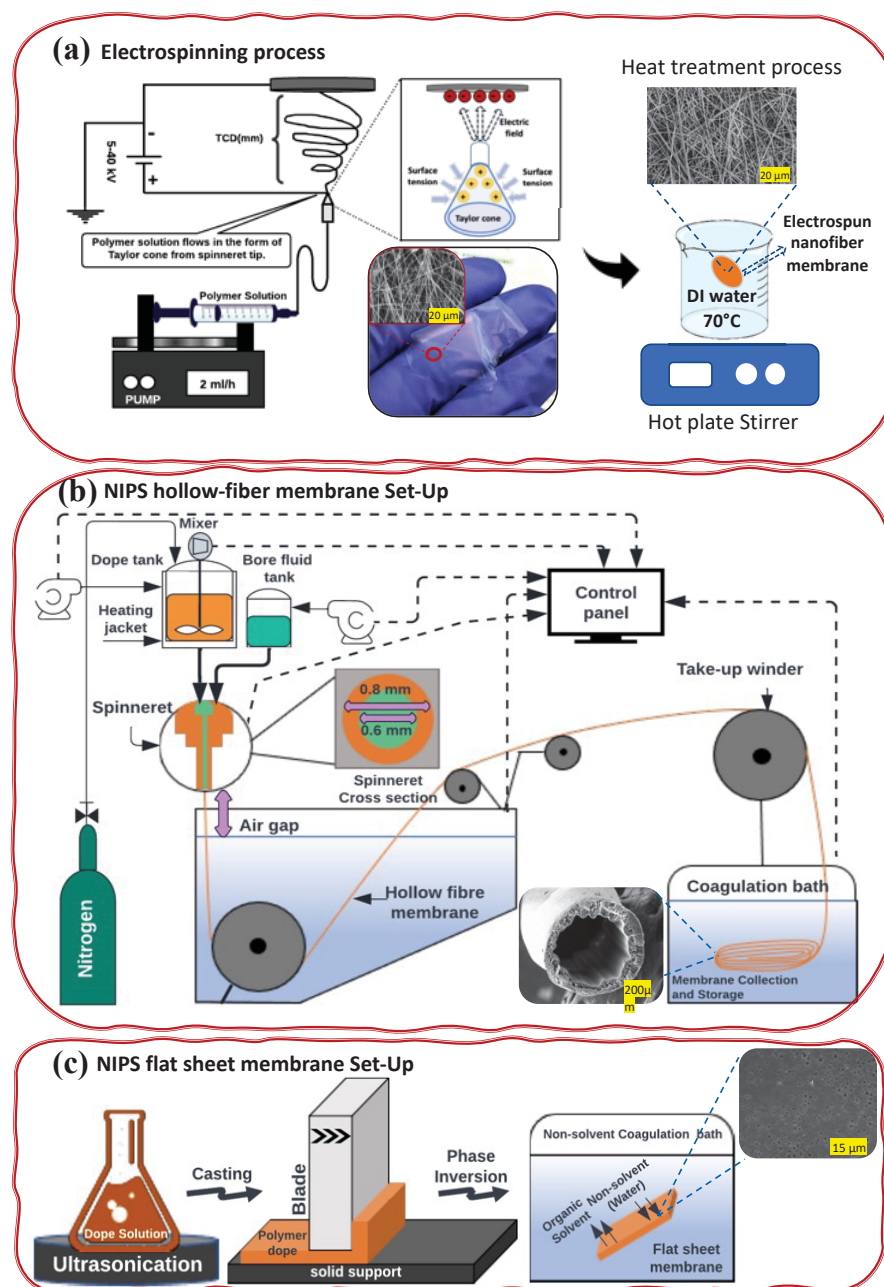


Figure 3.2 Various conventional and innovative methods for membrane fabrication in a glance: (A) Electrospinning process along with heat treatment, (B) Hollow-fiber fabrication by Non-solvent Induced Phase Separation (NIPS), (C) Flat sheet membrane fabrication by NIPS method

A pump controls the feed rate of the solution. The produced nanofiber samples are collected using a collector that is covered with aluminum foil to facilitate the peeling off the membrane from the collector. Furthermore, a power supplier (0-40 kV) is used to make the spinneret and the collector as two electrodes to provide electrostatic force to form the nanofibrous membrane samples. The electrospinning process was performed in a temperature range from 20 °C to 26 °C and humidity range from 30% to 51%.

3.2.3 Hollow-fiber and flat-sheet membrane preparation by NIPS method

Figures 3.2 (b) and (c) schematically illustrate the fabrication process of hollow-fiber and flat sheet membranes via NIPS method, respectively. In both NIPS systems, before the spinning, the spinning solution has to be degassed in order to prevent bubble building.

For synthesizing HFM, as shown in Figure 3.2 (b), the pressurized polymer solution along with the injection of bore fluid is extruded through a spinneret into a coagulation bath filled with a non-solvent (mostly water) kept at a constant temperature. In the coagulation bath with the occurrence of phase separation, the polymer-lean phase (solvent, additive, and bore liquid) is mixed with the non-solvent bath, and the polymer-rich phase forms the porous HFM. Then the synthesized HFM is directed into a rinsing bath to extract the residue solvent from its structure and finally, the membrane samples were dried overnight at ambient temperature. The principles of phase separation are the same for flat sheet or hollow-fiber membranes. As can be seen from Figure 3.2 (b) and (c), the only difference between the two NIPS methods is the casting method. In the case of flat sheet membrane fabrication, the polymer solution is cast by a blade in a determined thickness. As a consequence of solvent and non-solvent exchange in the coagulation bath, the porous flat sheet membrane results.

3.2.4 Exploring Material and Operating Parameters in Electrospinning

The polymer solutions of various CA concentrations, i.e., 10, 15, and 20 wt%, and different compositions of the solvent, i.e., (1:0), (1:1), and (2:8) were prepared. Their morphological

structure was studied to determine the optimized material and electrospinning process parameters. Furthermore, the efficient values for electrospinning process parameters, i.e., voltage, polymer solution feed rate, tip to collector distance (TCD), and process time were determined in regard to the morphological study of the synthesized ENM samples.

3.2.5 Heat post-treatment of CNC/CA, TOCNF/CA composite nanofibers

The loose and fluffy texture of the ENMs makes it difficult to handle them after the fabrication step. HPT process (See Figure 3.2(a)) was conducted to improve the coherence structure and mechanical resistance of the CNC/CA and TOCNF/CA ENMs. HPT process was carried out in a glass beaker that contained deionized (DI) water at 70°C which must be higher than the boiling point of the solvent mixture in order to complete evaporation of the solvent from the synthesized ENMs and lower than the glass transition temperature of the CA matrix polymer (110°C) to form good connectivity between the nanofibers right after electrospinning step for 2 h. The nanofibrous membranes were stored at ambient temperature for 24 h to be dried.

3.2.6 Solution characterization

The electrical conductivity of spinning solutions was measured using a conductivity meter (OAKLON pH/CON 510 Benchtop Meter). The conductivity electrode was entirely submerged in the solution, and at room temperature, the conductivity measurement was carried out after stabilizing the reader. The viscosity of spinning solutions was determined by a digital viscometer (Brookfield) in a 20 mL cylindrical sample container at a constant solution temperature of 25°C using an S-31 spindle. The rotation frequency of the S-31 spindle was 50 rpm, and the shear rate was 10.2 S⁻¹.

3.2.7 Membrane characterization

The morphological structure of CNC/CA and TOCNF/CA composite nanofibers was investigated by a Scanning Electron Microscope (SEM), Hitachi Model S3600-N. The SEM was performed

at 5 kV in three magnifications. The SEM samples were coated with gold using a sputter coater (Quorum Technologies - Model K550X) under 35 mA current for 2 minutes. The fiber distribution and mean fiber diameter size were measured using image processing software (ImageJ, 2.0.0-rc-43/1.50e) based on 40 fibers.

The porosity (ϵ) of CA ENMs was measured by the deviation of the inter-fiber volume and the total volume of the membrane. For porous hydrophilic ENMs, it could be determined by a gravimetric method using DI water. The weighted dry membrane samples were immersed in DI water overnight. The porosity was calculated by measuring the weight of water absorbed in the inter-fiber volume of the ENMs Attari, Yegani & Jafarzadeh (2017); Etemadi, Yegani & Babaeipour (2017):

$$\epsilon(\%) = \frac{\frac{(W_w - W_d)}{\rho_w}}{\frac{(W_w - W_d)}{\rho_w} + \frac{W_d}{\rho_p}} \times 100 \quad (3.1)$$

Where W_w is the weight of the wet sample (g), W_d is the dry sample weight (g), ρ_w and ρ_p are the density of the water and polymer at 25 °C, respectively ($\text{g}\cdot\text{cm}^{-3}$).

Mechanical properties of samples were measured on a Pneumatic tensile machine (Alliance RF/200(MTS)) at a loading speed of 2 mm/min equipped with a load cell of 100 N. All the ENM samples were measured 70 mm long by 10 mm wide. The upper and lower grips were clamped to the sample at 10 mm. An average value from three replicates was taken for all samples. The room temperature and relative humidity were controlled constant at 25 °C and 50%, respectively.

Fourier transform infrared (FTIR, Perkin Elmer) spectroscopic analysis of all samples was performed with a resolution of 2 cm^{-1} by averaging 64 scans in the range of 4000–400 cm^{-1} . FTIR of all nanofibrous membranes was taken under an attenuated total reflection (ATR) mode using the corresponding accessory.

3.3 Life Cycle Assessment methodology

In this section, the methodology of the comparative life cycle assessment of membrane fabrication by electrospinning and the conventional NIPS methods is presented. The electrospinning technique is previously described in subsection 3.2.2. Wet spinning (NIPS) method is covered in the following subsection to provide a comparison between the two membrane fabrication methods. The application of LCA provides a standardized method (ISO 14040, ISO 14044) for comparative investigation of the environmental impacts of the membrane fabrication process by electrospinning and NIPS methods. It quantifies all the relevant emissions and resources consumed, as well as the related environmental and health impacts and resource depletion issues that are associated with the considered nanocomposite 0.25TOCNF/CA membrane as the final product. An LCA study should include four key phases to evaluate environmental impacts: definition of the goal and scope, life cycle inventory analysis (LCI), environmental impact assessment (LCIA), and interpretation of results. The goal and scope, system boundaries, and LCI are discussed in this section, while the LCIA and interpretation are described in section 4.

3.3.1 Goal and scope definition

The goal of this study was the comparative assessment of the environmental impact of nanocomposite CNF/CA membrane production associated with two different methods, i.e., electrospinning and NIPS methods. The preparation of one batch of the membrane using 50 gr of 0.25 wt% CNF/15 wt% CA nanocomposite polymer solution by each fabrication method was taken as the functional unit (FU) of the analysis. All inputs (material requirements and energy consumption) and outputs (emissions) were evaluated on a per-FU basis. The material and energy requirements for the fabrication of one batch of nanocomposite CNF/CA membrane by Electrospinning and NIPS methods are shown in Table 3.4 and Table 3.5, respectively. Identifying the production process steps that contribute the most to the total environmental footprint of the product is another aim of this study. It might be helpful when upscaling from the laboratory to large-scale production while maintaining the smallest-possible environmental footprints.

Table 3.4 Per FU based material requirements and energy consumption for 0.25TOCNF/CA electrospun membrane fabrication by Electrospinning method

	Unit	Solution Preparation	Membrane Production	Production	Heat Treatment
Deionised Water	kg	0	0		3
Tap Water	kg	5	0		0
Cellulose acetate	kg	0.0075	0		0
TEMPO-CNF	kg	0.00013	0		0
Acetone	kg	0.21188	0		0
DMF	kg	0.02119	0		0
Electricity	kWh	4.5	4		10
Transportation	km*kg	138.9062	0		0

Table 3.5 Per FU based material requirements and energy consumption for 0.25TOCNF/CA hollow-fiber membrane fabrication by NIPS method

	Unit	Solution preparation	Membrane production	Membrane washing
Deionised Water	kg	0	50.02	0
Tap Water	kg	0	10	10
Cellulose acetate	kg	0.0075	0	0
TEMPO-CNF	kg	0.00013	0	0
Acetone	kg	0.24352	0	0
DMF	kg	0.05895	0	0
Electricity	kWh	14.5	63.46949	0
Transportation	km*kg	127.3662	51.5838	0

3.3.2 System boundary

The LCA study in this work is nanocomposite membrane production-focused which means it is a "cradle-to-gate" analysis. As shown in Figure 3.3, the system boundary includes the processes beginning with the extraction or production of raw materials and energy supplies and ending with the fabrication of the final product in the laboratory. All of the relevant raw materials, energy, utilities (e.g., electricity and water), chemicals, and emissions involved at each stage were considered to be within the system boundary. Environmental impacts due to the production of machinery and the equipment for nanocomposite membrane fabrication were not considered. The environmental impacts of emissions on water were considered.

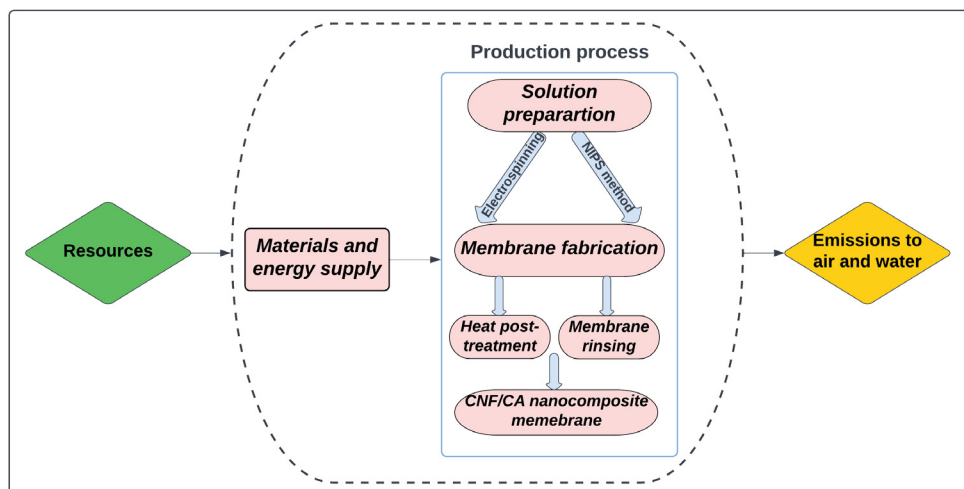


Figure 3.3 System boundary of electrospun nanocomposite membrane fabrication process

3.3.3 Life Cycle Inventory

All the data used in this LCA comes from the following four sources: Ecoinvent database (Version 3.7), original experimental data, literature, and estimations. Life Cycle Inventory data provided in Tables 3.7 and 3.6 were used per-FU basis.

The Ecoinvent database (Version 3.7) was used to evaluate the environmental impacts of the materials requirements and energy consumption in the fabrication process of 0.25TOCNF/CA nanocomposite membrane by two different methods (Table 3.6). The background upstream manufacturing data for electricity, transportation, water, and chemicals are provided using the inventory Ecoinvent database (Version 3.7).

Additionally, the synthesis process of CA and TOCNF, including materials and resources requirements and energy consumption data, was extracted from the literature Coletti, Valerio & Vismara (2013); Rodrigues Filho *et al.* (2008); Patiño-Masó *et al.* (2019); Saito, Kimura, Nishiyama & Isogai (2007); BERAICH, AROUCH, BAKASSE & Nasrellah and their environmental footprint was evaluated based on Ecoinvent database v3.7 (Table 3.7).

To produce cellulose acetate, the extracted cellulose fiber from wood pulp was stirred in a mixture of acetic acid, acetic anhydride, and sulphuric acid with determined portions at 50 °C for 2h until a homogeneous solution obtained. Following the cooling process at room temperature, the solution poured into 600 mL of a saturated sodium bicarbonate solution at 0 °C and stored at 4 °C overnight. The cellulose acetate that precipitated was subsequently filtered and rinsed with distilled water until it reached a neutral pH. Finally, the product was dried at 60 °C until it achieved a consistent mass BERAICH *et al.*; Coletti *et al.* (2013).

The initial step in TOCNF synthesis involves TEMPO-mediated oxidation. Kraft pulp is dispersed in deionized water using a pulper to achieve a predetermined concentration. Concurrently, in a container positioned beneath a mechanical stirrer, tetramethyl-piperidine-N-oxide (TEMPO) and KBr are dissolved in a small volume of deionized water. Once the paper pulp is homogeneously dispersed in water, the suspension is transferred to the container, and an appropriate amount of water is added. While continuously stirring the solution, a pH meter and two drip funnels are set up above the container. One funnel contains an aqueous solution of NaClO, and the other contains NaOH. Sodium hypochlorite (NaClO) is gradually added to the cellulose suspension, and the pH is monitored to maintain it within the range of 10.5-11 by adding sodium hydroxide (NaOH). The solution is left to stir overnight for 12-16 hours. Subsequently, the oxidized cellulose is acidified using concentrated hydrochloric acid (HCl) to aggregate the cellulose fibers, facilitating their separation from water. The oxidized cellulose is then filtered through a funnel with a tissue filter and washed with deionized water until it reaches a neutral pH. The refining and homogenization steps are performed using the same method as described above, resulting in a suspension of TEMPO-oxidized nanocellulose Patiño-Masó *et al.* (2019); Saito *et al.* (2007).

In the TOCNF production process, there are two key reactants that were not available in the existing Ecoinvent database. TEMPO was not included in the inventory because very limited information about its environmental impact is available. Moreover, NaBr is not available in any of the OpenLCA databases, and it was replaced with NaCl for impact estimation because the two chemicals share many similarities in the industrial manufacturing processes and environmental

Table 3.6 Per FU based life cycle inventory for the production of 0.25TOCNF/CA nanocomposite membrane by electrospinning and wet spinning methods

Inputs	Unit	Amount	Description	source
Electrospinning method				
Deionised Water	kg	3	Market for water, deionised Cutoff, U - RoW	Ecoinvent 3.7
Tap Water	kg	5	Market for tap water Cutoff, U - CA-QC	Ecoinvent 3.7
Cellulose acetate	kg	0.0075	Cellulose acetate production	Literature
TEMPO-CNF	kg	0.00013	TEMPO-Cellulose nanofiber production	Literature
Acetone	kg	0.212	Market for acetone, liquid Cutoff, U - RoW	Ecoinvent 3.7
DMF	kg	0.0212	Market for N,N-dimethylformamide Cutoff, U - GLO	Ecoinvent 3.7
Electricity	kWh	18.5	Market for electricity, medium voltage Cutoff, U-CA-QC	Ecoinvent 3.7
Transportation	km*kg	138.91	Market group for transport, Cutoff, U-GLO	Ecoinvent 3.7
Outputs				
Waste water	kg	8	Emission to water	
0.25CNF/CA ENM sample	number	1	Final product	
Inputs	Unit	Amount	Description	source
NIPS method				
Deionised Water	kg	50.02	Market for water, deionised Cutoff, U-RoW	Ecoinvent 3.7
Tap Water	kg	20	Market for tap water Cutoff, U-CA-QC	Ecoinvent 3.7
Cellulose acetate	kg	0.0075	Cellulose acetate production	Literature
TEMPO-CNF	kg	0.00013	TEMPO-Cellulose nanofiber production	Literature
Acetone	kg	0.244	Market for acetone, liquid Cutoff, U-RoW	Ecoinvent 3.7
DMF	kg	0.059	Market for N,N-dimethylformamide Cutoff, U-GLO	Ecoinvent 3.7
Electricity	kWh	77.97	Market for electricity, medium voltage Cutoff, U-CA-QC	Ecoinvent 3.7
Transportation	km*kg	178.95	Market group for transport, Cutoff, U-GLO	Ecoinvent 3.7
Outputs				
Waste water	kg	70.02	Emission to water	
0.25CNF/CA HFM sample	number	1	Final product	

outputs Li *et al.* (2013b). Furthermore, for some process data such as the volume of the utilized tap water in the washing process, we estimated the value from experience.

Table 3.7 Synthesis data inventory for the production of 1.14 gr CA and 10 gr TEMPO-CNF

Cellulose acetate			
Inputs	Unit	Amount	Description
Deionised Water	kg	6.22	Market for water, deionised Cutoff, U - RoW
Acetic acid	kg	0.063	Market for acetic acid, without water, in 98% solution state Cutoff, U - GLO
Cellulose fiber	kg	0.001	Market for cellulose fibre Cutoff, U - RoW
Acetic anhydride	kg	0.0043	Market for acetic anhydride Cutoff, U - GLO
Sodium bicarbonate	kg	1.32	Market for sodium bicarbonate Cutoff, U - GLO
Sulfuric acid	kg	0.0004	Market for sulfuric acid Cutoff, U - RoW
Electricity	kWh	4.7	Market for electricity, medium voltage Cutoff, U - CA-QC
Outputs	Unit	Amount	Description
Cellulose acetate	kg	0.00114	Final product
Waste water	kg	6.216	Emission to water
TEMPO-Oxidized CNF			
Inputs	Unit	Amount	Description
Deionised Water	kg	22	Market for water, deionised Cutoff, U - RoW
Ethanol	kg	504.96	Market for ethanol, without water, in 99.7% solution state, from ethylene Cutoff, U - RoW
Kraft paper	kg	0.040	Market for kraft paper kraft paper Cutoff, U - RoW
Piperidine	kg	0.24	Market for piperidine Cutoff, U - GLO
Sodium chloride	kg	0.0055	Market for sodium chloride, powder Cutoff, U - GLO
Sodium hydroxide	kg	0.43	market for sodium hydroxide, without water, in 50% solution state Cutoff, U - GLO
Electricity	kWh	331.216	Market for electricity, medium voltage Cutoff, U - CA-QC
Sodium hypochlorite	kg	0.097	market for sodium hypochlorite, without water, in 15% solution state Cutoff, U - RoW
Outputs	Unit	Amount	Description
Waste water	kg	22	Emission to water
TEMPO-CNF	kg	0.01	Final product

To conduct this analysis, we assumed that: 1) While membrane fabrication via NIPS method, Nitrogen pressure is constant at 1 bar in the entire spinning. 2) Wastewater treatment system was not considered in the analysis. 3) Emissions to air due to solvent volatility during the membrane synthesis process were not considered in the analysis.

3.3.4 Life Cycle Impact Assessment

LCA results depend critically on the utilized impact assessment method. These methods use different scientific models to translate the inventory amounts into environmental impacts using characterization factors. Several impact assessment methods were used in this analysis. Environmental impacts were assessed using the characterization factors specified for the IMPACT2002+ method, which is a more appropriate model among other non-North-American methods Jolliet *et al.* (2003); Toffoletto, Bulle, Godin, Reid & Deschênes (2007). The IMPACT2002+ method was developed by the US Environmental Protection Agency (EPA) and is based on North American data and environmental indicators. As a result, it is well-aligned with the environmental conditions, regulatory frameworks, and industrial practices prevalent in North America. The IMPACT2002+ method relies on extensive databases of emissions and environmental impacts specific to North America. This ensures that the assessment is based on up-to-date and regionally relevant data, enhancing the accuracy and reliability of the results for North American LCA studies. IMPACT2002+ was used to provide an endpoint damage assessment using the fifteen midpoint impact categories shown in Figure 3.4(a). The potential impact categories assessed are aquatic acidification potential (AAP; kg SO_2 eq.), aquatic ecotoxicity potential (AEP; kg TEG water), aquatic eutrophication potential (AEUP; kg PO_4 P-lim), global warming potential (GWP; kg CO_2 eq.), ionizing radiation potential (IRP; kBq C-14 eq.), mineral extraction potential (MEP; MJ surplus), human carcinogenic toxicity potential (HCTP; kg C_2H_3Cl eq), human non-carcinogenic toxicity potential (HNCTP; kg C_2H_3Cl eq), land use potential (LUP; $m^2_{org.arable}$), non-renewable energy potential (NREP; MJ primary), ozone layer depletion potential (OLDP; kg CFC-11 eq.), respiratory inorganics potential (RIP; kg $PM_{2.5}$ eq.), respiratory organics potential (ROP, kg C_2H_4 eq.), terrestrial acid/nutri potential (TANP; kg SO_2 eq.), terrestrial ecotoxicity potential (TEP; kg TEG soil). Midpoint impacts are weighted and grouped into four endpoint damage categories: human health (HH, DALY), ecosystem quality (EQ, $PDF.m^2.yr$), climate change (CC, kg CO_2), and resource depletion (RD, MJ).

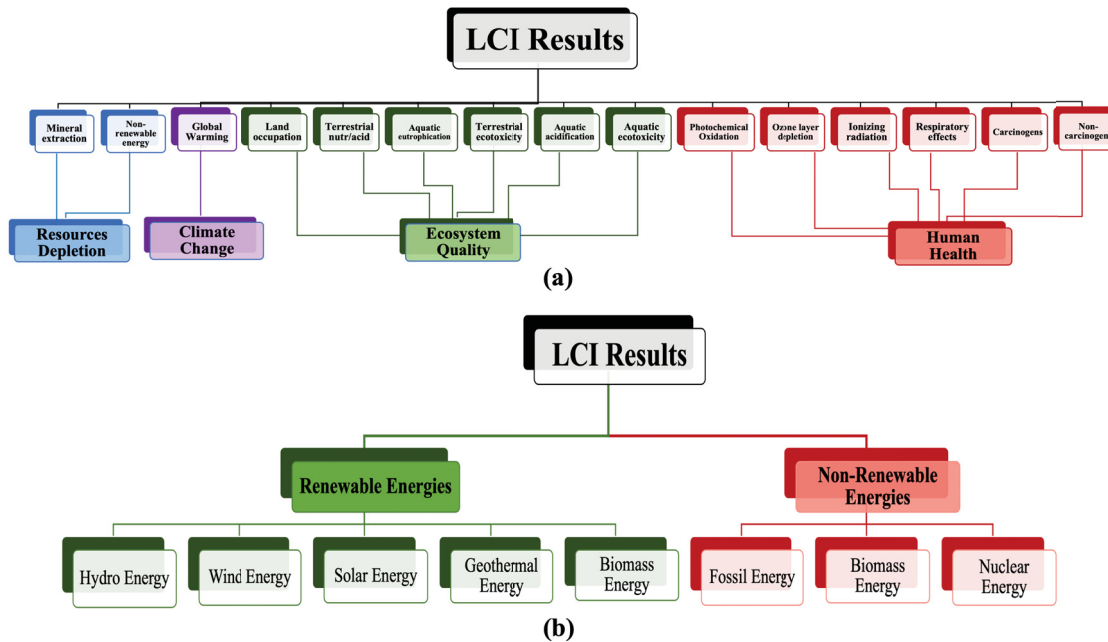


Figure 3.4 Overall scheme of a)IMPACT2002+ and b)CED impact assessment methods, an interconnection between LCI results and damage categories based on midpoint and energy categories

While energy is the most often quantified environmental impact, cumulative energy demand (CED; MJ) was used to analyze the overall energy consumption during the membrane production process and also to compare the energy use of two synthesis methods. The CED method is categorized into renewable (hydro, wind, solar, geothermal, and biomass) and non-renewable (fossil, biomass, and nuclear) energies (See Figure 3.4(b)).

3.3.5 Life Cycle Interpretation

Various sources contribute to both uncertainty and variability. Variability represents natural fluctuations in real-world conditions, while uncertainty primarily arises from imprecise measurements, data gaps, and model assumptions. LCA typically involves the use of extensive data, and

the uncertainty associated with these parameters can lead to uncertainties in the study's ultimate findings. Common sources of parameter uncertainty include empirical inaccuracies (resulting from imprecise measurements), unrepresentative data (incomplete or outdated measurements), and data gaps (where no measurements are available). We performed an uncertainty analysis on the model outputs, taking into account the variability in inventory data provided in Tables 3.7 and 3.6 for the production of a single batch of 0.25TOCNF/CA nanocomposite membrane. To evaluate the reliability of LCIA results in response to this variability, we conducted a Monte Carlo analysis with 1000 runs using OpenLCA software version 1.10.3. Our analysis assumed a uniform distribution at a confidence interval of 95% for electricity, transportation, water usage, and emissions into water data. The calculations included mean, maximum, minimum, standard deviation, and coefficient variation (CV) values as detailed in subsection 4.3.5.

CHAPTER 4

RESULTS

In this investigation, nanofibrous membranes based on cellulose were created using the electrospinning technique for water purification purposes. The first phase of the project focuses on optimizing the electrospinning process and material parameters, the outcomes of which are presented in section 4.1. Subsequently, during the second stage of the project, we investigated the mechanical improvement of the synthesized nanocomposite cellulose acetate membranes, exploring the influence of nanofiller loading and thermal treatment. The results of this phase are detailed in section 4.2. Following that, during the third stage of the project, we conducted a Life Cycle Assessment (LCA) to evaluate the environmental impacts of the electrospun membrane manufacturing process. Additionally, we conducted a comparative Life Cycle Assessment (LCA) between the electrospinning method and the conventional non-solvent induced phase separation (NIPS) method. The results of LCA are described in section 4.3.

4.1 Optimization of the Electrospinning Process

The optimization of the electrospinning process plays a pivotal role in enhancing the efficiency and quality of electrospun nanofibrous membranes (ENMs). This section delves into the intricate details of optimizing various parameters involved in the electrospinning process, a crucial step in tailoring the properties of ENMs for specific applications. By systematically adjusting factors such as polymer concentration, solvent composition, spinning solution flow rate, voltage field, tip-to-collector distance (TCD), and electrospinning processing time, we aim to achieve an ideal balance that ensures the formation of high-quality nanofibers. The discussion encompasses the impact of each parameter on the morphology, structure, and porosity of the resulting ENMs. Through this exploration, we aim to uncover optimal conditions that contribute to the production of electrospun nanofibrous membranes with desired characteristics, laying the foundation for their successful application in water purification processes.

4.1.1 Material and electrospinning process parameters

To explore the impact of material and electrospinning parameters on the morphology and nanostructure of Electrospun Nanocomposite Membranes (ENMs), nine distinct Cellulose Acetate (CA) membranes were produced in the laboratory using the electrospinning method. SEM, optical microscopy, and porosity measurements were employed to investigate the influence of polymer concentration, solvent composition, spinning solution flow rate, voltage field, tip-to-collector distance (TCD), and electrospinning processing time on the structure of the CA ENMs. Table 3.2 provides an overview of nine spinning solutions prepared with varying polymer concentrations and solvent compositions for CA ENM fabrication under different electrospinning conditions. Notably, an increased volume fraction of Dimethylformamide (DMF) in the solvent and higher CA concentration lead to elevated viscosity and conductivity. The results demonstrate a strong correlation between the viscosity and electrical conductivity of the spinning solutions with the fiber formation process. Fiber formation is significantly influenced by the interplay between solution viscosity and conductivity, emphasizing the importance of maintaining a balance between these parameters for successful fiber formation. Therefore, we closely monitored the values of these parameters for all solutions prepared in this study.

Table 3.2 details the synthesis of nine electrospun membrane samples, each produced using different spinning solutions and varied electrospinning process parameters. The success of fiber formation is closely tied to material parameters and solution characteristics, such as CA concentration, solvent mixture composition, solution viscosity, and solution conductivity. During the electrospinning process, fiber spinning for 15CA1/0, 15CA2/8, 20CA1/0, 20CA1/1, and 20CA2/8 solutions faced challenges due to various reasons. Morphological results indicated that increasing CA concentration from 10 wt% to 15 wt% led to a reduction in bead formation, attributed to heightened solution viscosity and surface tension. However, further elevating CA concentration to 20 wt% increased viscosity to a point where nanofiber formation became nearly impossible. The increased viscosity hindered fiber synthesis under constant electrospinning conditions. Additionally, the high volatility of acetone in the DMF/acetone solvent mixture (2/8) resulted in needle tip blocking. Moreover, the substantial surface tension of DMF led to

bead formation during the spinning process for 15CA1/0 and 20CA1/0. The optimization of electrospinning process conditions and material parameters was guided by the synthesis of the nine Electrospun Nanofibrous Membrane (ENM) samples, as outlined in Table 3.2.

4.1.2 Structural effects of material parameters

Figure 4.1 depicts SEM micrographs of the CA ENMs produced via electrospinning using polymeric solutions with two CA concentrations: 10 wt.% and 15 wt.%, in varying DMF:acetone solvent mixture compositions of 1:0, 1:1, and 2:8.

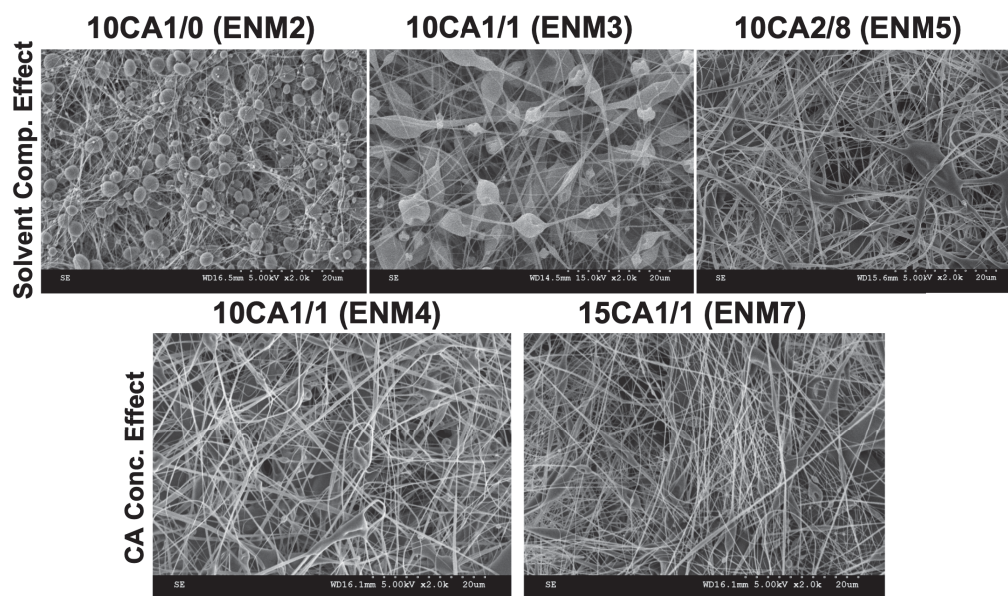


Figure 4.1 The morphological characterization of synthesized nanofibrous ENM samples to investigate the structural effects of material parameters

The top three images in Figure 4.1 illustrate a decline in bead formation and enhanced fiber formation with an increase in acetone volume fraction in the solvent mixture. Specifically, transitioning from pure DMF (1:0) to an equal volume mixture of DMF and acetone (1:1), and then to a mixture containing 20 V/V% DMF and 80 V/V% acetone (2:8) significantly improved fiber formation by reducing beads in the structure. Therefore, solution properties like CA concentration and solvent composition exert considerable influence on the electrospinning process. Optimizing these parameters becomes crucial for controlling nanofiber structure Lee

et al. (2018); Liu & Tang (2007); Phan *et al.* (2018). The significance of solvent parameters such as conductivity, solubility parameter, shear viscosity, surface tension, and concentration on ENM structure cannot be understated Lee *et al.* (2018); Han, Youk, Min, Kang & Park (2008); Uyar & Besenbacher (2008). The SEM micrograph in Figure 4.1 for 10CA1/0 (ENM2) highlights the inability to form a nanofibrous-structured membrane at low polymer concentration and acetone composition due to low viscosity and surface tension. Additionally, the comparison among SEM images of ENM2, ENM3, and ENM5 illustrates the interaction between polymer concentration and solvent composition, indicating that decreasing DMF volume ratio in the solvent enhances nanofiber formation by reducing surface tension at constant polymer concentration. In Figures 4.1- 10CA1/1 (ENM4) and 15CA1/1 (ENM7), a substantial increase in nanofiber formation is evident with an increase in polymer concentration. Notably, elevating the polymer concentration from 10 wt.% to 15 wt.%, dissolved in a solvent with 50 V/V% DMF, demonstrates the dominance of polymer concentration over the high DMF volume fraction in the solvent. This dominance leads to the formation of a smooth and bead-free nanofibrous structure.

4.1.3 Structural effects of electrospinning parameters

The morphological effects of electrospinning parameters, such as the applied voltage field, feed flow rate, processing time, and tip-to-collector distance (TCD), were examined based on SEM micrographs of eight ENM samples presented in Figure 4.2. The influence of processing time on ENM structure is evident in Figure 4.2- ENM1 and ENM2, where increased processing time in ENM2 resulted in higher bead density per surface unit. Moreover, a reduction in polymer solution flow rate from 5 ml/h to 2 ml/h, as depicted in Figure 4.2-ENM3 and ENM4, led to the formation of thinner fibers and decreased accumulation of polymer solution and beads in the electrospun membrane mat. Samples in Figure 4.2- ENM5 and ENM6, fabricated with different TCDs of 150 mm and 100 mm, respectively, demonstrated variations in fiber size due to TCD's impact on electrostatic force strength and residual solvent evaporation rate, resulting in thinner fibers in ENM5 Matabola & Moutloali (2013). Additionally, an increase in voltage field from 25 kV to 35 kV in Figure 4.2- ENM8 and ENM9 produced thinner fibers and reduced

polymer accumulation and bead formation, attributed to heightened electrostatic force between the electrodes, elongating the fibers into thinner sizes Sill & Von Recum (2008). These findings align with the morphological effects of spinning solution electrical conductivity, outlined in Table 3.2. Elevated electrical conductivity prompts increased charge repulsion and elongation during electrospinning, leading to thinner fibers in the same processing conditions Tijing, Woo, Yao, Ren & Shon (2017).

4.1.4 The effects of material and electrospinning parameters on the porosity of ENM samples

Porosity (ϵ) is a crucial parameter influencing the efficiency of electrospun nanofibrous membranes in separation processes. The interconnected porosity and pore size of nanofibers play a pivotal role in selective water filtration. This section delves into the examination of the impact of material and electrospinning parameters on the porosity of the electrospun nanofibrous membranes (ENMs). The outcomes of the porosity measurement analysis are succinctly presented in Figures 4.3, 4.4, and 4.5.

The observed trend in Figure 4.3 reveals that the porosity of ENM2, ENM3, and ENM5 increases from 58% to 75%, and then to 81% as the DMF volume ratio decreases from 100 v/v% to 50 v/v%, and finally to 20 v/v%, respectively. As discussed in subsection 4.1.2, the reduction in the volume fraction of DMF suppresses bead formation, consequently leading to an increase in porosity in the CA ENMs. In Figure 4.4, the impact of CA concentration on the porosity of ENMs is illustrated. The elevation of CA concentration from 10 wt% to 15 wt% results in a notable increase in porosity from 82% to 97%. Since bead formation in the membrane structure can cause pore blockage, the suppression of bead formation with the increase in CA concentration in the spinning solution contributes to the enhanced porosity of the ENM7 sample compared to the ENM4 sample.

Figure 4.5 presents the porosity levels of eight CA ENM samples, aiming to explore the influence of electrospinning parameters on ENM porosity. The figure illustrates that the enhanced porosity observed with an increase in electrospinning process time from 1h to 2h, as seen in ENM1 and

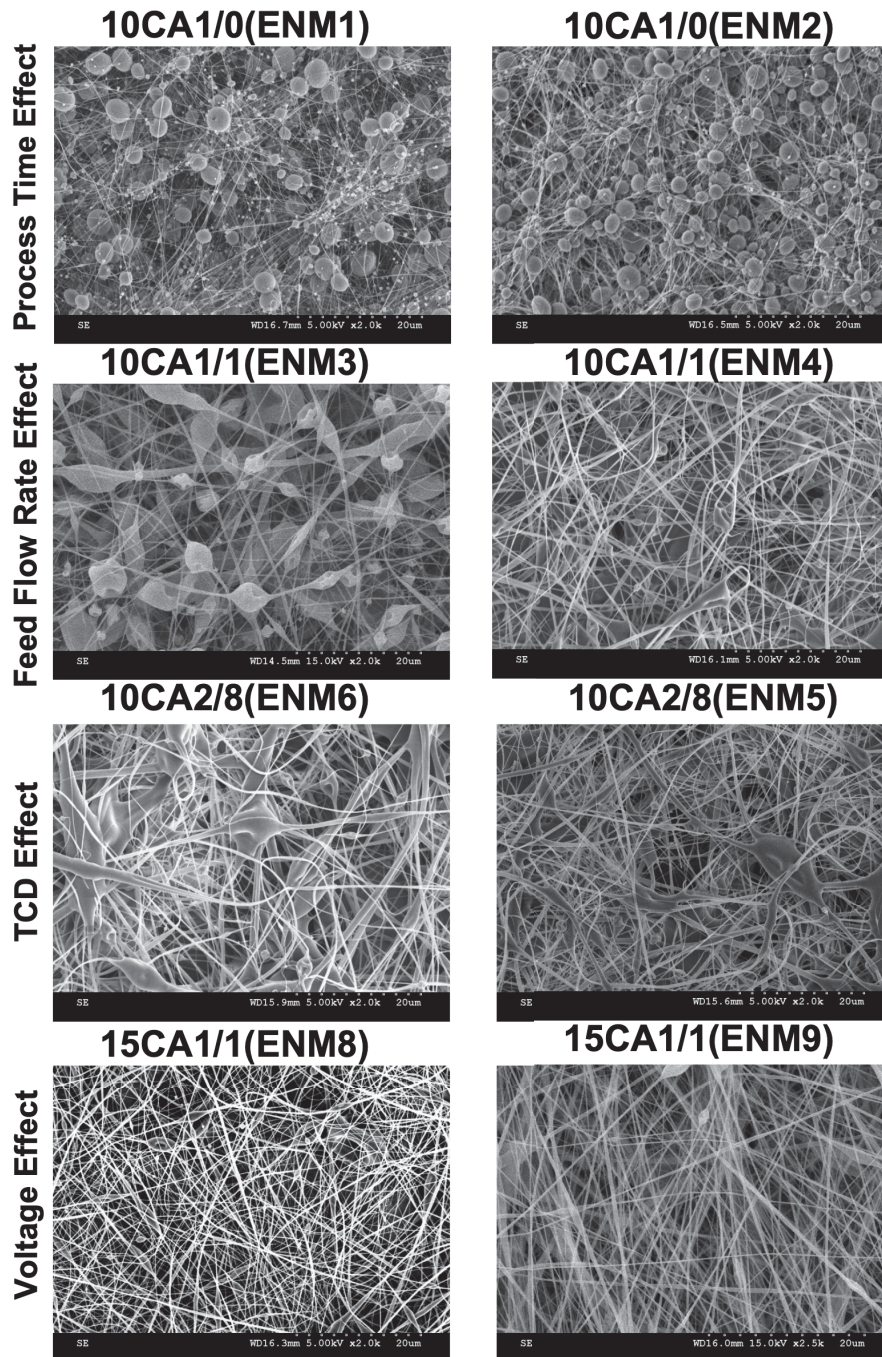


Figure 4.2 The morphological characterization of synthesized nanofibrous ENM samples to investigate the structural effects of electrospinning process parameters

ENM2 samples, is attributed to the augmented fiber formation, corroborated by the porosity test. Furthermore, the reduction in feed flow rate from 5 ml/h to 2 ml/h in ENM3 and ENM4 samples,

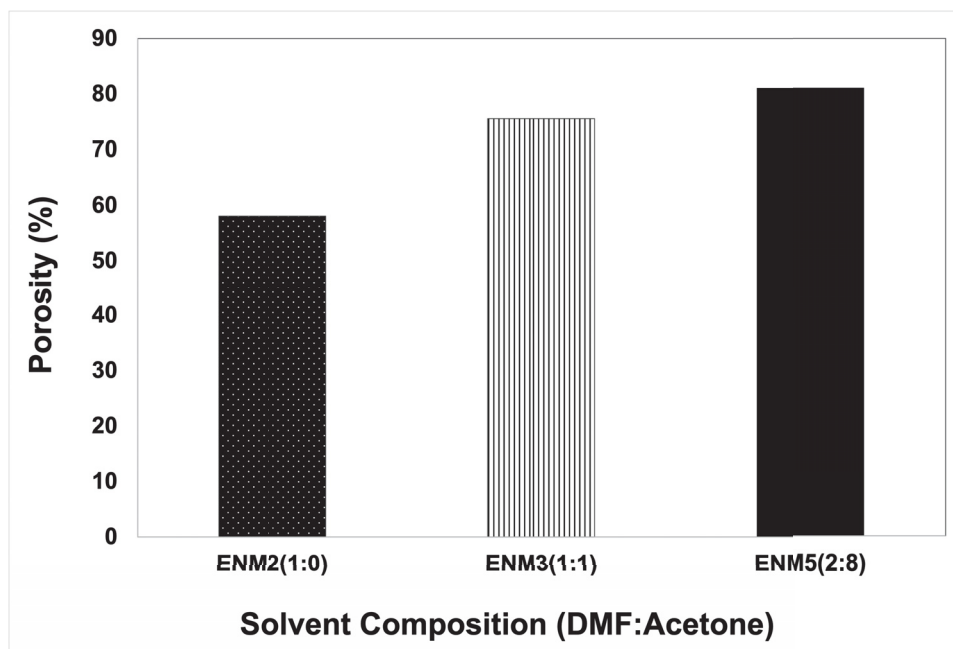


Figure 4.3 The effect of different compositions of DMF/acetone solvent mixtures on porosity(ϵ) of the synthesized ENM samples with the same CA concentration of 10 wt.% at constant electrospinning conditions

leading to a higher fiber formation rate and reduced accumulation of beads in the membrane structure, resulted in increased porosity. As detailed in subsection 4.1.3, the decrease in the distance between the spinneret tip and the collector from 150mm to 100mm in ENM5 and ENM6 samples caused more beads and polymer accumulation in the membrane structure, leading to a decline in porosity. Additionally, elevating the applied voltage field from 25 kV to 35 kV in ENM8 and ENM9 samples suppressed bead formation, consequently increasing porosity.

4.1.5 Conclusion

In summary, achieving the ideal balance between material selection and electrospinning process parameters involves a nuanced and multifaceted approach. Various considerations, including the physical attributes of prepared solutions, electrospinning parameters, and environmental conditions, must be taken into account. Through meticulous experimentation and thorough analysis, ideal material parameters—specifically, cellulose acetate (CA) concentration and

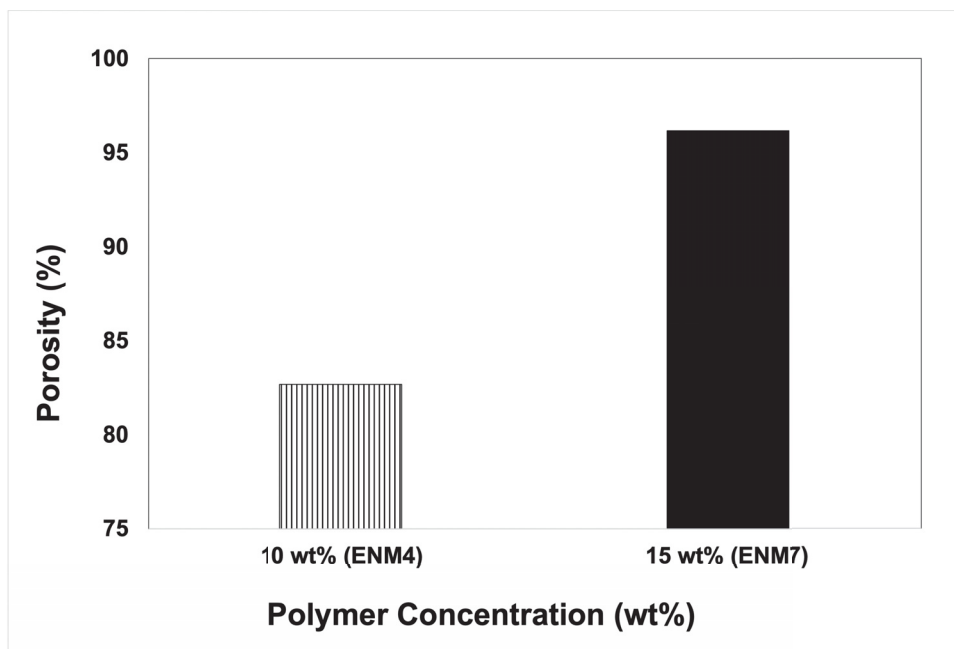


Figure 4.4 The effect of CA concentration on porosity(ϵ) of the synthesized ENM samples with the same solvent composition of (1:1) at constant electrospinning conditions

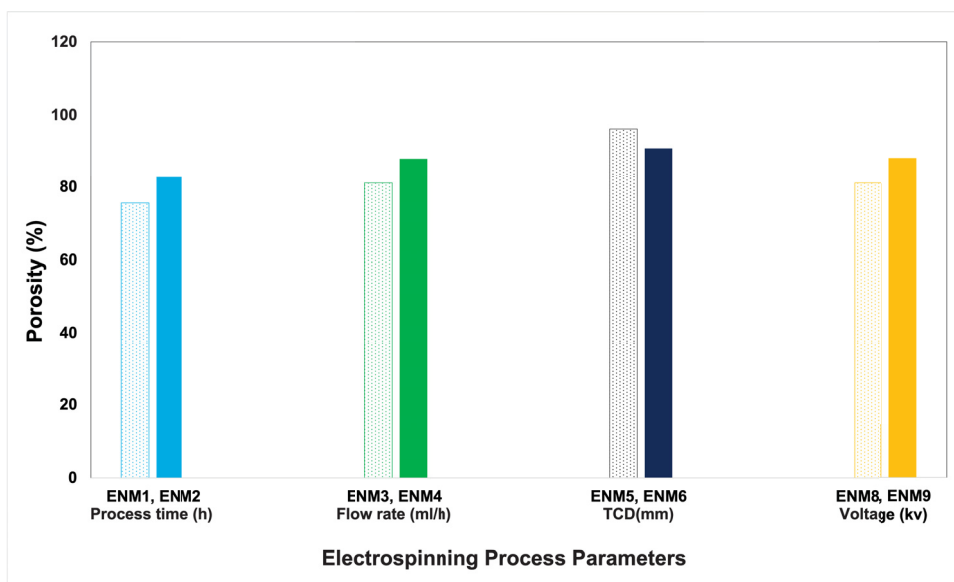


Figure 4.5 The effect of various electrospinning parameters on porosity(ϵ) of the synthesized ENM samples at constant CA concentration and solvent mixture composition

solvent mixture composition—and electrospinning process parameters—such as voltage, feed flow rate, tip-to-collector distance (TCD), and processing time—can be discerned. These best parameters contribute to the production of high-quality nanofibers with desired characteristics. Morphological assessments identified the ideal polymer solution as having a 15 wt% CA concentration and an equal 50 v/v% composition of dimethylformamide (DMF) and acetone (1:1) as the solvent mixture. Additionally, electrospinning process parameters were maintained at efficient values, including a constant voltage of 25 kV, feed flow rate of 2 ml/h, TCD of 100 mm, and processing time of 2 hours, as determined through morphological studies. The subsequent section will delve into the discussion of the reinforcing effects of cellulose nanofillers and heat post-treatment on these optimized CA electrospun nanofibrous membranes (ENMs).

4.2 Mechanical reinforcement of cellulose acetate nanofibrous membranes

This section aims to explore the enhancement of mechanical properties in cellulose-based electrospun nanofibrous membranes (ENMs) achieved through the incorporation of nanofillers and subsequent heat post-treatment. Solutions containing cellulose acetate (CA) as the matrix polymer at a concentration of 15 wt%, along with four different loadings of cellulose nanocrystals (CNC) or cellulose nanofibers (TOCNF) (i.e., 0.25, 0.5, 0.75, and 1 wt%), were electrospun using a 1:1 volume ratio of dimethylformamide (DMF) and acetone mixture as the solvent, under constant electrospinning conditions determined to be optimal. The ensuing sections delve into the influence of the heat post-treatment (HPT) process and provide a comparative analysis of the effects of CNC and TOCNF reinforcing agents on the bead-free morphological structure, subsequently impacting the mechanical properties of the CA nanocomposite samples.

4.2.1 Nanocomposite spinning solution characterization

In the context of nanofiber morphology, various solution parameters, particularly viscosity and conductivity, play a pivotal role. Figures 4.6(a) and (b) present bar graphs depicting the impact of nanofiller loading on the conductivity and viscosity of composite spinning solutions.

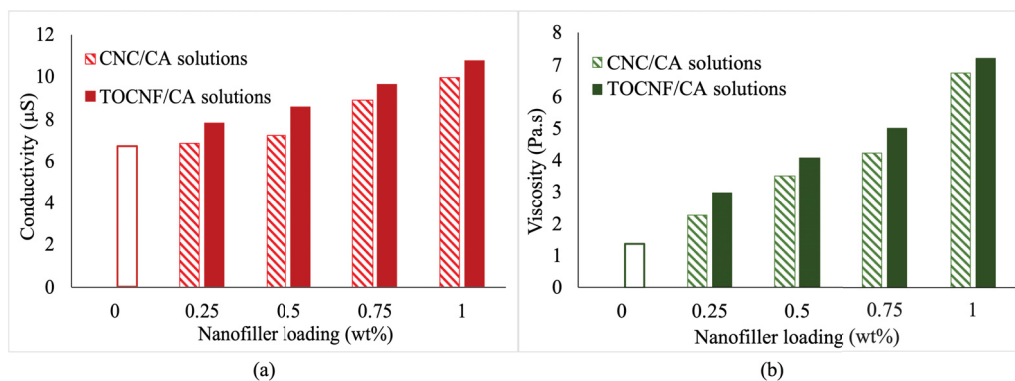


Figure 4.6 The impact of CNC/TOCNF loading on a) conductivity and b) viscosity of the spinning solutions

Notably, at equivalent nanofiller loading, TOCNF/CA solutions exhibit higher viscosity and conductivity compared to CNC/CA solutions. The fibrous nature of TOCNFs influences the entanglement of cellulose acetate (CA), resulting in increased viscosity. TEMPO-mediated oxidation of cellulose nanofibers (CNF) introduces stable charged carboxyl groups, enhancing the anionic character of TOCNFs (refer to Table 3.1). Consequently, the heightened conductivity in TOCNF/CA solutions can be attributed to stronger ionic interactions between negatively charged TOCNFs and positively charged CA chains Campano *et al.* (2018); Habibi *et al.* (2006). Examination of the red and green unfilled as well as hatched bar graphs in Figures 4.6(a) and (b), corresponding to data on pure CA and CNC/CA spinning solutions, reveals an increase in conductivity and viscosity for CNC/CA spinning solutions as CNC loading rises from 0 wt% to 1 wt%. This trend is similarly observed in the red and green unfilled and solid bar graphs representing TOCNF/CA spinning solutions.

4.2.2 Structural effects: HPT process

Figures 4.7 (a) and (b) display the SEM micrographs of pristine CA ENMs in their as-synthesized state and post-heat post-treatment (HPT). These visual representations serve as concrete evidence indicating an overall increase in fiber diameter after the HPT process. The subplots positioned

in the bottom corner of each micrograph depict the size distribution of fibers, showcasing a distribution pattern akin to a normal curve.

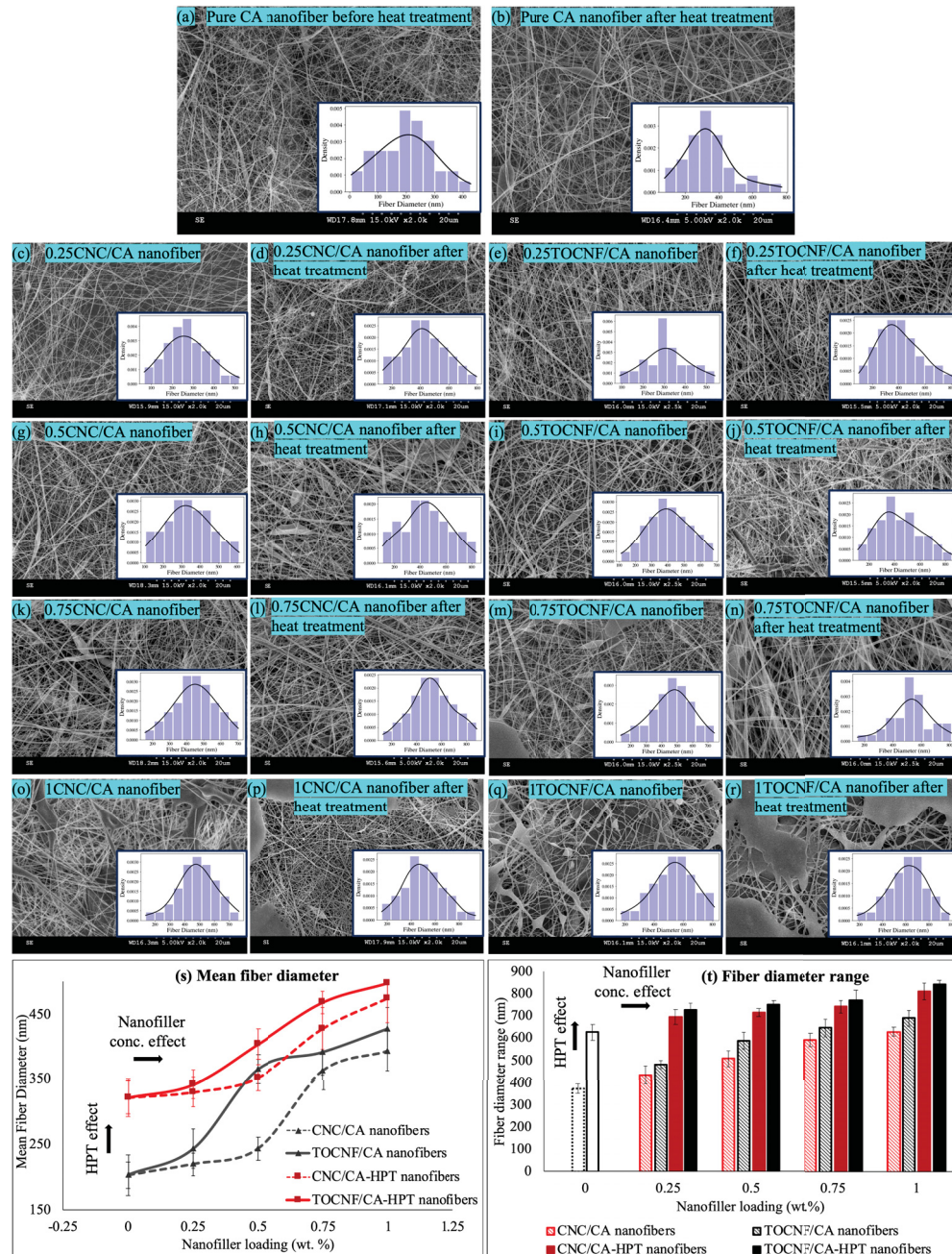


Figure 4.7 SEM images, fiber diameter distribution and range for pristine CA nanofibers and CNC/CA and TOCNF/CA ENMs as-spun and after HPT process (a)Pristine CA nanofibers as-synthesized (b)Pristine CA nanofibers after HPT (c) to (r) CNC/CA and TOCNF/CA composite nanofibers as-spun and after HPT process (s) Mean fiber diameter vs. nanofiller loading (t)Fiber diameter range vs. nanofiller loading

The image analysis yielded the mean and range of fiber diameters, as presented in Figure 4.7(s) and Figure 4.7(t), respectively, providing further insights into the morphological impact of nanofiller loading and the HPT process. For pure CA nanofibers, the mean diameter increased from 203 nm to 322 nm after HPT, and the fiber distribution widened, expanding the diameter range from 372 nm to 626 nm.

In addition to pure CA ENMs, Figures 4.7 (c) to (r) showcase micrographs of nanocomposite CNC/CA and TOCNF/CA ENMs before and after HPT, demonstrating variations in fiber diameter with different reinforcing agent loadings. Initial visual inspection indicates an increase in fiber diameter post-HPT, attributed to the physical connection of fibers and a mild melting on the surface, as reported in You, Lee, Lee & Park (2006).

Utilizing image analysis, the mean fiber diameter and fiber diameter range of the ENM samples were acquired and are depicted in Figures 4.7 (s) and (t). These graphs visually capture the structural impact of the HPT process. In Figure 4.7 (s), the comparison between dashed and solid red lines and also comparing the solid and dashed black lines together highlights the enhancing effect of HPT on increasing the fiber diameter for both CNC/CA and TOCNF/CA ENMs. A parallel trend is observed in Figure 4.7 (t), indicating a noticeable rise in the fiber diameter range with the implementation of HPT for both types of composite samples.

4.2.3 Structural effects: nanofiller loading

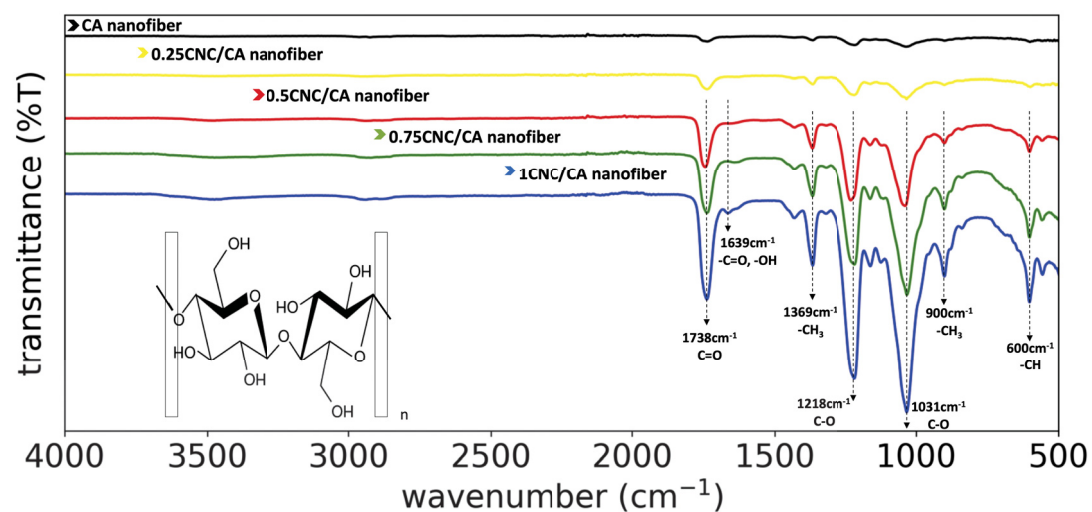
The SEM micrographs and corresponding fiber diameter distribution graphs of CNC/CA and TOCNF/CA ENMs with varying loadings from 0 wt% to 1 wt% are illustrated in Figures 4.7 (a) to (r). Visual inspection indicates that as the nanofiller loading increases from 0 wt% to 1 wt%, thicker fibers with a broader diameter range are obtained, as seen from the upper to the lower graphs. Furthermore, the fiber distribution curve tends to shift towards larger diameters, signifying an increase in the density of thicker fibers with higher nanofiller loading in the spinning solution.

As depicted in the summarized image analysis results in Figure 4.7 (s), the red dashed line graph illustrates that with an increase in CNC loading from 0 wt% to 1 wt%, the mean fiber diameter of CNC/CA nanocomposite ENMs rises from 203 nm to 404 nm. The black dashed line graph in Figure 4.7 (s) depicts changes in mean fiber diameter concerning loading for TOCNF/CA nanocomposite ENMs. With the addition of 1 wt% TOCNF to the spinning solution, the mean fiber diameter of the pristine CA ENM sample increases from 203 nm to 447 nm. The slope of both dashed red and black graphs, representing the variation rate of mean fiber diameter concerning nanofiller loading, increases after 0.5 wt% CNC and 0.25 wt% TOCNF. At the same nanofiller loading, the fibrous structure of TOCNF results in higher viscosity in the spinning solution, leading to a thicker and broader fiber diameter distribution in TOCNF/CA membranes compared to CNC/CA samples. The addition of reinforcing agents further increases the viscosity of the polymer solution. With higher viscosity, the polymer spinning solution is more resistant to stretching from the electric field force, resulting in thicker fibers Jiang *et al.* (2020). In Figure 4.7 (t), based on solid bar charts, in addition to the incremental effect of HPT, the increase in nanofiller loading from 0 wt% to 1 wt% has enhanced the fiber diameter range from 626 nm to 810 nm and from 626 nm to 841 nm for CNC/CA and TOCNF/CA composite ENMs, respectively.

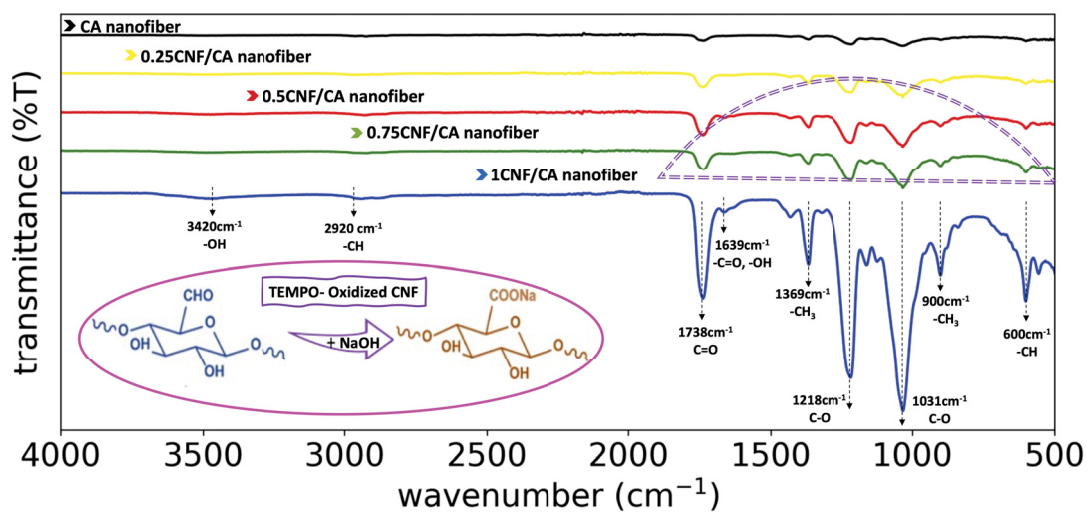
4.2.4 FTIR spectroscopy

FTIR spectroscopy was employed to explore the chemical interactions between the reinforcing agents and CA in the membrane samples. The FTIR spectra of CNC/CA and TOCNF/CA samples, featuring different loadings of the nanofillers, are presented in Figures 4.8 (a) and (b), respectively. The chemical structure of cellulose nanocrystals and TEMPO-oxidized cellulose nanofibrils is illustrated in the left corner of Figures 4.8 (a) and (b), respectively.

The dominant spectral bands within the wavenumber range of 500-4000 cm^{-1} are associated with the stretching vibrations of C-O and -C=O carboxyl groups originating from residual acetate groups in the CA matrix, notably at 1031 cm^{-1} , 1218 cm^{-1} , and 1738 cm^{-1} . In Figure 4.8 (a), the addition of CNCs to the fibers significantly enhances the relative intensity of peaks related to



a)



b)

Figure 4.8 FTIR spectra of ENMs (a) CNC/CA composite ENMs (b) TOCNF/CA composite ENMs as-spun

cellulose, particularly the most intense absorption band at 1031 cm^{-1} . Bands near 900 cm^{-1} and 1369 cm^{-1} correspond to the C-H bending vibration of the $-\text{CH}_3$ group, while the peak around 600 cm^{-1} represents the bending vibration of $-\text{CH}$. The presence of a band at 1639 cm^{-1}

indicates -OH bending, suggesting water in the nanofiber structure. Higher nanofiller loading increases the peak area, reflecting more -OH vibrations from water adsorption. Figures 4.8 (a) and (b) show that increasing CNC loading strengthens absorption peaks gradually. In contrast, for TOCNFs, absorption peaks slightly increase as nanofiller loading rises to 0.75 wt%, with further increases to 1 wt% resulting in stronger absorption peaks. This difficulty in distribution and dispersion of fibrous CNFs in the polymer matrix, compared to CNCs, is the cause. The FTIR spectra of 1TOCNF/CA composite ENM exhibit small peaks at 2920 cm^{-1} (-CH stretching vibrations from alkyl groups) and 3420 cm^{-1} (free -OH stretching vibrations of -OH groups), indicating H-bonding between the TOCNF molecule and adsorbed water.

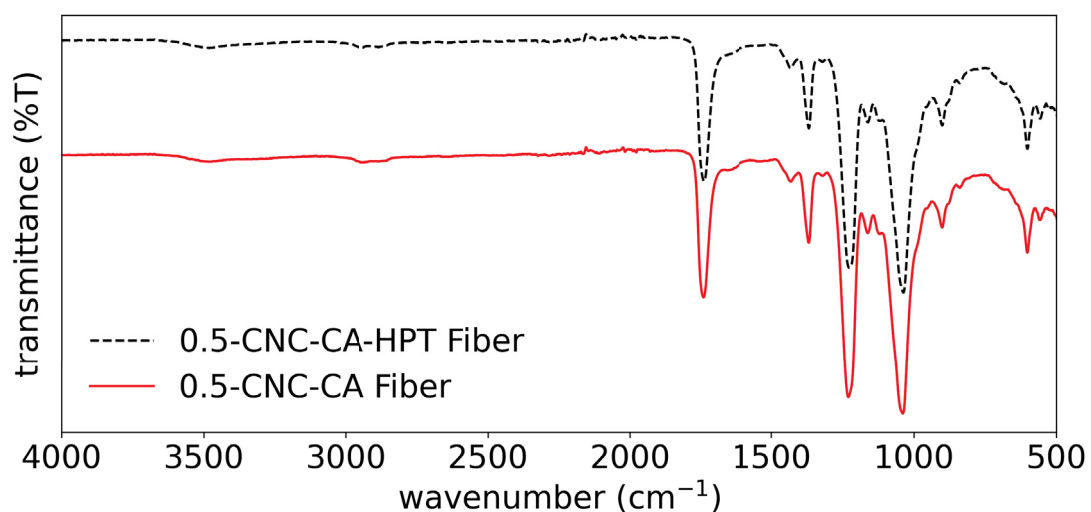


Figure 4.9 FTIR spectra of 0.5CNC/CA electrospun nanofibrous membrane samples as-spun and after HPT process

The FTIR spectra presented in Figure 4.9 depict the spectra obtained from the 0.5CNC/CA ENM samples before and after the HPT process. The overlapping peaks indicate that the HPT process does not induce any alterations in the composition of the membrane samples.

4.2.5 Mechanical properties

The mechanical characteristics of nanocomposite membrane samples were scrutinized to assess the reinforcing effects of nanocellulose fillers and the HPT process. Figures 4.10 (a) and (b) depict stress-strain curves for CNC/CA and TOCNF/CA nanocomposite ENMs with varying loadings of reinforcing agents in their as-spun and post-HPT states. Tables 4.1 and 4.2 provide a summary of key mechanical properties, including mean fiber diameter, fiber diameter range, ultimate tensile strength (UTS), elongation at the breakpoint, and Young's modulus. In Figures 4.10 (a) and (b), solid and dashed lines represent tensile curves for ENM samples before and after the HPT process, respectively. Initial stages of straining the as-synthesized samples (solid lines) exhibit notable resistance to deformation at the onset of the tensile test. According to Tables 4.1 and 4.2, increasing the content of CNC and TOCNF nanofillers results in a peak Young's modulus of 4.2 GPa and 5.3 GPa for as-spun 0.5CNC/CA and 0.25TOCNF/CA ENMs, respectively. This heightened resistance, compared to pure CA ENM, is attributed to increased fiber-to-fiber connections and the formation of collective intermolecular forces within the fiber mass. The stronger intermolecular forces in TOCNF/CA composite ENMs contribute to higher deformation resistance, as observed in Figure 4.10 (b), i.e., solid curves. Further deformation leads to more severe failure of fiber connections, resulting in a reduced cross-section of the specimen.

The pristine CA nanofibrous membrane exhibits a UTS of 5.1 MPa and an elongation at break of 0.76% before undergoing the HPT process. With an increase in CNC loading from 0 wt% to 1 wt% in the spinning solution, both UTS and fracture strain peak at 15.4 MPa and 1.18%, respectively, at a CNC loading of 0.5 wt%, showing a three-fold and 1.5-fold improvement over the pristine CA membrane (Figure 4.10 (a) i.e., solid curves). Comparable studies introducing CNCs as nanofillers in nanofiber structures demonstrated UTS improvements of 1.4 times (Sun *et al.* (2015) and 2.2 times (Jiang *et al.* (2020) in CNC/CA composite nanofibers compared to CA nanofibers (See Table 2.1).

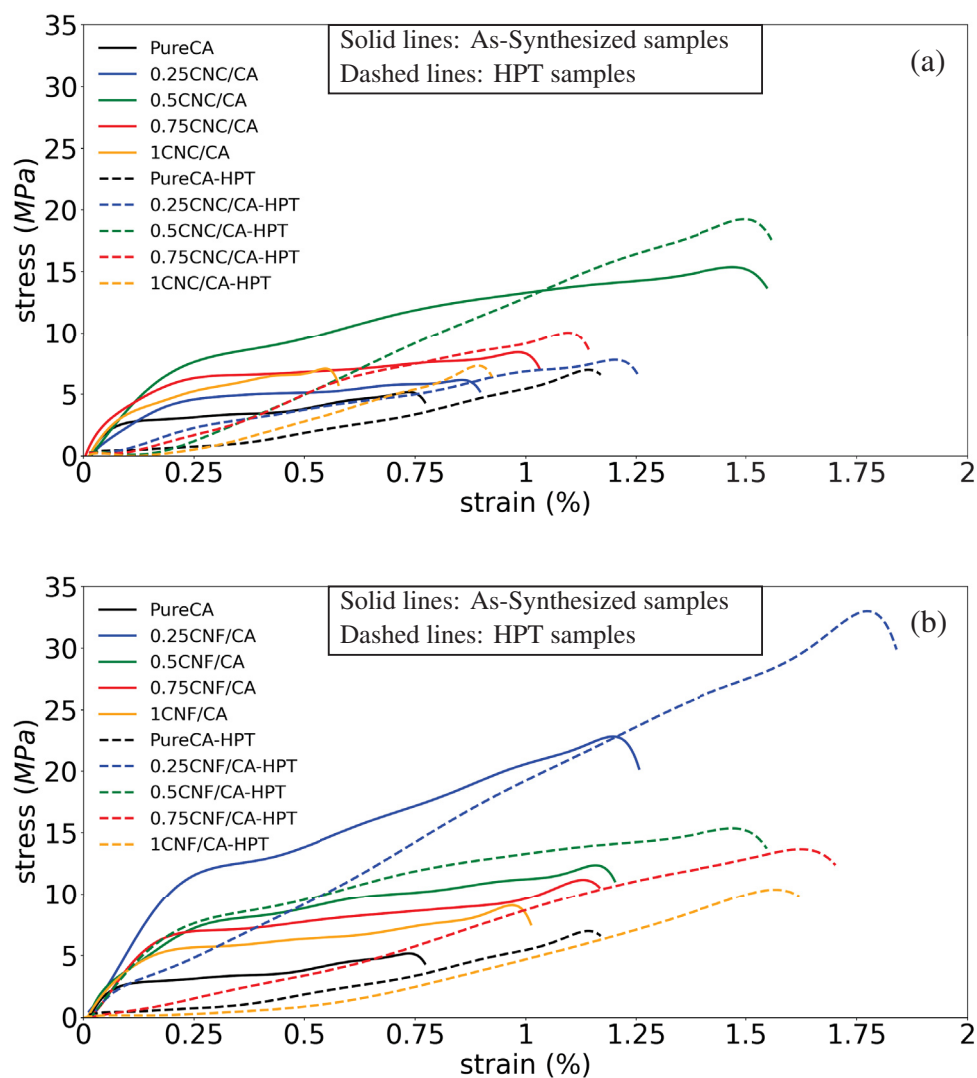


Figure 4.10 The effect of (a) CNC and (b) TOCNF nanofillers on mechanical properties of CA ENMs as-spun and after HPT process

In Figure 4.10 (b), i.e., solid curves, the 0.25TOCNF/CA membrane sample prior to the HPT process achieves maximum UTS and fracture strain of 22.6 MPa and 1.25%, respectively. These values are 4.4 times and 1.6 times higher than those of pristine CA nanofiber membranes. Limited studies exist on electrospun CNF/CA nanocomposite membranes and their mechanical properties to the best of the authors' knowledge.

CNF/CA nanocomposite membranes synthesized by Sharma et al. Sharma *et al.* (2021) and Cindradewi et al. Cindradewi *et al.* (2021) using phase inversion methods lack a nanofibrous structure, resulting in UTS values of 65 MPa and 47.6 MPa, respectively. This is attributed to the dense and bulk structure of the membranes (See Table 2.1).

Figures 4.10 (a) and (b) showcase similar trends in the tensile strength of CNC/CA and TOCNF/CA ENMs. Both types of composite ENMs demonstrate that an increase in nanofiller loading in the spinning solution, and consequently mean fiber diameter, results in enhanced tensile strength, reaching a peak for 0.5CNC/CA and 0.25TOCNF/CA ENMs. Subsequently, a decline in tensile strength is observed with further nanofiller loading, as illustrated in Figure 4.7 (s). The slope of the red dashed and black dashed curves in Figure 4.7 (s) sharpens after 0.5 wt% CNC and 0.25 wt% TOCNF for CNC/CA and TOCNF/CA composite nanofibers, respectively. This increasing trend suggests a correlation between mean fiber diameter and tensile strength, possibly indicating the maximum stress value and a reduction in fiber connections and length at the same membrane area density. Additionally, nanofiller aggregation could contribute to the observed decrease in tensile strength. Figures 4.10 (a) and (b) show that the decrease in tensile strength with TOCNF loading above 0.25 wt% is more pronounced than in the case of CNCs. This disparity might be attributed to the easier aggregation and stronger hydrogen bond formation of TOCNFs. The distribution and dispersion of nanofillers significantly impact the mechanical properties of ENMs. The remarkable improvement in fracture strength of composite nanofibrous membranes is attributed to the reinforcement effect of CNCs and TOCNFs. ENMs containing TOCNFs exhibit higher tensile strength, possibly due to stronger ionic interactions and better cross-linking with the CA matrix, stemming from the fibrous structure of TOCNFs. The dashed curves in Figures 4.10 (a) and (b) depict how the HPT process influences the mechanical properties of CNC/CA and TOCNF/CA composite nanofibers with varying nanofiller loadings.

As illustrated in Figures 4.10 (a) and (b), nanocomposite membranes subjected to thermal treatment exhibit markedly different stress-strain behavior compared to samples before the HPT process. During the heat treatment, the yield points nearly vanish, resulting in a more linear

behavior. These findings indicate that the heat-treated samples possess tougher, stronger, and more cohesive structures. The results show an enhancement in both ultimate tensile strength (UTS) and fracture strain after heat treatment. Additionally, heat treatment contributes to improved membrane integrity by eliminating solvents from the nanofibers.

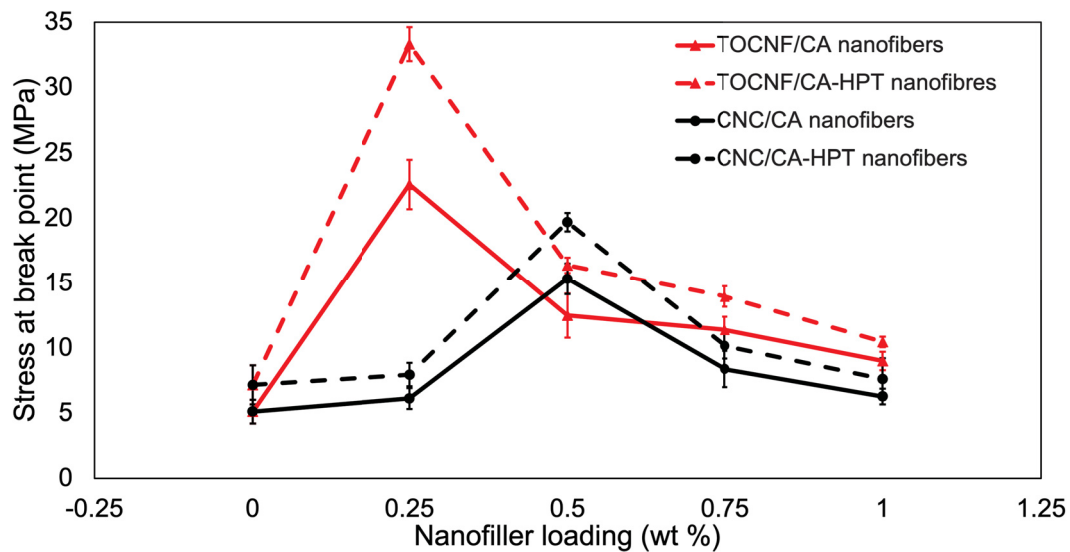


Figure 4.11 Variations of tensile strength of CNC/CA and TOCNF/CA ENMs as a function of nanofiller loading and heat treatment process

Table 4.1 The mechanical properties of CNC/CA nanocomposite ENMs

Sample Code	CA		0.25CNC/CA		0.5CNC/CA		0.75CNC/CA		1CNC/CA	
	AS*	HPT*	AS	HPT	AS	HPT	AS	HPT	AS	HPT
Mean Diameter(nm)	203±20	322±24	219±17	330±23	243±18	352±20	362±28	428±32	404±21	474±19
Diameter Range(nm)	372±22	626±35	434±38	694±33	507±36	716±18	592±30	741±27	629±19	810±38
UTS(MPa)	5.1±0.9	7.2±1.5	6.1±0.8	8±0.9	15.3±1.2	19.7±0.7	8.4±1.4	10.2±1	6.3±0.6	7.6±1.6
Strain at Break(%)	0.76±0.11	1.17±0.32	0.89±0.21	1.22±0.31	1.54±0.38	1.55±0.35	1.02±0.26	1.13±0.27	0.57±0.09	0.91±0.11
Modulus(GPa)	1.13±0.21		1.6±0.17		4.2±0.51		3.4±0.33		1.8±0.19	

★ AS: As-Synthesized, HPT: After Heat Treatment Process

Table 4.2 The mechanical properties of TOCNC/CA composite ENMs

Sample Code	CA		0.25CNC/CA		0.5CNC/CA		0.75CNC/CA		1CNC/CA	
	AS*	HPT*	AS	HPT	AS	HPT	AS	HPT	AS	HPT
Mean Diameter(nm)	203±20	322±24	233±30	342±22	345±22	404±23	411±35	468±17	447±31	498±13
Diameter Range(nm)	372±22	626±35	480±18	727±28	587±37	749±19	646±40	772±45	690±35	841±20
UTS(MPa)	5.1±0.9	7.15±1.5	22.6±1.9	33.31±1.3	12.5±1.7	16.4±0.6	11.4±1	13.97±0.8	8.99±0.7	10.46±0.4
Strain at Break(%)	0.76±0.11	1.17±0.32	1.25±0.27	1.83±0.41	1.19±0.17	1.54±0.19	1.17±0.22	1.69±0.35	0.99±0.13	1.61±0.48
Modulus(GPa)	1.13±0.21		5.3±1.69		3.5±1.08		2.7±0.79		1.5±0.58	

★ AS: As-Synthesized, HPT: After Heat Treatment Process

Figure 4.11 presents comparisons of ultimate tensile strength (UTS) among pristine CA nanofibers, CNC nanofiller-reinforced CA composite ENMs, and TOCNF nanofiller-reinforced CA composite ENMs concerning nanofiller loadings and the HPT process. Overall, the incorporation of CNC and TOCNF reinforcements into the CA matrix leads to an increase in tensile strength. The highest UTS of 33.31 MPa and maximum elongation at the breakpoint of 1.83% were achieved for the heat-treated 0.25TOCNF/CA composite ENM sample. The addition of TOCNFs enhances the flexibility of the TOCNF/CA composite ENM sample by fostering good interfacial bonding between the CA matrix and fibrils Liu, Sun, Tian, Maiti & Ma (2013); Wu *et al.* (2019). As depicted in Figure 4.11, further increases in TOCNF weight percentage from 0.25 wt% to 1 wt% in the polymer spinning solution result in a decrease in tensile strength. This decline may be attributed to the inhomogeneous distribution of TOCNF nanofiller in the CA polymer matrix, influenced by the high aspect ratio of TOCNFs, leading to the formation of aggregations through strong hydrogen bonds and swollen clusters due to water in the solution.

4.2.6 Conclusion

These findings provide evidence of the feasibility of manipulating the structure of CA ENMs through an effective procedure to attain the desired morphology. In summary, the characterization of the structural and mechanical properties of the NCs/CA electrospun fibers revealed that they were smooth, bead-free, and their mean fiber diameter was significantly influenced by nanofiller loading and heat treatment. With an increase in CNC and TOCNF loading in the polymer spinning solution, individual fibers in ENM samples became thicker, resulting in larger mean fiber diameters. Similarly, after heat post-treatment, ENM samples exhibited an increased mean fiber diameter. The mean fiber diameter and tensile strength showed a correlation, with heat-treated 0.25TOCNF/CA ENM samples demonstrating the maximum ultimate tensile strength (UTS) and elongation at break. To address long-term sustainability, the subsequent section delves into the environmental impacts of the 0.25TOCNF/CA modified ENM sample over its life cycle, encompassing sourced materials and the fabrication process.

4.3 Life Cycle Assessment: environmental impacts of cellulose-based nanocomposite membrane fabrication process

In the pivotal third phase of this Ph.D. research, we embark on a comprehensive examination of the environmental footprint associated with the fabrication process of cellulose-based nanocomposite membranes. This phase, dedicated to Life Cycle Assessment (LCA), delves into the intricate interplay between the sourced materials, and manufacturing procedures of the membrane. As we transition from structural and mechanical characterizations to a holistic analysis, our focus broadens to evaluate the sustainability implications of the cradle-to-gate life cycle of the 0.25TOCNF/CA modified ENM sample. This meticulous investigation aims to quantify and understand the environmental impacts stemming from raw material extraction, through the fabrication process of the nanocomposite membrane. By systematically exploring each stage, we aspire to provide valuable insights into the ecological considerations surrounding cellulose-based nanocomposite membrane technology, paving the way for informed decision-making and sustainable advancements in membrane fabrication.

4.3.1 Life Cycle Impact Assessment (CED and IMPACT2002+ methods)

Upon completing the life cycle inventory, the subsequent phase involves the impact evaluation, where elementary and economic flows within the system are translated into environmental indicators. Table 4.3 provides a comprehensive summary of the total energy demand for membrane fabrication processes, encompassing both NIPS and electrospinning methods. This assessment takes into account the energy requirements for all material production processes, including electricity, water, and transportation. Beyond energy impacts, Table 4.3 presents the variability in results associated with fifteen midpoint impact categories and four endpoint damages, as determined by the IMPACT2002+ assessment method.

The subsequent sections will meticulously examine the consumed energy, environmental midpoint impact categories, and endpoint damages incurred during the manufacturing stages of nanofibrous membrane sample through electrospinning and hollow-fiber membrane sample via

Table 4.3 Per FU Based CED and IMPACT2002+ results for the production of 0.25TOCNF/CA nanocomposite membrane by Electrospinning and NIPS methods

Cumulative Energy Demand (MJ)	NIPS	Electrospinning
CED total energy	1030	768
CED for CA production process	290	290
CED for TOCNF production process	382	382
CED for electricity	337	80
CED for Solvent	21	16.5
CED for water	0.46	0.04
CED for transportation	0.41	0.31
Renewable energy	467	229
Non-renewable energy	563	539
IMPACT2002+	NIPS	Electrospinning
Midpoint Impact Categories		
Aquatic acidification potential (AAP; kg SO ₂ eq.)	0.192	0.185
Aquatic ecotoxicity potential (AEP; kg TEG water)	6275	5471
Aquatic eutrophication potential (AEUP; kg PO ₄ P-lim)	0.01	0.012
Global warming potential (GWP; kg CO ₂ eq.)	26.56	25.03
Ionizing radiation potential (IRP; kBq Carbon-14 eq.)	503.6	391.652
Mineral extraction potential (MEP; MJ surplus)	1.5	1.4
Human carcinogenic toxicity potential (HCTP; kg C ₂ H ₃ Cl eq)	1.214	1.14
Human non-carcinogenic toxicity potential (HNCTP; kg C ₂ H ₃ Cl eq)	2.68	2.36
land use potential (LUP; m ² org.arable)	2.23	1.4
Non-renewable energy potential (NREP; MJ primary)	562.55	539
Ozone layer depletion potential (OLDP; kg CFC-11 eq.)	9.7e-7	8.97e-7
Respiratory inorganics potential (RIP; kg PM2.5 eq.)	0.035	0.0336
Respiratory organics potential (ROP, kg C ₂ H ₄ eq.)	0.0173	0.0170
terrestrial acid/nutri potential (TANP; kg SO ₂ eq.)	0.7732	0.73
terrestrial ecotoxicity potential (TEP; kg TEG soil)	1126	1081.5
Endpoint Damages	NIPS	Electrospinning
Human Health (HH, DALY)	3e-5	2.88e-5
Ecosystem Quality (EQ, PDF.m ² .yr)	3.9	2.87
Climate Change (CC, kg CO ₂)	26.56	25
Resource Depletion (RD, MJ)	606	581

the NIPS method. This analysis will be conducted through a detailed contribution analysis to discern the nuanced environmental implications of each fabrication approach.

4.3.2 Environmental impacts of synthesis process of 0.25TOCNF/CA nanofibrous membrane by electrospinning technique

As highlighted in preceding sections, the manufacturing process of the electrospun membrane sample, specifically the 0.25TOCNF/CA variant, is illustrated in Figure 3.2(a). This section delves into the environmental ramifications associated with the single-batch production of the 0.25TOCNF/CA electrospun membrane. The discussion encompasses all process steps, the materials utilized, and the energy requirements involved in the production.

CED impact value for 0.25TOCNF/CA electrospun membrane

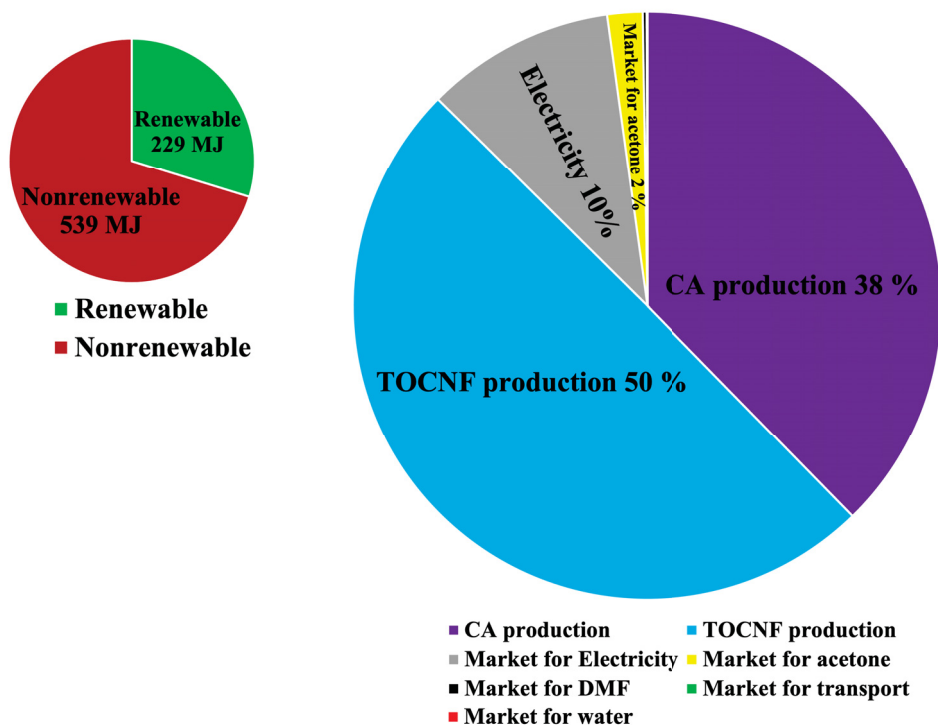
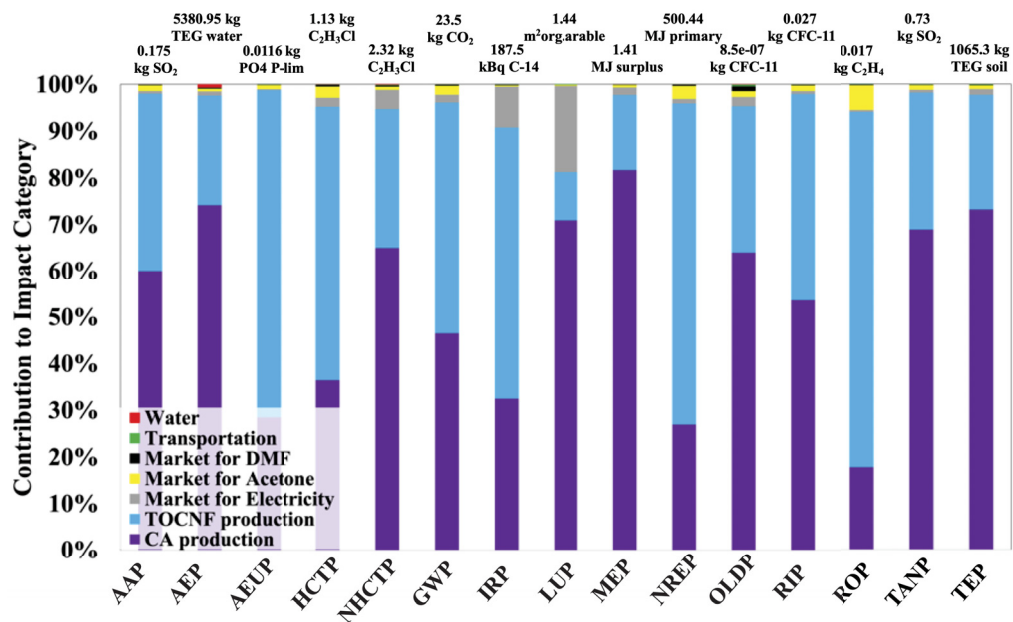
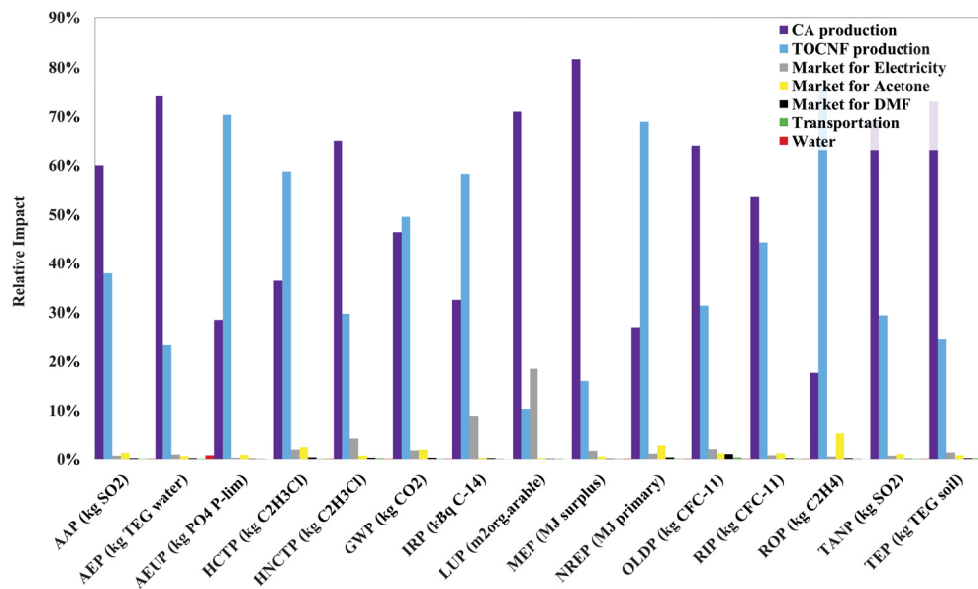


Figure 4.12 CED for material and energy requirement processes of electrospinning 50gr 0.25TOCNF/CA



a)



b)

Figure 4.13 IMPACT2002+ results (a) contribution to impact category (b) relative Impact, for the environmental impacts of producing 0.25CNF/CA electrospun nanofibrous membrane

The cumulative energy demand for the material, electricity, water, and transportation processes involved in the production of the 0.25TOCNF/CA ENM sample is visualized in Figure 4.12. The accompanying pie chart on the right side of the figure highlights that TOCNF, CA, and electricity collectively account for the majority of the energy demand, constituting 50%, 38%, and 10% of the total energy consumption, respectively. In the electrospinning of 50 grams of the 0.25TOCNF/CA polymeric solution, the total energy expenditure, as indicated in Table 4.3, amounted to 768 MJ. Notably, TOCNF production (382 MJ), CA production (290 MJ), and electricity (80 MJ) emerged as the predominant contributors to this total consumption. The substantial energy demand in TOCNF production is predominantly attributed to non-renewable fossil energy consumed during the Ethanol production process. Similarly, in the CA production process, the elevated energy demand stems from both non-renewable fossil energy and renewable water energy, utilized in the sodium bicarbonate production process and hydroelectric power, respectively. It's worth noting that the Quebec province of Canada, where the study is conducted, heavily relies on hydroelectric resources, contributing significantly to the total cumulative energy demand. The breakdown of total energy demand into renewable and nonrenewable sources is depicted in the pie chart on the left side of Figure 4.12, revealing that 70% of the total demand (539 MJ) is derived from nonrenewable sources.

Figure 4.13 visually presents the life cycle environmental impacts associated with the production of 0.25TOCNF/CA ENM. In Figure 4.13 (a), the contribution of material, electricity, water, and transportation processes to the fifteen mid-point impact categories, as per the IMPACT2002+ assessment method, is depicted using stacked columns. Notably, the larger contributions across all mid-point categories stem from the CA and TOCNF production processes. To facilitate a comparative analysis of the environmental impacts of different processes, Figure 4.13 (b) illustrates the relative impacts of CA, TOCNF, Acetone, and DMF production processes, alongside the electricity, water, and transportation requirements.

The aquatic ecotoxicity (AEP) midpoint category in the overall electrospun membrane fabrication process is predominantly influenced by the CA production process, contributing over 74%, and the TOCNF production process, contributing over 23%. The primary contributors to the AEP

impact category are soda (over 49%) and DI water (over 10%) used in CA production and ethanol (over 21%) used in TOCNF production processes. The environmental impact related to aquatic toxicity is mainly attributed to the heat production and lime used in soda production and the ethylene and heat production for ethanol required in CA and TOCNF production processes.

In terms of the global warming potential (GWP) impact category, sodium bicarbonate, electricity, and acetic acid requirements in the CA production process, ethanol consumption in the TOCNF production process, and the acetone production process significantly contribute to the environmental burden. Specifically, sodium bicarbonate, ethanol, and the aforementioned requirements contribute over 41%, over 43%, and over 10%, respectively, to the total GWP environmental burden.

The potential damage to human health encompasses midpoint impact categories such as carcinogens (HCTP), non-carcinogens (HNCTP), ionizing radiation (IRP), ozone layer depletion (OLDP), and respiratory (RIP and ROP) effects. The utilization of soda, acetic acid, and ethanol in the CA and TOCNF production processes, along with acetone and electricity consumption, plays a predominant role in contributing to embedded carcinogenic and non-carcinogenic toxicity potentials. In Figure 4.13 (a), it is evident that the TOCNF production process, primarily due to ethylene consumption, is the dominant contributor to carcinogenic toxicity potential, while the CA production process, specifically the soda production process, holds the main risk burden for non-carcinogenic toxicity potential. Additionally, ethanol consumption significantly impacts respiratory health, contributing to 76% of associated risks, while sodium bicarbonate and electricity voltage transformation account for 15% and 79% of ionizing radiation risks, respectively.

4.3.3 Environmental impacts of synthesis process of 0.25CNF/CA hollow-fiber membrane via NIPS method

The wet spinning method, also known as the non-solvent induced phase separation (NIPS) method, is a traditional approach involving the extrusion of a polymer solution through a spinneret into a coagulation bath (refer to Figure 3.2 (b)). In terms of cost-effectiveness and the mechanical and

electrical properties of the resulting materials, numerous comparative studies have demonstrated the efficiency, affordability, and scalability of electrospinning for the production of one-dimensional nanofibers with intriguing mechanical and electrical characteristics Haghghat Bayan, Afshar Taromi, Lanzi & Pierini (2021); Mohammadzadehmoghadam, Dong & Jeffery Davies (2015). However, comparing the environmental impacts of both methods poses challenges due to the limited availability of comparative life cycle assessment studies. This subsection presents an environmental impact analysis of the batch production process of 0.25TOCNF/CA hollow-fiber membranes (HFMs) by NIPS method.

CED impact value for 0.25TOCNF/CA hollow-fiber membrane

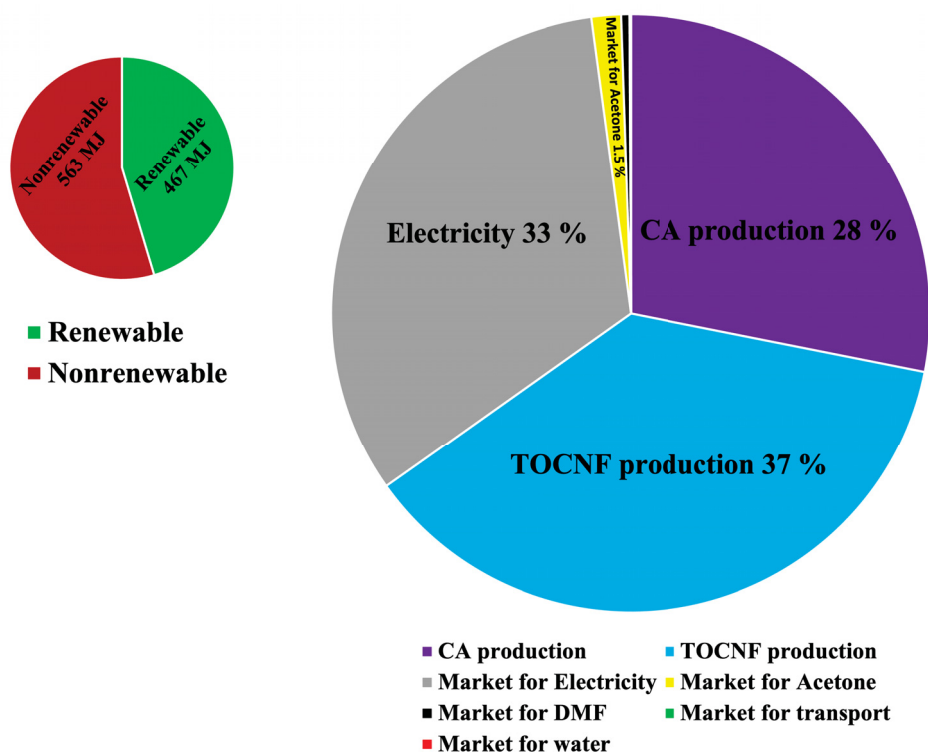
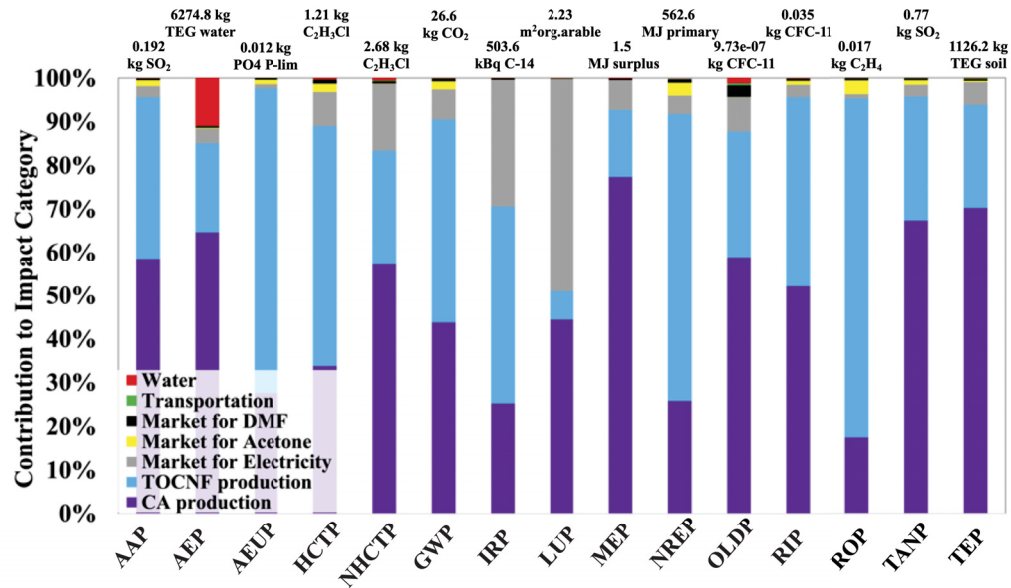
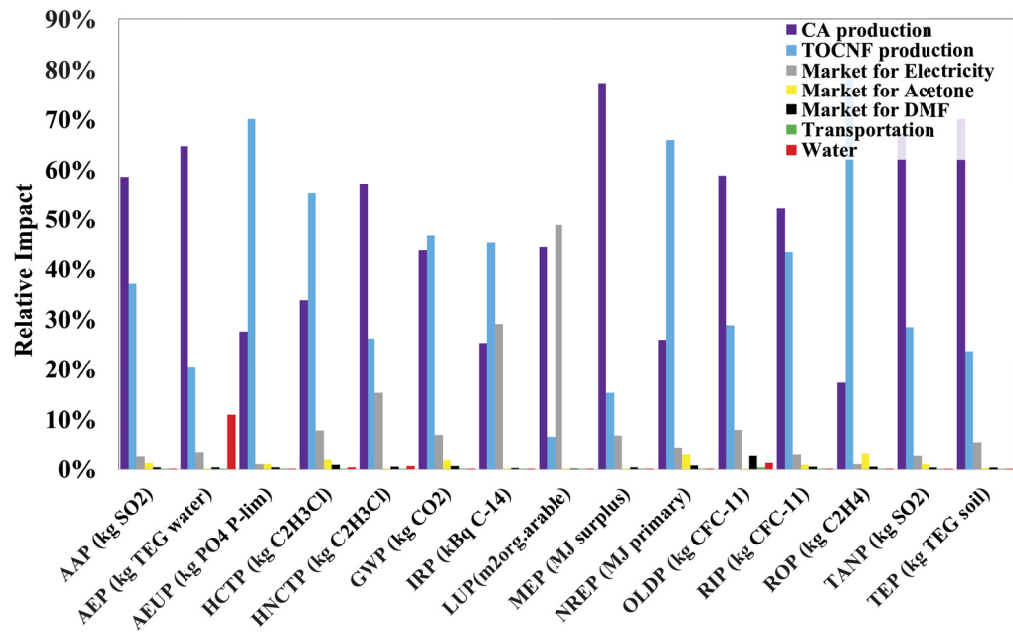


Figure 4.14 CED results for the environmental impacts of producing 0.25CNF/CA hollow-fiber membrane via NIPS method



a)



b)

Figure 4.15 IMPACT2002+ results (a) Contribution to impact category (b) Relative Impact, for the environmental impacts of producing 0.25CNF/CA hollow-fiber membrane via NIPS method

Figure 4.14 offers a comprehensive view of the combined energy requisites encompassing material, electricity, water, and transportation needs for fabricating 0.25TOCNF/CA HFM sample. The pie chart on the right side of the figure delineates that CA production, TOCNF production, and electricity consumption constitute the bulk of the energy demand, accounting for 28%, 37%, and 33% of the total energy consumption, respectively, surpassing the energy needs of solvent production, transportation, and water requirements. An in-depth analysis detailed in Table 4.3 reveals that the total energy expenditure for extruding 50 grams of the 0.25TOCNF/CA polymeric solution via the NIPS method amounted to 1029.706 MJ. Among these, CA production (290 MJ), TOCNF production (382 MJ), and electricity (337 MJ) emerged as the primary contributors to the overall consumption. Further delineating the energy distribution, the left-side pie chart in Figure 4.14 dissects the total energy demand into renewable and nonrenewable sources. Predominantly stemming from nonrenewable origins, 55% (563 MJ) of the total demand draws from nonrenewable fossil fuels utilized in sodium bicarbonate and ethanol production for CA and TOCNF processes, respectively. Alternatively, renewable energy usage, totaling 467 MJ, predominantly hails from hydroelectricity, representing 94% of Quebec's power generation and marking renewable water resources as a significant contributor to the cumulative energy landscape.

Figure 4.15 illustrates the life cycle environmental impacts entwined with the manufacture of 0.25TOCNF/CA HFM. Employing the IMPACT2002+ assessment method, material, electricity, water, and transportation processes contribute to 15 mid-point impact categories, showcased in Figure 4.15 (a). The stacked columns reveal that predominant contributions across all mid-point categories stem from CA production, TOCNF production, and electricity consumption. Furthermore, the grouped bars in Figure 4.15 (b) are strategically presented to facilitate a comparative analysis of the relative environmental impacts of diverse processes, encompassing CA, TOCNF, Acetone, and DMF production processes, in addition to electricity, water, and transportation requirements.

The aquatic toxicity midpoint impact categories are predominantly influenced by the CA production process, primarily due to the requirements for sodium bicarbonate and electricity. In

addition to CA production, the TOCNF production process significantly contributes to aquatic toxicity impacts, particularly through the consumption of ethylene and the associated heat production required for ethanol. As illustrated in Figure 4.15, water consumption plays a considerable role in aquatic ecotoxicity (AEP), indicating substantial water usage in NIPS with significant repercussions on aquatic ecosystems.

Climate change damage, quantified through the global warming potential metric, is a highly assessed environmental impact. In the overall fabrication process of hollow-fiber membrane, the TOCNF production process contributes over 47%, the CA production process contributes over 44%, and the electricity market accounts for 7% of the global warming potential (GWP) midpoint impact. This impact is primarily driven by soda requirements (over 39%) in the CA production process and ethanol (over 41%) and electricity (over 7%) consumption in the TOCNF production process. Notably, the non-renewable sources used for electricity generation in the TOCNF production process, sourced from the Cellulose Lab in New Brunswick, exhibit higher negative environmental impacts compared to the hydroelectricity used in CA production in Quebec.

The cumulative impacts on the Human Health endpoint damage result from carcinogens (HCTP), non-carcinogens (HNCTP), ionizing radiation (IRP), ozone layer depletion (OLDP), and respiratory (RIP and ROP) midpoint categories. Significant contributions to carcinogenic and non-carcinogenic toxicity potentials stem from soda production and electricity requirements in the CA production process, along with the ethylene hydration process employed in TOCNF production. The carcinogenic toxicity associated with TOCNF is notably more pronounced than that of CA, attributed to the utilization of ethylene in the TOCNF production process. Conversely, CA production bears the primary risk burden in non-carcinogenic toxicity, primarily due to soda production for sodium bicarbonate requirements. Land use (LUP) and ionizing radiation (IRP) impact categories are significantly influenced by electricity consumption, particularly from non-renewable sources of power generation.

4.3.4 Comparative analyses of 0.25TOCNF/CA membrane production by electrospinning and wet spinning methods

There is a noticeable scarcity of studies focusing on the environmental aspects of membrane fabrication processes. Furthermore, the primary objective of the current LCA study is to conduct a comparative analysis of the environmental impacts between the traditional NIPS method and the innovative electrospinning technique, employing IMPACT2002+ and CED impact assessment methods. The comprehensive results presented in table 4.3 undeniably highlight the substantial influence of the membrane fabrication method on environmental performance.

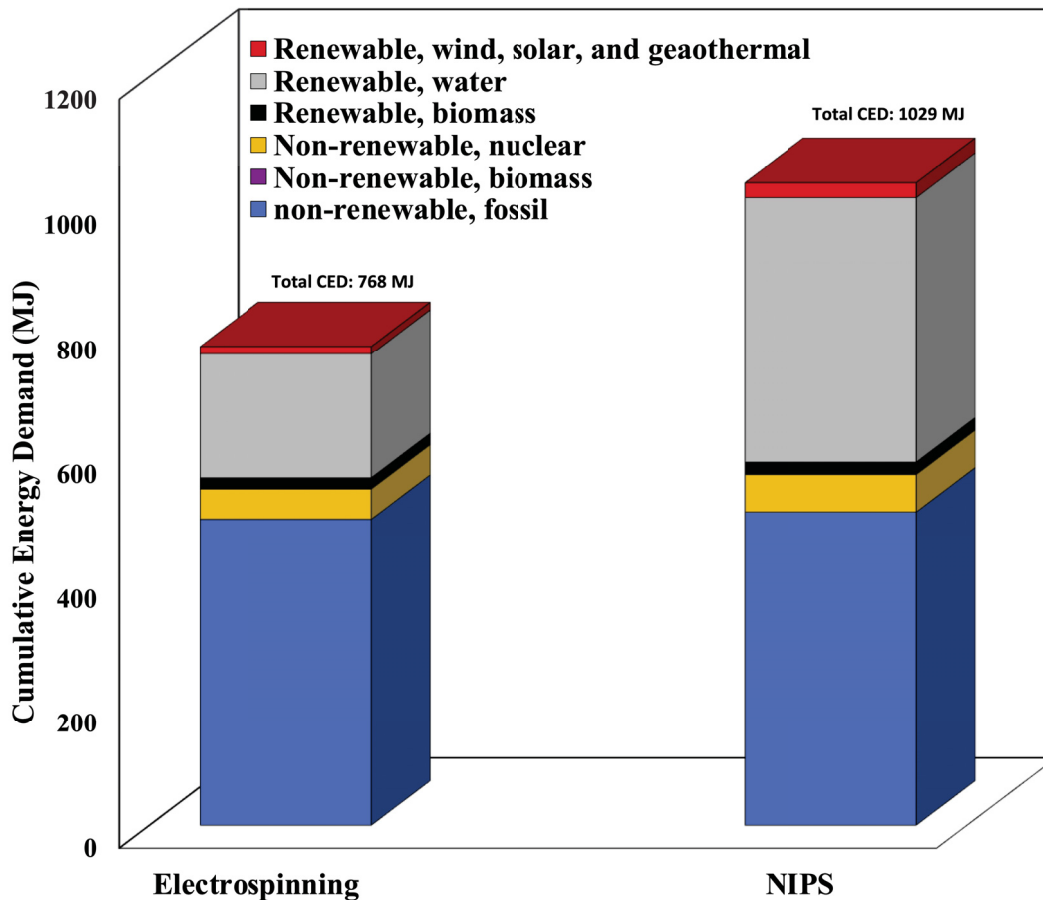


Figure 4.16 Comparative CED results for the energy consumption for the production of 0.25CNF/CA ENM and HFM via Electrospinning and NIPS methods

Figure 4.16 presents a comparative analysis of the total cumulative energy demand for the synthesis of 0.25TOCNF/CA membranes using both the NIPS and electrospinning methods. Clearly, the 0.25TOCNF/CA HFM sample exhibits a significantly higher energy burden across almost all energy impact categories compared to the 0.25TOCNF/CA ENM sample. A quick glance reveals that the NIPS method has a total energy demand of 1029 MJ, surpassing the electrospinning technique's demand of 768 MJ, primarily due to increased electricity and water consumption in the NIPS synthesis process. The 3D-stacked bars in figure 4.16 highlight that nonrenewable fossil fuels, represented by the blue part in the bars, contribute significantly to the cumulative energy demand for both membrane synthesis methods. For the 0.25TOCNF/CA ENM, fossil fuel non-renewable energy is mainly attributed to ethanol (324 MJ) and sodium bicarbonate (106 MJ) production in the background upstream processes for TOCNF and CA production. In the case of 0.25TOCNF/CA HFM fabricated by the NIPS method, ethanol and sodium bicarbonate production also dominate nonrenewable fossil fuel energy use. The overall consumption of non-renewable energy is higher in the NIPS method compared to the electrospinning method, owing to increased solvent, electricity, water, and transportation requirements.

In both membrane fabrication processes, the renewable water energy source, represented by the grey part in the 3D stacked bars (See figure 4.16), emerges as the second most significant contributor to the total cumulative energy demand (CED). Notably, Quebec, Canada, stands as the largest generator of hydroelectricity, with 94% of its electricity sourced from renewable resources. The production of 0.25TOCNF/CA ENM requires approximately 86 MJ of hydroelectricity, while the electric power needed for synthesizing the 0.25TOCNF/CA HFM sample is around 310 MJ. The results of the CED impact assessment underscore the efficiency of the electrospinning method, which demands less electrical power than the NIPS method, positioning it as a more environmentally favorable choice in terms of energy consumption.

The yellow sections in the stacked bars denote non-renewable nuclear energy consumption, totaling 60 MJ for the NIPS method and 48 MJ for the electrospinning technique. The NIPS

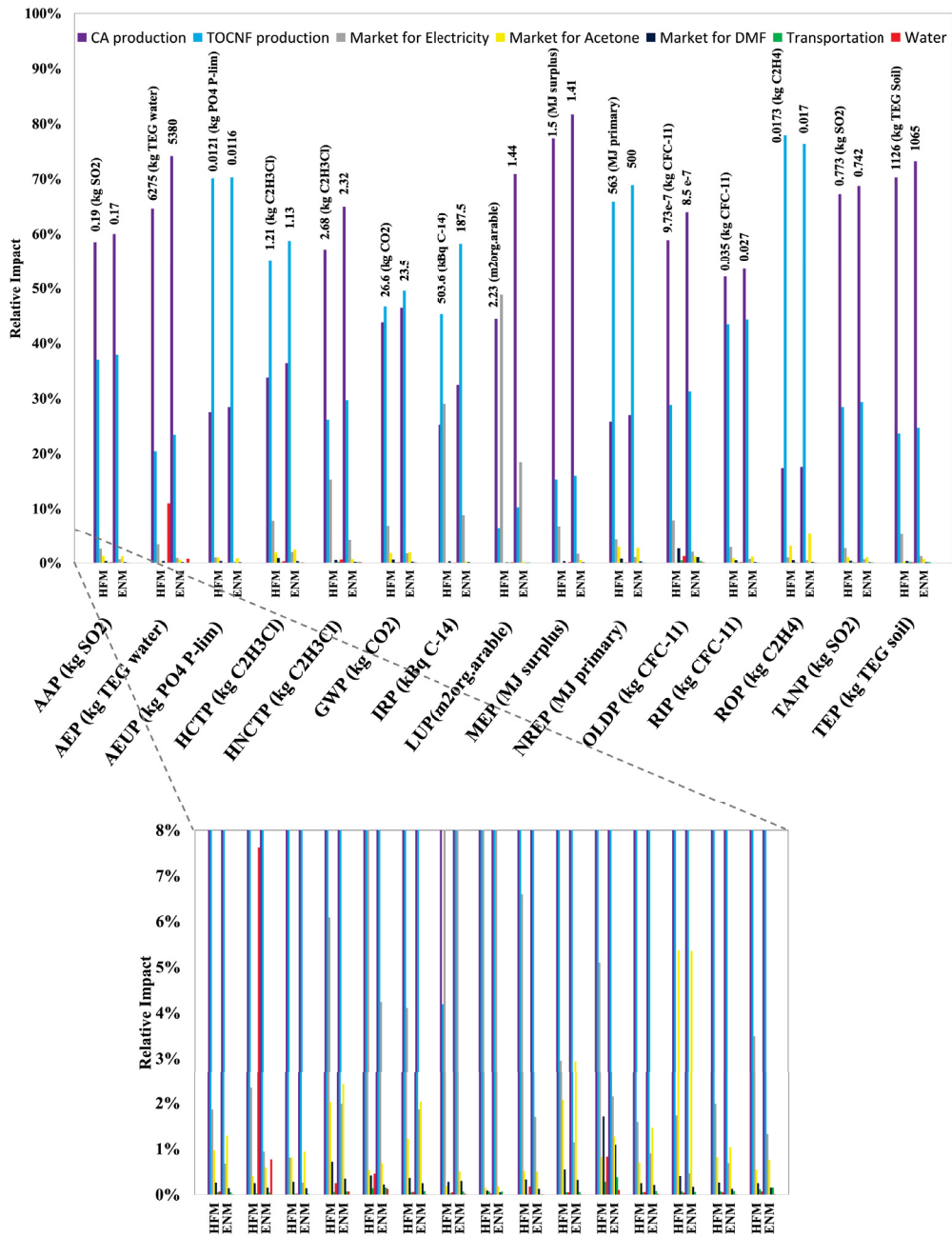


Figure 4.17 Comparing IMPACT2002+ results for the environmental impacts of producing 0.25CNF/CA ENM and HFM via Electrospinning and NIPS methods

method's higher consumption of electrical power, water, and solvent results in a more pronounced negative environmental impact from an energy perspective.

In addition to the energy impact assessment, for the purpose of environmental comparison between NIPS and electrospinning methods, the relative midpoint impacts of utilized materials, transportation, electricity, and water requirements for both 0.25TOCNF/CA ENM and HFM samples are visually presented in Figure 4.17. The zoomed graph at the bottom of Figure 4.17 provides a clear view of the results for the relative midpoint impacts within the range of 0% to 20%.

Analyzing the results obtained from the IMPACT2002+ assessment (refer to Table 4.3), a comparative analysis reveals that the NIPS method exhibits significantly higher impact potentials in aquatic ecotoxicity, human carcinogenic toxicity, human non-carcinogenic toxicity, global warming, ionizing radiation, land usage, non-renewable energy, and ozone layer depletion impact categories. The clustered bars representing aquatic ecotoxicity impact demonstrate that the NIPS method (6275 kg TEG water) has a more detrimental effect on the toxicity burden in aquatic ecosystems compared to the electrospinning method (5380 kg TEG water). The red bars denote water consumption in the membrane fabrication process. The zoomed figure clearly indicates that the NIPS method consumes more water than electrospinning, releasing a substantial amount of solvent-contaminated wastewater into the environment and causing more negative impacts on aquatic ecosystems.

In terms of human carcinogenic and non-carcinogenic toxicity, as evident in Figure 4.17, the NIPS method (4 kg C_2H_3Cl eq) contributes more than electrospinning (3.5 kg C_2H_3Cl eq), primarily due to higher electricity demand (grey bars) for producing the HFM sample compared to the ENM sample.

Electricity, being the dominant contributor to the land use potential impact category, results from voltage transformation and heat and power co-generation processes in the background upstream. Consequently, the NIPS method has a greater environmental impact due to its higher electricity usage.

Depletion of the ozone layer leads to increased levels of UV radiation reaching the Earth's surface, posing risks to human health. UV radiation also has repercussions on terrestrial and

aquatic ecosystems, influencing growth, food chains, and biochemical cycles. The analysis of results reveals that the production processes of soda, acetic acid, ethanol, dimethylamine, and carbon monoxide in the background production processes of CA, TOCNF, acetone, and DMF significantly contribute to the OLDP impact category. Consequently, higher solvent consumption leads to increased impact on ozone layer depletion in the NIPS method.

An integrated midpoint/endpoint-oriented approach has been introduced through the IMPACT 2002+ LCIA methodology. Endpoint indicators were examined to obtain a more comprehensive and tangible understanding of the environmental effects of the membrane production process. Various substances, products, and processes can be characterized by utilizing damage characterization factors of reference substances, multiplied by the midpoint characterization. The reference damage characterization factors are outlined in Table 4.4. In addition to the intermediate midpoint impacts, the calculated endpoint damages are presented in Table 4.3.

Figure 4.18 illustrates the comprehensive environmental damages incurred throughout the entire membrane fabrication process for the synthesized 0.25TOCNF/CA HFM and ENM samples, allowing for a comparison between the NIPS and electrospinning methods. The depicted results underscore that the production of 0.25TOCNF/CA HFM sample through the NIPS method exhibits significantly more adverse effects on human health, resource depletion, ecosystem quality, and climate change endpoint damages. This environmental impact dominance of the NIPS method is rooted in the substantial amounts of energy, materials, and water consumed during the production process.

Figure 4.19 depicts the contribution of materials and process steps to the endpoint indicators in the IMPACT2002+ methodology for both HFM and ENM samples. The figure underscores that the production processes involving CA and TOCNF in the synthesis of HFM and ENM samples exert the most significant environmental burdens. These findings suggest that the TOCNF production process is responsible for 69% and 66% of the resource depletion damage in the production processes of HFM and ENM samples, respectively. This can be attributed

¹ Source of the data: Jolliet *et al.* (2003)

Table 4.4 Damage characterization factors (CFs) of reference substances¹

Midpoint Categories	Damage CFs	Units
Aquatic Ecotoxicity Potential	8.86E-05	PDF.m ² .yr/kg TEG water
Human Carcinogenic Toxicity Potential	1.45E-06	DALY/kg C ₂ H ₃ Cl eq
Human Non-Carcinogenic Toxicity Potential	1.45E-06	DALY/kg C ₂ H ₃ Cl eq
Global Warming Potential	1	kg CO ₂ eq./kg CO ₂ eq.
Ionizing Radiation Potential	2.10E-10	DALY/kBq C-14 eq.
Mineral Extraction Potential	5.10E-02	MJ/kg iron
Land Use Potential	1.09	PDF.m ² .yr/m ² org.arable
Non-Renewable Energy Potential	45.6	MJ/kg crude oil
Ozone Layer Depletion Potential	1.05E-03	DALY/kg CFC-11
Respiratory Inorganics Potential	7.00E-04	DALY/kg PM2.5
Respiratory Organics Potential	2.13E-06	DALY/Bq carbon-14
Terrestrial acid/nutri Potential	8.86E-05	PDF-m ² .yr/kg SO ₂
Terrestrial Ecotoxicity Potential	1.04	PDF.m ² .yr/kg.TEG soil

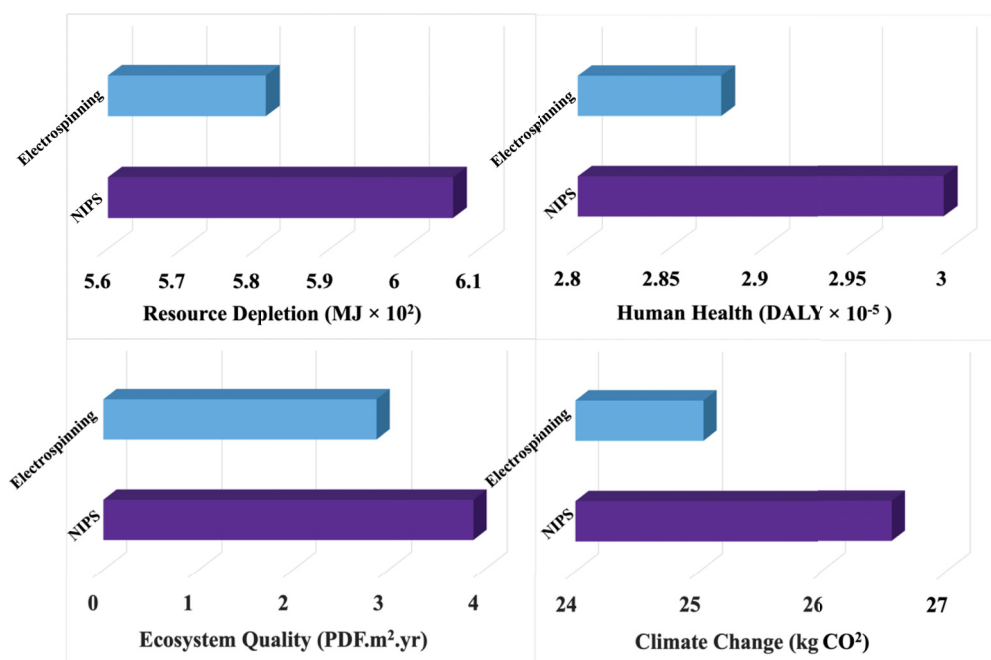


Figure 4.18 Relative endpoint damages of producing one functional unit of the final product by NIPS and electrospinning processes

to the fact that a substantial portion of the electricity used in TOCNF production is derived from non-renewable energy sources. Notably, the TOCNF for this study was procured from

Cellulose Lab in New Brunswick, Canada, where approximately 70% of electricity is sourced from non-renewable resources. It is worth noting that the other required materials and energy were obtained from the province of Quebec, where 94.3% of electricity is generated from hydro, representing a renewable resource.

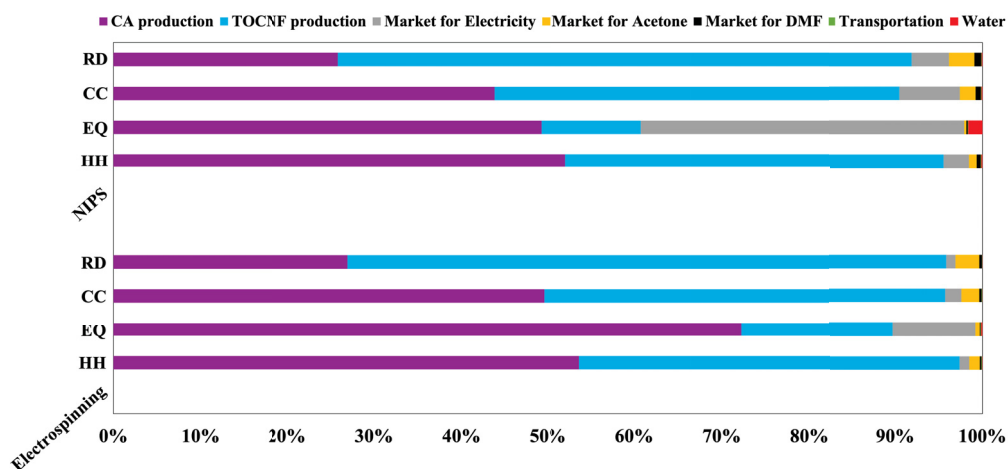


Figure 4.19 Contribution to endpoint damages of producing one functional unit of the final product by NIPS and electrospinning processes

Furthermore, the EQ stacked bar's prominent red section in Figure 4.19 highlights the significant water consumption in the NIPS process, resulting in substantial amounts of wastewater contaminated with solvents being discharged into the environment. This discharge negatively impacts the aquatic ecosystem midpoint category and, consequently, the ecosystem quality endpoint indicator.

Additionally, the NIPS method, in comparison to electrospinning, incurs higher electricity consumption throughout the entire membrane fabrication process, as indicated by the gray section of the stacked bars at the top of the figure. The investigation into midpoint categories reveals that land use potential is the primary affected category by electricity generation and voltage transformation. Since the electricity used is predominantly derived from hydropower, it aligns with a study by Lovering et al., stating that 80% of global land use for electricity production is attributed to hydroelectric dams Lovering, Swain, Blomqvist & Hernandez (2022).

4.3.5 Interpretation of environmental impacts of synthesizing 0.25TOCNF/CA ENM and HFM samples

Upon finalizing the Life-Cycle Impact Assessment (LCIA) for each process and the resulting product, the last phase of an LCA analysis involves the interpretation of the obtained results pertaining to the impact categories. The reliability of the LCA study hinges on accurate data, which is not always readily available Heijungs (1996); Guo & Murphy (2012); Heijungs (1996). Multiple factors such as the assumptions due to the inherent complexity of the system, the novelty of the subject matter, and the lack of data, and inaccurate measurements mainly contribute to the uncertainty in LCA studies. Consequently, this significantly impacts the reliability of research findings. Researchers often resort to incorporating assumptions and relying on average or secondary data to mitigate these uncertainties Santero (2010); Huijbregts (1998).

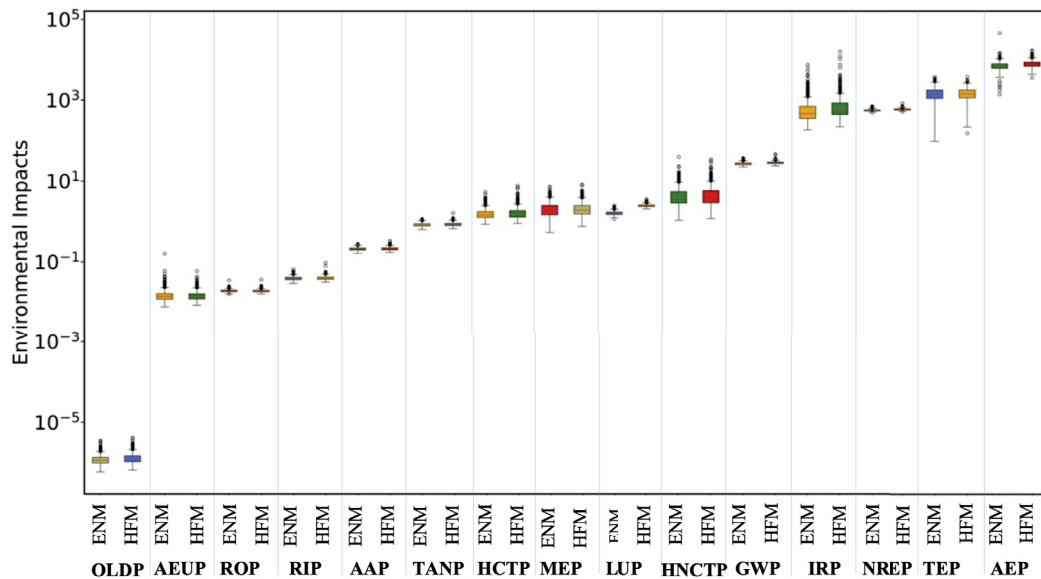


Figure 4.20 Comparative uncertainty boxplots for ENM and HFM samples manufacturing processes by electrospinning and NIPS methods

We quantified the uncertainties associated with the most influential materials and processes that contribute to the LCA results. The uncertainty realizations of modeled fifteen midpoint impact categories for the fabrication processes of HFM and ENM samples by electrospinning and NIPS methods and their statistical distributions are summarized in Table 4.5 and are presented in

Table 4.5 Uncertainty results for life cycle impact assessment of 0.25TOCNF/CA ENM and HFM

Impact category	Mean		STD		CV (%)		Max		Min	
	ENM	HFM	ENM	HFM	ENM	HFM	ENM	HFM	ENM	HFM
Ozone layer depletion (kg CFC-11 eq)	1.2e-6	1.34e-6	3.5e-7	4.13e-7	28.8	30.9	3.5E-6	4.15e-6	5.9E-7	4.02E-7
Aquatic eutrophication (kg PO4 P-lim)	0.015	0.0148	0.007	0.0047	44.8	31.7	0.159	0.059	0.008	0.0045
Respiratory organics (kg C2H4 eq)	0.019	0.019	0.0013	0.0016	7.1	8.4	0.035	0.036	0.016	0.0014
Respiratory inorganics (kg PM2.5 eq)	0.039	0.04	0.0042	0.005	10.7	12.6	0.065	0.0945	0.0293	0.0046
Aquatic acidification (kg SO2 eq)	0.207	0.211	0.018	0.021	8.8	9.8	0.162	0.329	0.278	0.0194
Terrestrial acid/nutrient (kg SO2 eq)	0.829	0.851	0.085	0.096	10.2	11.3	1.166	1.611	0.629	0.0899
Carcinogens (kg C2H3Cl eq)	1.566	1.664	0.491	0.643	31.3	38.7	5.334	7.625	0.851	0.615
Land occupation (m ² org.arable)	1.601	2.445	0.161	0.215	10.1	8.8	2.464	3.522	1.153	0.199
Mineral extraction (MJ surplus)	2.062	2.103	0.865	0.884	41.9	42.0	7.23	8.25	0.531	0.748
Noncarcinogens (kg C2H3Cl eq)	4.553	4.932	2.792	3.269	61.3	66.3	39.512	34.329	1.059	1.174
Global warming (kg CO2 eq)	26.886	28.329	2.063	2.35	7.7	8.3	37.208	46.589	22.542	2.121
Ionizing radiation (Bq C-14 eq)	628.52	819.995	548.16	1025.88	87.2	125.1	7541.83	16001.5	183.85	218.903
Nonrenewable energy (MJ primary)	565.72	587.623	27.996	34.745	4.9	5.9	719.28	834.5	495.96	28.86
Terrestrial ecotoxicity (kg TEG soil)	1447.11	1452.99	499.52	494.4	34.5	34.0	3717.39	3807.89	94.033	145.32
Aquatic ecotoxicity (kg TEG water)	7038.4	7781.6	1906.1	1500.1	27.1	19.3	45699.2	16959.5	1380.9	1453.8

the form of box plots in Figure 4.20. According to the Table 4.5, variations in the coefficient of variation (CV) are observed across the electrospinning and NIPS manufacturing processes and different midpoint impact categories. This discrepancy arises because each process has a distinct influence on specific impacts. Non-renewable Energy, Global Warming, Respiratory Effects, Aquatic Acidification, Terrestrial acid/nutrient, and Land Use have the lowest uncertainty of all the impact categories, with the coefficient of variations (CVs) between 4.9% and 12.6%, signifying lower uncertainty in the LCI data associated with these impacts. The box plots

presented in Figure 4.20 for the NREP, GWP, ROP, RIP, AAP, and LUP impact categories exhibit the least variation from the mean, aligning with the findings from the CV values. The strong confidence in LCA outcomes, particularly for GWP and NREP impact categories, signifies that the environmental assessments of both membrane fabrication processes are reliable in these categories, offering a solid foundation for LCA comparisons between the two methods. Conversely, the uncertainty for Ionizing Radiation, Human Health Toxicity, Eco Toxicity, Mineral Extraction, Marine Eutrophication, and Ozone Layer Depletion impact categories varies between 30% and 125.1%. The increasing trend of high uncertainty signifies a notable level of ambiguity within the life cycle inventory (LCI) data concerning these impact categories in both the electrospinning and NIPS manufacturing processes. This uncertainty stems from data quality, compounded uncertainties within the model's multiple layers, and limited understanding of the environmental impacts of various compounds.

CHAPTER 5

DISCUSSION

The achieved mechanical improvements, evident in heightened tensile strength and Young's modulus, validate the success of the employed nanofiller addition and heat post-treatment (HPT) processes. This outcome aligns with the primary objective of addressing limitations in membrane mechanical strength, a crucial factor influencing their performance in pressure-driven filtration processes. Furthermore, the successful integration of nanofillers and HPT offers a promising pathway for advancing membrane technology. The improved fiber linkages and enhanced mechanical properties contribute to the durability and longevity of membranes, crucial in applications where mechanical strength is pivotal, such as water purification and industrial processes. These findings not only advance our fundamental understanding of polymer-based membrane materials but also present practical implications for the design and fabrication of robust membranes with superior mechanical characteristics.

In the realm of sustainability, the Life Cycle Assessment (LCA) findings highlight the favorable aspects of electrospinning over the NIPS method concerning energy efficiency, electricity, and water consumption. Notably, the increased water usage in the NIPS method leads to the discharge of significant amounts of solvent-contaminated wastewater, resulting in more pronounced adverse effects on aquatic ecosystems. The Cumulative Energy Demand (CED) impact assessment reinforces the environmental benefits of the electrospinning method, particularly in terms of energy consumption. Specifically, the 0.25TOCNF/CA Hollow Fiber Membrane (HFM) sample crafted via NIPS exhibits considerably higher energy burdens across nearly all energy impact categories compared to the 0.25TOCNF/CA Electrospun Nanofibrous Membrane (ENM) sample. The overall non-renewable fossil fuel energy consumption is greater in the NIPS method due to heightened requirements for solvent, electricity, water, and transportation. The modeled uncertainty realizations across fifteen midpoint impact categories for HFM and ENM samples produced by electrospinning and NIPS methods reveal that Non-renewable Energy, Global Warming, and Land Use have the lowest uncertainty among all impact categories. Additionally,

the IMPACT2002+ assessment underscores that the NIPS fabrication process for HFM imposes a more substantial burden on Land Use, Global Warming, and Non-renewable Energy compared to the electrospinning process for ENM synthesis. These findings underscore the complexity of sustainability assessments, necessitating a balanced consideration of multiple factors. In achieving the research objectives, the LCA outcomes provide a valuable understanding of the environmental trade-offs between electrospinning and NIPS methods. The comprehensive analysis allows for informed decision-making in membrane fabrication processes, emphasizing the need for a holistic approach that considers both energy efficiency and chemical usage. However, uncertainties persist, particularly in areas such as the long-term effects of emitted solvents and the broader environmental impacts of the different methods.

Achieving the research objectives, the mechanical improvements and sustainability assessments collectively contribute to a more robust understanding of membrane fabrication processes. LCA outcomes provide a valuable understanding of the environmental trade-offs between electrospinning and NIPS methods. These advancements not only address mechanical limitations but also lay the foundation for informed decision-making in selecting fabrication methods based on environmental considerations and emphasizing the need for a holistic approach that considers both energy efficiency and chemical usage.

Looking ahead, the prospects for future research lie in refining and optimizing the nanofiller addition and HPT processes. Further investigation could explore alternative nanofillers to ascertain the optimal parameters for achieving the desired mechanical improvements. Additionally, research could delve into the scalability and practical implementation of these enhanced membranes in real-world applications, addressing challenges related to large-scale production and compatibility with existing filtration systems. Furthermore, the research opens avenues for recommendations aimed at mitigating the environmental implications of membrane fabrication. Exploring solvent alternatives or implementing closed-loop systems in electrospinning processes could significantly reduce environmental burdens. Additionally, in-depth investigations into the fate and transport of emitted solvents are vital for a more comprehensive assessment. Additional prospects for future research lie in refining the comparative LCA methodology, incorporating

more precise data on solvent emissions, and extending the analysis to include other relevant environmental impact categories. Continued efforts to optimize the electrospinning and NIPS processes for sustainability, such as developing greener solvents or enhancing energy efficiency, are essential. Collaborations with industry stakeholders can facilitate the practical implementation of these recommendations and promote the adoption of more sustainable membrane fabrication practices.

In conclusion, the results obtained in this study hold significant implications for the mechanical improvement of polymer-based membranes, opening avenues for further research and practical applications. The enhanced understanding of the relationships between nanofillers, heat post-treatment, and membrane mechanical properties contributes to the broader field of membrane technology. As we continue to refine these techniques, the potential benefits extend beyond the laboratory, impacting industries reliant on efficient and robust membrane-based filtration processes. Moreover, the LCA results and uncertainties presented in this dissertation contribute valuable insights into the environmental implications of electrospinning and NIPS membrane fabrication methods. While achieving the research objectives, the findings highlight the need for a nuanced understanding of sustainability considerations in membrane technology. The recommendations provided offer a pathway for mitigating negative environmental impacts, and future research endeavors can build upon this foundation to further enhance the sustainability and benefits of membrane fabrication processes.

CONCLUSION

The sustainable development of membrane technology involves exploring optimization concepts and conducting a life cycle assessment of all processes associated with the fabrication process. Within this doctoral dissertation, we initially fine-tuned the electrospinning process and examined the mechanical enhancement of CA membranes, taking into account the influence of various parameters. Subsequently, we conducted an evaluation of the environmental impacts associated with the optimized electrospun membrane sample, drawing comparisons with the hollow-fiber membrane produced through the NIPS method. Furthermore, a dedicated section delves into the significance of achieving a balance between sustainability and efficiency in the realm of membrane technology.

The electrospinning and fiber formation are significantly influenced by the viscosity and electrical conductivity of the spinning solutions and their interplay. Notably, solutions like 15CA1/0, 15CA2/8, 20CA1/0, 20CA1/1, and 20CA2/8 faced challenges during fiber spinning due to distinct reasons. Elevated viscosity resulting from a higher CA concentration (20 wt%) hindered fiber synthesis under constant electrospinning conditions. Conversely, the pronounced volatility of acetone in the DMF/acetone solvent mixture composition of 2/8 led to needle tip blocking. Additionally, the substantial surface tension of DMF caused bead formation during the spinning process of 15CA1/0 and 20CA1/0. Our findings revealed that, concerning material parameters, 15 wt% CA concentration and a 50 v/v% composition (1/1) of DMF/acetone mixture solvent were optimal. We also examined the effects of processing parameters on the structure of the ENM samples. Optimal electrospinning processing time was determined to be 2 hours, facilitating easier removal of the nanofibrous membrane mats from the collector and handling post-fabrication. Regarding spinning solution flow rate, tip-to-collector distance, and voltage field parameters, the optimal levels were 2 ml/h, 100 mm, and 25 kV, respectively, due to the high formation rate of fibers and reduced accumulation of polymer solution and beads in the membrane sample structure.

Investigating the impacts of nanofiller loading and thermal treatment on mechanical properties of the ENMs revealed that the incorporation of nanocellulose fillers led to an enhancement in the

mechanical properties of the ENMs, resulting in increased Young's modulus and tensile strength. Notably, ENMs containing TOCNFs exhibited higher tensile strength compared to those with CNCs, potentially attributed to the more robust ionic interaction between the negatively charged TOCNFs and positively charged CA chains. Additionally, the fibrous structure of TOCNFs likely played a role in heightened interaction and cross-linking with the CA matrix. The findings indicate that heat-treated ENM samples demonstrated tougher, stronger, and more cohesive structures due to cross-linking between nanofibers, resulting in improved ultimate tensile strength (UTS) and fracture strain post-heat treatment. Moreover, heat treatment contributed to enhanced mechanical properties and membrane integrity by solvent removal and nanofiber cross-linking. The heat-treated 0.25TOCNF/CA composite ENM sample, in particular, exhibited a maximum UTS of 33.31 MPa and a maximum elongation at the breakpoint of 1.83%.

Our endeavor in this project was motivated by the aspiration to strike a harmonious balance between sustainability and operational efficiency. The environmental footprints of the traditional wet spinning method (NIPS) and the innovative dry spinning technique (electrospinning) was conducted through the utilization of the IMPACT2002+ and CED life cycle impact assessment methodologies. The findings underscore the substantial influence of the membrane fabrication method on environmental performance. A comprehensive assessment of the total cumulative energy demand for the synthesis of 0.25TOCNF/CA membrane using NIPS and electrospinning methods revealed that the electrospinning technique exhibited a lower environmental impact compared to the NIPS method. The NIPS method demonstrated a higher total cumulative energy demand (1029 MJ) than the electrospinning technique (768 MJ), primarily due to increased electricity and water consumption in the NIPS synthesis process.

In line with the IMPACT2002+ assessment, the NIPS method exhibited significantly greater impact potential across various categories, including aquatic ecotoxicity, human carcinogenic toxicity, human non-carcinogenic toxicity, global warming, ionizing radiation, land usage, non-renewable energy, and ozone layer depletion. The NIPS method's heightened water consumption suggests the release of substantial amounts of solvent-contaminated wastewater into the environment, leading to more adverse effects on aquatic ecosystems. Additionally,

the NIPS method's elevated electricity consumption, compared to electrospinning, throughout the membrane fabrication process, contributes to negative impacts in the land use category and subsequent damages to ecosystem quality. Endpoint damages analysis indicated that the production of the 0.25TOCNF/CA HFM sample by the NIPS method had more detrimental impacts on human health, resource depletion, ecosystem quality, and climate change compared to the electrospinning method. These environmental impacts from the NIPS method can be attributed to the substantial energy, material, and water consumption during the production process.

RECOMMENDATIONS

This study has offered valuable insights into enhancing the mechanical properties of electrospun cellulose-based membranes through the incorporation of nanocellulose fillers and subsequent heat post-treatment. Furthermore, the implementation of a cradle-to-gate Life Cycle Assessment (LCA) for membrane fabrication has unveiled the environmental implications of this process. Nonetheless, there are several prospects for future research that could further advance the comprehension and application of these findings.

Primarily, extending the cradle-to-gate Life Cycle Assessment (LCA) of the manufactured cellulose-based membranes to encompass the entire life cycle, including usage and disposal stages, is recommended. Such an extension would facilitate a comprehensive cradle-to-grave evaluation of the membranes' environmental impact, pinpointing areas for potential improvement. The LCA scope could be broadened to encompass factors like energy consumption, water usage, and waste generation throughout the membrane's entire life cycle.

Moreover, it would be advantageous to assess the extended-term stability and durability of the modified cellulose-based membranes. This evaluation could involve subjecting the membranes to accelerated aging tests, such as exposure to harsh environmental conditions or continuous mechanical stress, while monitoring their mechanical properties over an extended period. The outcomes of these examinations would be instrumental in gauging the suitability of these membranes for practical applications, including water filtration or separation processes.

Additionally, exploring the scalability of the fabrication process for these modified membranes is essential. Examining the feasibility of up-scaling production to industrial levels, maintaining desired mechanical properties, and minimizing environmental impact is crucial for the commercialization and widespread adoption of these membranes.

Furthermore, the implementation of a cradle-to-gate Life Cycle Assessment (LCA) for membrane fabrication offers valuable insights into the environmental impact of the manufacturing process. To enhance the accuracy and reliability of LCA results, future research should incorporate

sensitivity analysis. This analysis would involve varying key parameters, such as energy consumption, raw material sourcing, and waste management, to assess their influence on the overall environmental performance of the membrane fabrication process.

Finally, the real-world application of these cellulose-based membranes warrants exploration. Conducting pilot studies or collaborating with industry partners to test the membranes' performance in practical settings can provide valuable feedback and insights for further improvements.

In conclusion, this section on future work underscores potential research areas to build upon the findings of this PhD dissertation. By delving deeper into the mechanical enhancement of electrospun cellulose-based membranes through nanocellulose fillers and heat treatment, and broadening the scope of cradle-to-gate LCA, researchers can continue advancing the field and contributing to the development of sustainable and efficient membrane fabrication techniques.

BIBLIOGRAPHY

- Abbasi, S. A. (2014). *Exergetic Life Cycle Assessment of Electrospun Polyvinylidene Fluoride Nanofibers*. University of South Florida.
- Abdelrazeq, H., Khraisheh, M., Ashraf, H. M., Ebrahimi, P. & Kunju, A. (2021). Sustainable innovation in membrane technologies for produced water treatment: Challenges and limitations. *Sustainability*, 13(12), 6759.
- Abdullah, N., Yusof, N., Lau, W., Jaafar, J. & Ismail, A. (2019). Recent trends of heavy metal removal from water/wastewater by membrane technologies. *Journal of Industrial and Engineering Chemistry*, 76, 17–38.
- Abe, K., Tomobe, Y. & Yano, H. (2020). The reinforcement effect of cellulose nanofiber on Young's modulus of polyvinyl alcohol gel produced through the freeze/thaw method. *Journal of Polymer Research*, 27(8), 1–5.
- Aboamera, N. M., Mohamed, A., Salama, A., Osman, T. & Khattab, A. (2019). Characterization and mechanical properties of electrospun cellulose acetate/graphene oxide composite nanofibers. *Mechanics of Advanced Materials and Structures*, 26(9), 765–769.
- Adiga, S. P., Jin, C., Curtiss, L. A., Monteiro-Riviere, N. A. & Narayan, R. J. (2009). Nanoporous membranes for medical and biological applications. *Wiley Interdisciplinary Reviews: Nanomedicine and Nanobiotechnology*, 1(5), 568–581.
- Amiraliyan, N., Nouri, M. & Haghghat Kish, M. (2010). Structural characterization and mechanical properties of electrospun silk fibroin nanofiber mats. *Polymer Science Series A*, 52(4), 407–412.
- Arribas, P., Khayet, M., García-Payo, M. & Gil, L. (2014). Self-sustained electro-spun polysulfone nano-fibrous membranes and their surface modification by interfacial polymerization for micro-and ultra-filtration. *Separation and Purification Technology*, 138, 118–129.
- Arribas, P., García-Payo, M., Khayet, M. & Gil, L. (2019). Heat-treated optimized polysulfone electrospun nanofibrous membranes for high performance wastewater microfiltration. *Separation and Purification Technology*, 226, 323–336.
- Aruchamy, K., Mahto, A. & Nataraj, S. (2018). Electrospun nanofibers, nanocomposites and characterization of art: insight on establishing fibers as product. *Nano-Structures & Nano-Objects*, 16, 45–58.
- Attari, N. & Hausler, R. (2020). Morphological investigation of Cellulose Acetate nanofibrous membranes. *Proceedings of the 4rd International Conference of Recent Trends in Environmental Science and Engineering (RTESE'20)*.

- Attari, N. & Hausler, R. (2023). Reinforcing Effects of Fibrous and Crystalline Nanocelluloses on Cellulose Acetate Membranes. *Carbohydrate Polymer Technologies and Applications*, 100281.
- Attari, N., Yegani, R. & Jafarzadeh, Y. (2017). The Effects of Bore Fluid Composition and Coagulation Bath Temperature on the Structure and Performance of Polysulfone Hollow Fiber Membranes in Collagen Separation. *Iran. J. Polym. Sci. Technol.(Persian)*, 29, 561–572.
- Babaei-Ghazvini, A. & Acharya, B. (2022). Influence of cellulose nanocrystal aspect ratio on shear force aligned films: Physical and mechanical properties. *Carbohydrate Polymer Technologies and Applications*, 3, 100217.
- Banerjee, P. (2023). Life Cycle Analysis of Polymeric Membrane-Based Processes. *Membranes for Water Treatment and Remediation*, 277–292.
- Basile, A., Cassano, A. & Rastogi, N. K. (2015). *Advances in membrane technologies for water treatment: materials, processes and applications*. Elsevier.
- Battirola, L. C., Andrade, P. F., Marson, G. V., Hubinger, M. D. & do Carmo Gonçalves, M. (2017). Cellulose acetate/cellulose nanofiber membranes for whey and fruit juice microfiltration. *Cellulose*, 24(12), 5593–5604.
- Bay, R. K., Zarybnicka, K., Jancar, J. & Crosby, A. J. (2020). Mechanical Properties of Ultrathin Polymer Nanocomposites. *ACS Applied Polymer Materials*, 2(6), 2220–2227.
- BERAICH, F. Z., AROUCH, M., BAKASSE, M. & Nasrellah, H. From waste to an ecological material: a new way to value the waste paper.
- Bonton, A., Bouchard, C., Barbeau, B. & Jedrzejak, S. (2012). Comparative life cycle assessment of water treatment plants. *Desalination*, 284, 42–54.
- Burger, C., Hsiao, B. S. & Chu, B. (2006). Nanofibrous materials and their applications. *Annual review of materials research*, 36(1), 333–368.
- Cai, S., Li, Y., Liu, H.-Y. & Mai, Y.-W. (2019). Effect of electrospun polysulfone/cellulose nanocrystals interleaves on the interlaminar fracture toughness of carbon fiber/epoxy composites. *Composites Science and Technology*, 181, 107673.
- Campano, C., Merayo, N., Balea, A., Tarrés, Q., Delgado-Aguilar, M., Mutjé, P., Negro, C. & Blanco, Á. (2018). Mechanical and chemical dispersion of nanocelluloses to improve their reinforcing effect on recycled paper. *Cellulose*, 25(1), 269–280.

- chand Katakam, H. (2015). *Fabrication and Characterization of Polycarbonate Polyurethane (PCPU) Nanofibers Impregnated with Nanofillers*. University of South Florida.
- Chen, D., Liu, T., Zhou, X., Tjiu, W. C. & Hou, H. (2009). Electrospinning fabrication of high strength and toughness polyimide nanofiber membranes containing multiwalled carbon nanotubes. *The Journal of Physical Chemistry B*, 113(29), 9741–9748.
- Cho, M., Karaaslan, M. A., Renneckar, S. & Ko, F. (2017). Enhancement of the mechanical properties of electrospun lignin-based nanofibers by heat treatment. *Journal of Materials Science*, 52(16), 9602–9614.
- Choi, S.-S., Lee, Y. S., Joo, C. W., Lee, S. G., Park, J. K. & Han, K.-S. (2004). Electrospun PVDF nanofiber web as polymer electrolyte or separator. *Electrochimica Acta*, 50(2-3), 339–343.
- Cindradewi, A. W., Bandi, R., Park, C.-W., Park, J.-S., Lee, E.-A., Kim, J.-K., Kwon, G.-J., Han, S.-Y. & Lee, S.-H. (2021). Preparation and characterization of cellulose acetate film reinforced with cellulose nanofibril. *Polymers*, 13(17), 2990.
- Coday, B. D., Miller-Robbie, L., Beaudry, E. G., Munakata-Marr, J. & Cath, T. Y. (2015). Life cycle and economic assessments of engineered osmosis and osmotic dilution for desalination of Haynesville shale pit water. *Desalination*, 369, 188–200.
- Coletti, A., Valerio, A. & Vismara, E. (2013). *Posidonia oceanica* as a renewable lignocellulosic biomass for the synthesis of cellulose acetate and glycidyl methacrylate grafted cellulose. *Materials*, 6(5), 2043–2058.
- Coutinho de Paula, E. & Amaral, M. C. S. (2017). Extending the life-cycle of reverse osmosis membranes: A review. *Waste Management & Research*, 35(5), 456–470.
- Cseri, L., Razali, M., Pogany, P. & Szekely, G. (2018). Organic solvents in sustainable synthesis and engineering. In *Green chemistry* (pp. 513–553). Elsevier.
- Curran, M. A. (2013). Life cycle assessment: a review of the methodology and its application to sustainability. *Current Opinion in Chemical Engineering*, 2(3), 273–277.
- Davoodi, A. H., Mazinani, S., Sharif, F. & Ranaei-Siadat, S. O. (2018). GO nanosheets localization by morphological study on PLA-GO electrospun nanocomposite nanofibers. *Journal of Polymer Research*, 25(9), 1–11.
- Del Río De Vicente, J. I. (2021). Cellulose nanocrystals functionalized cellulose acetate electrospun membranes for adsorption and separation of nanosized particles.

- Divya, S. & Oh, T. H. (2022). Polymer Nanocomposite Membrane for Wastewater Treatment: A Critical Review. *Polymers*, 14(9), 1732.
- Doshi, J. & Reneker, D. H. (1995). Electrospinning process and applications of electrospun fibers. *Journal of electrostatics*, 35(2-3), 151–160.
- du Quebec, G. (1995). *Quebec Ministry of the Environment: 25 years of industrial wastewater treatment in Quebec - report*.
- Earles, J. M. & Halog, A. (2011). Consequential life cycle assessment: a review. *The International Journal of Life Cycle Assessment*, 16(5), 445–453.
- Etemadi, H., Yegani, R. & Babaeipour, V. (2016). Study on the reinforcing effect of nanodiamond particles on the mechanical, thermal and antibacterial properties of cellulose acetate membranes. *Diamond and Related Materials*, 69, 166–176.
- Etemadi, H., Yegani, R. & Babaeipour, V. (2017). Performance evaluation and antifouling analyses of cellulose acetate/nanodiamond nanocomposite membranes in water treatment. *Journal of applied polymer science*, 134(21).
- Fane, A., Wang, R. & Jia, Y. (2011). *Membrane technology: past, present and future*. Springer.
- Fischer, S., Thümmel, K., Volkert, B., Hettrich, K., Schmidt, I. & Fischer, K. (2008). Properties and applications of cellulose acetate. *Macromolecular symposia*, 262, 89–96.
- Foroughi, F., Rezvani Ghomi, E., Morshedi Dehaghi, F., Borayek, R. & Ramakrishna, S. (2021). A review on the life cycle assessment of cellulose: From properties to the potential of making it a low carbon material. *Materials*, 14(4), 714.
- Gaitán, A. & Gacitúa, W. (2018). Morphological and mechanical characterization of electrospun polylactic acid and microcrystalline cellulose. *BioResources*, 13(2), 3659–3673.
- Gallo Stampino, P., Riva, L., Punta, C., Elegir, G., Bussini, D. & Dotelli, G. (2021). Comparative Life Cycle Assessment of Cellulose Nanofibres Production Routes from Virgin and Recycled Raw Materials. *Molecules*, 26(9), 2558.
- Geng, S., Wloch, D., Herrera, N. & Oksman, K. (2020). Large-scale manufacturing of ultra-strong, strain-responsive poly (lactic acid)-based nanocomposites reinforced with cellulose nanocrystals. *Composites Science and Technology*, 108144.
- Ghasemi, S., Behrooz, R., Ghasemi, I., Yassar, R. S. & Long, F. (2018). Development of nanocellulose-reinforced PLA nanocomposite by using maleated PLA (PLA-g-MA). *Journal of Thermoplastic Composite Materials*, 31(8), 1090–1101.

- Glater, J. (1998). The early history of reverse osmosis membrane development. *Desalination*, 117(1-3), 297–309.
- Goetz, L. A., Naseri, N., Nair, S. S., Karim, Z. & Mathew, A. P. (2018). All cellulose electrospun water purification membranes nanotextured using cellulose nanocrystals. *Cellulose*, 25(5), 3011–3023.
- Golizadeh, M., Karimi, A., Gandomi-Ravandi, S., Vossoughi, M., Khafaji, M., Joghataei, M. T. & Faghihi, F. (2019). Evaluation of cellular attachment and proliferation on different surface charged functional cellulose electrospun nanofibers. *Carbohydrate polymers*, 207, 796–805.
- Goodenough, J. B. (2014). Electrochemical energy storage in a sustainable modern society. *Energy & Environmental Science*, 7(1), 14–18.
- Gu, H., Reiner, R., Bergman, R. & Rudie, A. (2015). LCA study for pilot scale production of cellulose nano crystals (CNC) from wood pulp. *Proceedings from the LCA XV Conference*, pp. 33–42.
- Guo, M. & Murphy, R. (2012). LCA data quality: sensitivity and uncertainty analysis. *Science of the total environment*, 435, 230–243.
- Habibi, Y., Chanzy, H. & Vignon, M. R. (2006). TEMPO-mediated surface oxidation of cellulose whiskers. *Cellulose*, 13(6), 679–687.
- Haghighat Bayan, M. A., Afshar Taromi, F., Lanzi, M. & Pierini, F. (2021). Enhanced efficiency in hollow core electrospun nanofiber-based organic solar cells. *Scientific Reports*, 11(1), 21144.
- Han, S. O., Youk, J. H., Min, K. D., Kang, Y. O. & Park, W. H. (2008). Electrospinning of cellulose acetate nanofibers using a mixed solvent of acetic acid/water: Effects of solvent composition on the fiber diameter. *Materials Letters*, 62(4-5), 759–762.
- Hancock, N. T., Black, N. D. & Cath, T. Y. (2012). A comparative life cycle assessment of hybrid osmotic dilution desalination and established seawater desalination and wastewater reclamation processes. *Water research*, 46(4), 1145–1154.
- Hazarika, K. K., Konwar, A., Borah, A., Saikia, A., Barman, P. & Hazarika, S. (2023). Cellulose nanofiber mediated natural dye based biodegradable bag with freshness indicator for packaging of meat and fish. *Carbohydrate Polymers*, 300, 120241.
- Heijungs, R. (1996). Identification of key issues for further investigation in improving the reliability of life-cycle assessments. *Journal of Cleaner Production*, 4(3-4), 159–166.

- Hivechi, A., Bahrami, S. H., Siegel, R. A., B. Milan, P. & Amoupour, M. (2020). In vitro and in vivo studies of biaxially electrospun poly (caprolactone)/gelatin nanofibers, reinforced with cellulose nanocrystals, for wound healing applications. *Cellulose*, 1–18.
- Hu, S., Qin, Z., Cheng, M., Chen, Y., Liu, J. & Zhang, Y. (2018). Improved properties and drug delivery behaviors of electrospun cellulose acetate nanofibrous membranes by introducing carboxylated cellulose nanocrystals. *Cellulose*, 25(3), 1883–1898.
- Huijbregts, M. et al. (2001). *Uncertainty and variability in environmental life-cycle assessment*. Citeseer.
- Huijbregts, M. A. (1998). Application of uncertainty and variability in LCA. *The International Journal of Life Cycle Assessment*, 3, 273–280.
- Ismail, N., Venault, A., Mikkola, J.-P., Bouyer, D., Drioli, E. & Kiadeh, N. T. H. (2020). Investigating the potential of membranes formed by the vapor induced phase separation process. *Journal of Membrane Science*, 597, 117601.
- Janeca, A., Rodrigues, F. S., Gonçalves, M. C. & Faria, M. (2021). Novel Cellulose Acetate-Based Monophasic Hybrid Membranes for Improved Blood Purification Devices: Characterization under Dynamic Conditions. *Membranes*, 11(11), 825.
- Jiang, L., Li, K., Yang, H., Liu, X., Li, W., Xu, W. & Deng, B. (2020). Improving mechanical properties of electrospun cellulose acetate nanofiber membranes by cellulose nanocrystals with and without polyvinylpyrrolidone. *Cellulose*, 27(2), 955–967.
- Jin, K., Tang, Y., Zhu, X. & Zhou, Y. (2020). Polylactic acid based biocomposite films reinforced with silanized nanocrystalline cellulose. *International Journal of Biological Macromolecules*, 162, 1109–1117.
- Jolliet, O., Margni, M., Charles, R., Humbert, S., Payet, J., Rebitzer, G. & Rosenbaum, R. (2003). IMPACT 2002+: a new life cycle impact assessment methodology. *The international journal of life cycle assessment*, 8(6), 324–330.
- Jonoobi, M., Harun, J., Mathew, A. P. & Oksman, K. (2010). Mechanical properties of cellulose nanofiber (CNF) reinforced polylactic acid (PLA) prepared by twin screw extrusion. *Composites Science and Technology*, 70(12), 1742–1747.
- Juber, F. A. H., Jawad, Z. A., Chin, B. L. F., Yeap, S. P. & Chew, T. L. (2021). The prospect of synthesis of PES/PEG blend membranes using blend NMP/DMF for CO₂/N₂ separation. *Journal of Polymer Research*, 28(5), 1–26.

- Judd, S. (2008). The status of membrane bioreactor technology. *Trends in biotechnology*, 26(2), 109–116.
- Jung, J. T., Kim, J. F., Wang, H. H., Di Nicolo, E., Drioli, E. & Lee, Y. M. (2016). Understanding the non-solvent induced phase separation (NIPS) effect during the fabrication of microporous PVDF membranes via thermally induced phase separation (TIPS). *Journal of Membrane Science*, 514, 250–263.
- Kausar, A. (2017). Overview on conducting polymer in energy storage and energy conversion system. *Journal of Macromolecular Science, Part A*, 54(9), 640–653.
- Kim, J. (2020). Recent progress on improving the sustainability of membrane fabrication. *Journal of Membrane Science and Research*, 6(3), 241–250.
- Kocabaş, D. S., Akçelik, M. E., Bahçegül, E. & Özbek, H. N. (2021). Bulgur bran as a biopolymer source: Production and characterization of nanocellulose-reinforced hemicellulose-based biodegradable films with decreased water solubility. *Industrial Crops and Products*, 171, 113847.
- Kugarajah, V., Ojha, A. K., Ranjan, S., Dasgupta, N., Ganesapillai, M., Dharmalingam, S., Elmoll, A., Hosseini, S. A., Muthulakshmi, L., Vijayakumar, S. et al. (2021). Future applications of electrospun nanofibers in pressure driven water treatment: A brief review and research update. *Journal of Environmental Chemical Engineering*, 9(2), 105107.
- Lalia, B. S., Kochkodan, V., Hashaikh, R. & Hilal, N. (2013). A review on membrane fabrication: Structure, properties and performance relationship. *Desalination*, 326, 77–95.
- Lalia, B. S., Guillen, E., Arafat, H. A. & Hashaikh, R. (2014). Nanocrystalline cellulose reinforced PVDF-HFP membranes for membrane distillation application. *Desalination*, 332(1), 134–141.
- Lawler, W., Alvarez-Gaitan, J., Leslie, G. & Le-Clech, P. (2015). Comparative life cycle assessment of end-of-life options for reverse osmosis membranes. *Desalination*, 357, 45–54.
- Lee, H., Nishino, M., Sohn, D., Lee, J. S. & Kim, I. S. (2018). Control of the morphology of cellulose acetate nanofibers via electrospinning. *Cellulose*, 25, 2829–2837.
- Levanic, J., Šenk, V. P., Nadrah, P., Poljanšek, I., Oven, P. & Haapala, A. (2020). Analyzing TEMPO-oxidized cellulose fiber morphology: new insights into optimization of the oxidation process and nanocellulose dispersion quality. *ACS Sustainable Chemistry & Engineering*, 8(48), 17752–17762.

- Li, L., Hashaikeh, R. & Arafat, H. A. (2013a). Development of eco-efficient micro-porous membranes via electrospinning and annealing of poly (lactic acid). *Journal of membrane science*, 436, 57–67.
- Li, N., Zheng, J., Hadi, P., Yang, M., Huang, X., Ma, H., Walker, H. W. & Hsiao, B. S. (2019). Synthesis and characterization of a high flux nanocellulose–cellulose acetate nanocomposite membrane. *Membranes*, 9(6), 70.
- Li, N. N., Fane, A. G., Ho, W. W. & Matsuura, T. (2011). *Advanced membrane technology and applications*. John Wiley & Sons.
- Li, Q., McGinnis, S., Wong, A. & Renneckar, S. (2013b). Nanocellulose life cycle assessment. *ACS Sustainable Chemistry & Engineering*, 1(8), 919–928.
- Liang, Y., Cheng, S., Zhao, J., Zhang, C., Sun, S., Zhou, N., Qiu, Y. & Zhang, X. (2013). Heat treatment of electrospun Polyvinylidene fluoride fibrous membrane separators for rechargeable lithium-ion batteries. *Journal of Power Sources*, 240, 204–211.
- Liao, Y., Loh, C.-H., Tian, M., Wang, R. & Fane, A. G. (2018). Progress in electrospun polymeric nanofibrous membranes for water treatment: Fabrication, modification and applications. *Progress in Polymer Science*, 77, 69–94.
- Liu, D., Sun, X., Tian, H., Maiti, S. & Ma, Z. (2013). Effects of cellulose nanofibrils on the structure and properties on PVA nanocomposites. *Cellulose*, 20(6), 2981–2989.
- Liu, H. & Hsieh, Y.-L. (2002). Ultrafine fibrous cellulose membranes from electrospinning of cellulose acetate. *Journal of Polymer Science Part B: Polymer Physics*, 40(18), 2119–2129.
- Liu, H. & Tang, C. (2007). Electrospinning of cellulose acetate in solvent mixture N, N-dimethylacetamide (DMAc)/acetone. *Polymer journal*, 39(1), 65–72.
- Liu, J., Vanderesse, N., Stinville, J.-C., Pollock, T., Bocher, P. & Texier, D. (2019). In-plane and out-of-plane deformation at the sub-grain scale in polycrystalline materials assessed by confocal microscopy. *Acta Materialia*, 169, 260–274.
- Loeb, S. & Sourirajan, S. (1962). *Sea water demineralization by means of an osmotic membrane*. ACS Publications.
- Lovering, J., Swain, M., Blomqvist, L. & Hernandez, R. R. (2022). Land-use intensity of electricity production and tomorrow’s energy landscape. *PLoS One*, 17(7), e0270155.

- Ma, H., Burger, C., Hsiao, B. S. & Chu, B. (2014). Fabrication and characterization of cellulose nanofiber based thin-film nanofibrous composite membranes. *Journal of Membrane Science*, 454, 272–282.
- Madushela, N. (2017). Life cycle assessment–A review. *Proceedings of the world congress on engineering*, 2.
- Malara, A., Pantò, F., Santangelo, S., Antonucci, P. L., Fiore, M., Longoni, G., Ruffo, R. & Frontera, P. (2021). Comparative life cycle assessment of Fe₂O₃-based fibers as anode materials for sodium-ion batteries. *Environment, Development and Sustainability*, 23(5), 6786–6799.
- Manda, B. K., Worrell, E. & Patel, M. K. (2014). Innovative membrane filtration system for micropollutant removal from drinking water–prospective environmental LCA and its integration in business decisions. *Journal of cleaner production*, 72, 153–166.
- Marcano, J. G. S. & Tsotsis, T. T. (2002). *Catalytic membranes and membrane reactors*. Wiley-VCH Weinheim.
- Marino, T., Galiano, F., Molino, A. & Figoli, A. (2019). New frontiers in sustainable membrane preparation: Cyrene™ as green bioderived solvent. *Journal of Membrane Science*, 580, 224–234.
- Marino, T., Blefari, S., Di Nicolò, E. & Figoli, A. (2017). A more sustainable membrane preparation using triethyl phosphate as solvent. *Green Processing and Synthesis*, 6(3), 295–300.
- Matabola, K. & Moutloali, R. (2013). The influence of electrospinning parameters on the morphology and diameter of poly (vinylidene fluoride) nanofibers-effect of sodium chloride. *Journal of Materials Science*, 48, 5475–5482.
- Matsuura, T. (2020). *Synthetic membranes and membrane separation processes*. CRC press.
- Medina-Gonzalez, Y., Aimar, P., Lahitte, J.-F. & Remigy, J.-C. (2011). Towards green membranes: Preparation of cellulose acetate ultrafiltration membranes using methyl lactate as a biosolvent. *International Journal of Sustainable Engineering*, 4(01), 75–83.
- Mehrabani, S. A. N., Vatanpour, V. & Koyuncu, I. (2022). Green solvents in polymeric membrane fabrication: A review. *Separation and Purification Technology*, 298, 121691.
- Mohammadzadehmoghadam, S., Dong, Y. & Jeffery Davies, I. (2015). Recent progress in electrospun nanofibers: Reinforcement effect and mechanical performance. *Journal of Polymer Science Part B: Polymer Physics*, 53(17), 1171–1212.

- Mokhena, T., Jacobs, N. & Luyt, A. (2018). Nanofibrous alginate membrane coated with cellulose nanowhiskers for water purification. *Cellulose*, 25(1), 417–427.
- Morgan, M. G., Henrion, M. & Small, M. (1990). *Uncertainty: a guide to dealing with uncertainty in quantitative risk and policy analysis*. Cambridge university press.
- Nakhate, P. H., Moradiya, K. K., Patil, H. G., Marathe, K. V. & Yadav, G. D. (2020). Case study on sustainability of textile wastewater treatment plant based on lifecycle assessment approach. *Journal of Cleaner Production*, 245, 118929.
- Nasir, A., Masood, F., Yasin, T. & Hameed, A. (2019). Progress in polymeric nanocomposite membranes for wastewater treatment: Preparation, properties and applications. *Journal of Industrial and Engineering Chemistry*, 79, 29–40.
- Ni, X., Cheng, W., Huan, S., Wang, D. & Han, G. (2019). Electrospun cellulose nanocrystals/poly (methyl methacrylate) composite nanofibers: Morphology, thermal and mechanical properties. *Carbohydrate polymers*, 206, 29–37.
- Pan, C.-Y., Xu, G.-R., Xu, K., Zhao, H.-L., Wu, Y.-Q., Su, H.-C., Xu, J.-M. & Das, R. (2019). Electrospun nanofibrous membranes in membrane distillation: Recent developments and future perspectives. *Separation and Purification Technology*, 221, 44–63.
- Park, H. B., Hoek, E. & Tarabara, V. (2013). Gas separation membranes, Encyclopedia of membrane science and technology. John Wiley & Sons, Inc.
- Patiño-Masó, J., Serra-Parareda, F., Tarrés, Q., Mutjé, P., Espinach, F. X. & Delgado-Aguilar, M. (2019). TEMPO-oxidized cellulose nanofibers: a potential bio-based superabsorbent for diaper production. *Nanomaterials*, 9(9), 1271.
- Patterson, J. W. (1985). *Industrial wastewater treatment technology*. Butterworth Publishers, Stoneham, MA.
- Petroudy, S. R. D., Kahagh, S. A. & Vatankhah, E. (2021). Environmentally friendly superabsorbent fibers based on electrospun cellulose nanofibers extracted from wheat straw. *Carbohydrate Polymers*, 251, 117087.
- Phan, D.-N., Lee, H., Choi, D., Kang, C.-Y., Im, S. S. & Kim, I. S. (2018). Fabrication of two polyester nanofiber types containing the biobased monomer isosorbide: poly (ethylene glycol 1, 4-cyclohexane dimethylene isosorbide terephthalate) and poly (1, 4-cyclohexane dimethylene isosorbide terephthalate). *Nanomaterials*, 8(2), 56.

- Piccinno, F., Hischier, R., Seeger, S. & Som, C. (2015). Life cycle assessment of a new technology to extract, functionalize and orient cellulose nanofibers from food waste. *ACS Sustainable Chemistry & Engineering*, 3(6), 1047–1055.
- Piccinno, F., Hischier, R., Seeger, S. & Som, C. (2018). Predicting the environmental impact of a future nanocellulose production at industrial scale: Application of the life cycle assessment scale-up framework. *Journal of Cleaner Production*, 174, 283–295.
- Pinnau, I. & Freeman, B. (2000). *Formation and modification of polymeric membranes: overview*. ACS Publications.
- Prézéus, F., Tiruta-Barna, L., Guigui, C. & Remigy, J.-C. (2021). A generic process modelling–LCA approach for UF membrane fabrication: Application to cellulose acetate membranes. *Journal of Membrane Science*, 618, 118594.
- Rahman, A., Pullabhotla, V. R., Daniel, L. & Uahengo, V. (2021). Hybrid nanocomposites based on cellulose nanocrystals/nanofibrils and titanium oxide: Wastewater treatment. In *Cellulose Nanocrystal/Nanoparticles Hybrid Nanocomposites* (pp. 141–164). Elsevier.
- Razali, M., Kim, J. F., Attfield, M., Budd, P. M., Drioli, E., Lee, Y. M. & Szekely, G. (2015). Sustainable wastewater treatment and recycling in membrane manufacturing. *Green Chemistry*, 17(12), 5196–5205.
- Reid, C. & Breton, E. (1959). Water and ion flow across cellulosic membranes. *Journal of applied polymer science*, 1(2), 133–143.
- Rodrigues Filho, G., Monteiro, D. S., da Silva Meireles, C., de Assunção, R. M. N., Cerqueira, D. A., Barud, H. S., Ribeiro, S. J. & Messadeq, Y. (2008). Synthesis and characterization of cellulose acetate produced from recycled newspaper. *Carbohydrate Polymers*, 73(1), 74–82.
- Saito, T., Kimura, S., Nishiyama, Y. & Isogai, A. (2007). Cellulose nanofibers prepared by TEMPO-mediated oxidation of native cellulose. *Biomacromolecules*, 8(8), 2485–2491.
- Salama, A., Mohamed, A., Aboamera, N. M., Osman, T. & Khattab, A. (2018). Characterization and mechanical properties of cellulose acetate/carbon nanotube composite nanofibers. *Advances in Polymer Technology*, 37(7), 2446–2451.
- Santero, N. (2010). Life cycle assessment of pavements: a critical review of existing literature and research.
- Saud, A., Saleem, H. & Zaidi, S. J. (2022). Progress and Prospects of Nanocellulose-Based Membranes for Desalination and Water Treatment. *Membranes*, 12(5), 462.

- Selatile, M. K., Ray, S. S., Ojijo, V. & Sadiku, R. (2018). Recent developments in polymeric electrospun nanofibrous membranes for seawater desalination. *RSC advances*, 8(66), 37915–37938.
- Sharma, A., Mandal, T. & Goswami, S. (2021). Fabrication of cellulose acetate nanocomposite films with lignocellulosic nanofiber filler for superior effect on thermal, mechanical and optical properties. *Nano-Structures & Nano-Objects*, 25, 100642.
- Sheng, L., Jiang, R., Zhu, Y. & Ji, Y. (2014). Electrospun cellulose nanocrystals/polycaprolactone nanocomposite fiber mats. *Journal of Macromolecular Science, Part B*, 53(5), 820–828.
- Sidney, L. & Srinivasa, S. [US Patent 3,133,132]. (1964, 12). High flow porous membranes for separating water from saline solutions. Google Patents.
- Sill, T. J. & Von Recum, H. A. (2008). Electrospinning: applications in drug delivery and tissue engineering. *Biomaterials*, 29(13), 1989–2006.
- Sonia, Hassana, M. (2015). Chemical isolation and characterization of different cellulose-nanofibers from cotton stalks. *Carbohydrate Polymers*, 134, 8.
- Sonnemann, G. W., Schuhmacher, M. & Castells, F. (2003). Uncertainty assessment by a Monte Carlo simulation in a life cycle inventory of electricity produced by a waste incinerator. *Journal of cleaner production*, 11(3), 279–292.
- Stamatialis, D. F., Papenburg, B. J., Gironés, M., Saiful, S., Bettahalli, S. N., Schmitmeier, S. & Wessling, M. (2008). Medical applications of membranes: Drug delivery, artificial organs and tissue engineering. *Journal of Membrane Science*, 308(1-2), 1–34.
- Strathmann, H., Kock, K., Amar, P. & Baker, R. (1975). The formation mechanism of asymmetric membranes. *Desalination*, 16(2), 179–203.
- Suja, P., Reshmi, C., Sagitha, P. & Sujith, A. (2017). Electrospun nanofibrous membranes for water purification. *Polymer reviews*, 57(3), 467–504.
- Sun, C., Boluk, Y. & Ayranci, C. (2015). Investigation of nanofiber nonwoven meshes produced by electrospinning of cellulose nanocrystal suspensions in cellulose acetate solutions. *Cellulose*, 22(4), 2457–2470.
- Sun, C., Yin, H., He, J., Zou, L. & Xu, Y. (2021). Fabrication and characterization of nanofibrous gelatin/chitosan-poly (ethylene oxide) membranes by electrospinning with acetic acid as solvent. *Journal of Polymer Research*, 28(12), 1–13.

- Sun, S. & Ertz, M. (2020). Life cycle assessment and Monte Carlo simulation to evaluate the environmental impact of promoting LNG vehicles. *MethodsX*, 7, 101046.
- Szekely, G., Jimenez-Solomon, M. F., Marchetti, P., Kim, J. F. & Livingston, A. G. (2014). Sustainability assessment of organic solvent nanofiltration: from fabrication to application. *Green Chemistry*, 16(10), 4440–4473.
- Tijing, L., Woo, Y., Yao, M., Ren, J. & Shon, H. (2017). 1.16 Electrospinning for membrane fabrication: strategies and applications. *Comprehensive Membrane Science and Engineering; Elsevier: Oxford, UK*, 418–444.
- Toffoletto, L., Bulle, C., Godin, J., Reid, C. & Deschênes, L. (2007). LUCAS-A new LCIA method used for a Canadian-specific context. *The International Journal of Life Cycle Assessment*, 12(2), 93–102.
- Tucker, N., Stanger, J. J., Staiger, M. P., Razzaq, H. & Hofman, K. (2012). The history of the science and technology of electrospinning from 1600 to 1995. *Journal of engineered fibers and fabrics*, 7(2_suppl), 155892501200702S10.
- Tungprapa, S., Puangparn, T., Weerasombut, M., Jangchud, I., Fakum, P., Semongkhon, S., Meechaisue, C. & Supaphol, P. (2007). Electrospun cellulose acetate fibers: effect of solvent system on morphology and fiber diameter. *Cellulose*, 14, 563–575.
- Turk, J., Oven, P., Poljanšek, I., Lešek, A., Knez, F. & Rebec, K. M. (2020). Evaluation of an environmental profile comparison for nanocellulose production and supply chain by applying different life cycle assessment methods. *Journal of Cleaner Production*, 247, 119107.
- Uyar, T. & Besenbacher, F. (2008). Electrospinning of uniform polystyrene fibers: The effect of solvent conductivity. *Polymer*, 49(24), 5336–5343.
- Vaidya, R. & Wilkins, E. (1994). Effect of interference on amperometric glucose biosensors with cellulose acetate membranes. *Electroanalysis*, 6(8), 677–682.
- Vatanpour, V., Pasaoglu, M. E., Barzegar, H., Teber, O. O., Kaya, R., Bastug, M., Khataee, A. & Koyuncu, I. (2022). Cellulose acetate in fabrication of polymeric membranes: A review. *Chemosphere*, 295, 133914.
- Voisin, H., Bergström, L., Liu, P. & Mathew, A. P. (2017). Nanocellulose-based materials for water purification. *Nanomaterials*, 7(3), 57.

- Wang, D., Cheng, W., Wang, Q., Zang, J., Zhang, Y. & Han, G. (2019a). Preparation of electrospun chitosan/poly (ethylene oxide) composite nanofibers reinforced with cellulose nanocrystals: Structure, morphology, and mechanical behavior. *Composites Science and Technology*, 182, 107774.
- Wang, X., Cheng, W., Wang, D., Ni, X. & Han, G. (2019b). Electrospun polyvinylidene fluoride-based fibrous nanocomposite membranes reinforced by cellulose nanocrystals for efficient separation of water-in-oil emulsions. *Journal of Membrane Science*, 575, 71–79.
- Wang, Y., Ying, Z., Xie, W. & Wu, D. (2020). Cellulose nanofibers reinforced biodegradable polyester blends: Ternary biocomposites with balanced mechanical properties. *Carbohydrate Polymers*, 233, 115845.
- Wen, Y., Yuan, J., Ma, X., Wang, S. & Liu, Y. (2019). Polymeric nanocomposite membranes for water treatment: a review. *Environmental Chemistry Letters*, 17(4), 1539–1551.
- Wilderer, P. (2010). *Treatise on water science*. Newnes.
- Wong, D., Hartery, S., Keltie, E., Chang, R., Kim, J. S. & Park, S. S. (2021). Electrospun Polystyrene and Acid-Treated Cellulose Nanocrystals with Intense Pulsed Light Treatment for N95-Equivalent Filters. *ACS Applied Polymer Materials*, 3(10), 4949–4958.
- Wsoo, M. A., Shahir, S., Mohd Bohari, S. P., Nayan, N. H. M. & Razak, S. I. A. (2020). A review on the properties of electrospun cellulose acetate and its application in drug delivery systems: A new perspective. *Carbohydrate Research*, 491, 107978.
- Wu, Y., Tang, Q., Yang, F., Xu, L., Wang, X. & Zhang, J. (2019). Mechanical and thermal properties of rice straw cellulose nanofibrils-enhanced polyvinyl alcohol films using freezing-and-thawing cycle method. *Cellulose*, 26(5), 3193–3204.
- Yadav, P., Ismail, N., Essalhi, M., Tysklind, M., Athanassiadis, D. & Tavajohi, N. (2021). Assessment of the environmental impact of polymeric membrane production. *Journal of Membrane Science*, 622, 118987.
- Yang, J., Han, C.-R., Duan, J.-F., Ma, M.-G., Zhang, X.-M., Xu, F., Sun, R.-C. & Xie, X.-M. (2012). Studies on the properties and formation mechanism of flexible nanocomposite hydrogels from cellulose nanocrystals and poly (acrylic acid). *Journal of Materials Chemistry*, 22(42), 22467–22480.
- You, Y., Lee, S. W., Lee, S. J. & Park, W. H. (2006). Thermal interfiber bonding of electrospun poly (l-lactic acid) nanofibers. *Materials Letters*, 60(11), 1331–1333.

- Yue, Y., Han, J., Han, G., French, A. D., Qi, Y. & Wu, Q. (2016). Cellulose nanofibers reinforced sodium alginate-polyvinyl alcohol hydrogels: Core-shell structure formation and property characterization. *Carbohydrate Polymers*, 147, 155–164.
- Zhou, Z., Lin, W. & Wu, X.-F. (2016). Electrospinning ultrathin continuous cellulose acetate fibers for high-flux water filtration. *Colloids and Surfaces A: Physicochemical and Engineering Aspects*, 494, 21–29.

